

External Grant Award Nos. G09AP00065 and G09AP00066

**EFFECTS OF SHALLOW 3D STRUCTURE OF THE MISSISSIPPI EMBAYMENT ON GROUND-MOTION AMPLIFICATION: COLLABORATIVE RESEARCH WITH UNIVERSITY OF MINNESOTA, DULUTH, AND UNIVERSITY OF MEMPHIS**

David Dolenc  
Large Lakes Observatory, University of Minnesota, Duluth  
2205 E 5th Street  
Duluth, MN 55812  
Telephone: (218) 726-8136  
FAX: (218) 726-6979  
Email: ddolenc@d.umn.edu

Stephen Horton  
Center for Earthquake Research and Information, University of Memphis  
3890 Central Avenue  
Memphis, TN 38152  
Telephone: (901) 678-4896  
FAX: (901) 678-4734  
Email: shorton@memphis.edu

Start Date: June 1, 2009  
End Date: May 31, 2010

**EFFECTS OF SHALLOW 3D STRUCTURE OF THE MISSISSIPPI EMBAYMENT ON GROUND-MOTION AMPLIFICATION: COLLABORATIVE RESEARCH WITH UNIVERSITY OF MINNESOTA, DULUTH, AND UNIVERSITY OF MEMPHIS**

David Dolenc

Large Lakes Observatory, University of Minnesota, Duluth  
2205 E 5th Street, Duluth, MN 55812

Tel.: (218) 726-8136, FAX: (218) 726-6979, Email: ddolenc@d.umn.edu

Stephen Horton

Center for Earthquake Research and Information, University of Memphis  
3890 Central Avenue, Memphis, TN 38152

Tel.: (901) 678-4896, FAX: (901) 678-4734, Email: shorton@memphis.edu

**Abstract**

The Mississippi Embayment (ME) region contains the New Madrid Seismic Zone (NMSZ), the most seismically active region in the central and eastern United States that is capable of producing M7+ earthquakes. At the same time, the embayment region is covered with up to 1 km thick low-velocity unconsolidated sediments that are known to amplify ground motions at low frequencies while reducing amplitude at high frequencies. Because large earthquakes in the NMSZ are infrequent, the effects of the shallow structure on the wave propagation in the ME remain to be better quantified. We used finite-difference code WPP with 1D and 3D velocity models of the ME to simulate five M4.0-5.2 earthquakes that were well recorded on the regional broadband seismic network. The models included a 1D velocity model, a 1D velocity crustal model overlain by a 3D sedimentary structure, and a complete 3D velocity model. We compared the results to evaluate the effects of the shallow structure on the ground-motion amplification, trapping of the surface waves in the slow velocity structures, and any focusing and interference effects at the basin edge. We further compared the synthetic waveforms to the observations to evaluate the 3D velocity model. We used the U.S. Geological Survey's new and comprehensive 3D velocity model of the region (CUSVM v1). The results of our study showed that synthetics obtained with the CUSVM v1 3D velocity model fit well the observed ground motions of the M5.2 Mt. Carmel, IL earthquake. Three of the M4 events having depths between 9.7 and 23.8 km and located in the ME were also well modeled by the 3D velocity model. Modeling results for the M4 Bardwell event at 2.6 km depth, located in the NE part of the ME, suggested that additional testing and possible refinement of the 3D velocity model in this region are needed. The results also showed the importance of including a slow velocity layer as well as 3D structure in the numerical simulations within the ME.

**Project Results**

We report on our modeling results of the five M4.0-5.2 earthquakes in the larger Mississippi Embayment (ME) region using finite difference code WPP and U.S. Geological Survey's 3D velocity model (CUSVM v1).

**Introduction**

Examples from numerous earthquakes have shown that strong ground motions can be expected in sedimentary basins. For example, the 1985  $M_w$ 8.1 Michoacan earthquake produced large ground motions as a result of the seismic wave reverberations in the basin of Mexico City (e.g., Anderson et al., 1986; Singh et al., 1988). Another, more recent example is the 1995  $M_w$ 6.9 Kobe earthquake where the shallow basin sediments as well as focusing and interference effects of the basin edge produced ground motions that were much stronger than expected from an earthquake of this size (Pitarka et al., 1996; Kawase, 1996). The trapping of the seismic

energy in the shallow sediments is the result of the slow seismic velocities as well as the basin structure. On the other hand, studies of seismic wave attenuation in the New Madrid seismic zone showed that slow sedimentary layers also significantly reduce the amplitudes of body waves and thus reduce ground motions at higher frequencies (e.g., Al-Shukri et al., 1988; Al-Shukri and Mitchell, 1990; Chen et al., 1994; Liu et al., 1994; Langston, 2003a).

Numerical simulations using 3D seismic velocity and seismic attenuation models can be used to study the effects of the sedimentary basins on the seismic wave propagation in more detail and to estimate the expected ground motions as well as the duration of shaking in the basins. The 3D velocity and attenuation model should first be tested by simulating the past, well-recorded events. Once validated, the 3D model can further be used to simulate scenario events in the region and help us better prepare for future events.

### ***The Mississippi Embayment (ME) and the New Madrid Seismic Zone***

The Mississippi Embayment (ME) is a broad southwest-plunging trough filled with up to 1 km of unconsolidated sediments (Stearns, 1957; Stearns and Marcher, 1962). The large impedance contrast at the interface between the sediments and the basement rocks can trap seismic energy in the slow velocity layers, resulting in stronger and longer-duration ground motions. Located within the embayment is the New Madrid Seismic Zone (NMSZ) that generated a series of great earthquakes in 1811-1812. The magnitude values for the three mainshocks (12/16/1811, 01/23/1812, and 02/07/1812) have generally been based on the microseismic effects, with published values ranging from 7.0 to 8.75 (Hough, 2004). Based on the paleoseismic investigations, the repeat time for the New Madrid events has been estimated to be on the order of 400-500 years (Tuttle and Schweig, 1996; Tuttle et al., 2002). Because large earthquakes are infrequent in the NMSZ, the wave propagation effects within the embayment sediments are still not completely understood and additional modeling as well as development of more detailed 3D velocity model are needed in order to estimate ground shaking for possible future events.

### ***Previous Work***

Although several previous studies included modeling of seismic wave propagation in the ME (e.g., Saikia and Somerville, 1997; Atkinson and Beresnev, 2002; Langston, 2003a; Langston, 2003b; Langston et al., 2005), only one study so far used a 3D velocity model to estimate ground motion amplification in this region (Saikia et al., 2006). The main two reasons for this have been 1) the limited knowledge of the detailed 3D structures in the region, and 2) the limited computational resources to run large scale simulations that would include a significant part of the ME region, yet still have a fine enough space resolution to support inclusion of slow seismic velocities (minimum  $v_s \sim 500$  m/s) and simulate frequencies all the way up to  $\sim 0.5$  Hz.

### ***The U.S. Geological Survey 3D Velocity Model CUSVM***

With the approaching bicentennial of the 1811-1812 New Madrid earthquakes, U.S. Geological Survey is reevaluating the temporal and spatial distribution of shaking and damage from St. Louis to Memphis that could be expected from a repeat of the 1811-1812 events (Robert Williams and Steve Hartzell, 2008, personal communication). U.S. Geological Survey constructed a new and comprehensive 3D geologic and seismic velocity model of the ME from the existing data. The model will be used to simulate the 1811-1812 ground motions using 3D computer simulations.

### ***Wave Propagation Modeling***

In our study we focused on the 3D effects of the shallow, slow structures in the ME region on the seismic wave propagation and ground-motion amplification. We used a 1D velocity crustal model, a 1D velocity crustal model overlain by a 3D sedimentary structure, and a complete 3D velocity model (3D crustal and 3D sedimentary model). For the 3D model, we used the U.S. Geological Survey's 3D velocity model CUSVM v1.

We used finite-difference code Wave Propagation Program (WPP; Nilsson et al., 2007) to simulate propagation of the seismic waves through the velocity models. WPP is a parallel computer program for simulating time-

dependent elastic and viscoelastic wave propagation, developed by the Lawrence Livermore National Laboratory group. The code has been verified with the method of manufactured solutions and by comparing the response of canonical problems to archived solutions (Nilsson et al., 2007). The code has also been successfully used in the broadband waveform modeling of moderate earthquakes in the San Francisco Bay Area (Rodgers et al., 2008a), scenario earthquakes on the Hayward Fault (Rodgers et al., 2008b), and in the ground-motion modeling of the 1906 San Francisco Earthquake (Aagaard et al., 2008). The code is well documented and publicly available (<https://computation.llnl.gov/casc/serpentine/software.html>). WPP supports the use of non-uniform grid spacing. The ability to use a finer computation mesh only in the regions where finer resolution is needed (shallow parts of the model with slow velocities) significantly reduces the memory requirements for the simulations and thus enables use of larger models and/or higher-frequency ground motion simulations.

We simulated five M4.0-5.2 events that were well recorded on the regional broadband seismic network (Fig. 1 and Table 1). Four of the events were located in the ME region and varied greatly in the hypocenter depths. The 06/06/2003  $M_w$ 4.0 Bardwell, Kentucky, event was located further to the north, in the region where the sedimentary layer is shallower. The event was only 2.6 km deep and observations showed a substantial surface wave train at some of the stations. The three other events in the ME had increasing depths (Fig. 1 and Table 1) and modeling showed the relative importance of the 3D velocity model on body waves. The last event that we modeled (04/18/2008,  $M_w$ 5.2) was located in the Illinois basin and provided interesting contrast to the previous events as in this case the seismic waves entered the ME from the north.

We compared the simulations to evaluate the effects of the shallow structure on the ground-motion amplification. We further compared the synthetic waveforms to the observations to evaluate the 3D velocity model. We also simulated events using the finer grid spacing to compute higher-resolution waveforms (up to 1 Hz). We compared the results to previous simulations (up to 0.5 Hz) and observations to estimate the importance of using high-resolution simulations for the M4-5 events in the NMSZ.

### ***Velocity Models***

The size of the 3D velocity models used to simulate the 4 events in the ME region was 345 km x 225 km x 50 km. The size of the models used to simulate the April 18, 2008  $M_w$ 5.2 Illinois event was 500 km x 225 km x 50 km (see Fig. 1). To accommodate slow velocities in the shallower regions, a finer computational mesh was used for the shallow regions. For the low-resolution runs ( $f < 0.5$  Hz) the 500 m grid spacing was used in the lower parts of the model. Grid spacing of 250 m was used above 2.5 km depth and grid spacing of 125 m above 1.25 km depth. For the high-resolution runs ( $f < 1$  Hz) the 500 m grid spacing was used below 18 km depth, grid spacing of 250 m above 18 km depth, grid spacing of 125 m above 2.5 km depth, and grid spacing of 62.5 m above 1.25 km depth.

#### ***1D model***

We used the 1D velocity model from Horton et al. (2005). Density values were determined using the Nafe-Drake equation (Brocher, 2005). The 1D model values are listed in Table 2.

#### ***1D+3D model***

The top 340 m of the above 1D model were replaced with the 3D velocity model CUSVM v1. Simulations for the top 1000 m with 3D are being computed.

#### ***3D model***

The U.S. Geological Survey's 3D velocity model CUSVM v1 was used.

#### ***3DHR model***

Same as the above 3D model, only that finer grid spacing was used to allow high-resolution runs ( $f < 1$  Hz).

The slowest S-wave velocity included in the 3D models was 500 m/s. The values in the CUSVM v1 model that were slower were increased to this minimum value. Topography was not included in the modeling.

### *Models with Q*

Since the CUSVM v1 model did not include attenuation, we also constructed 3D models with Q. We used a simple attenuation model in which  $Q_S$  linearly increased from 70 to 700 as S-wave velocity increased from 500 to 2000 m/s. In addition, we ran simulations that included a uniform attenuation within the ME basin ( $Q_P=200$ ,  $Q_S=100$ ). Unfortunately WPP simulations that included attenuation resulted in waveforms with random steps and artificial arrivals (see Fig. 9). We have not included any of the attenuation results in this report and are working with the authors of the WPP code to resolve this issue before submitting our results for publication.

All simulations were performed on the Linux cluster *Calhoun* at the Minnesota Supercomputer Institute (MSI). The *Calhoun* cluster had 2040 processors (255 nodes, 8 processors/node) with 14 GB memory/node available to the user. Memory requirements for different models and simulations are listed in Table 3. The time of computation varied depending on the number of processors that were used in a particular simulation. The minimum number of processors needed for each simulation was determined by the memory requirements. The small-model low-resolution simulation without attenuation was completed in about 4 hours using 40 processors. The large-model high-resolution simulation without attenuation was completed in about 16 hours using 144 processors.

## **Results**

Events AR1, AR2, and AR3 had similar magnitude, focal mechanisms, and epicenter location. The main difference were the hypocenter depths that were 23.8 km for AR1, 15.5 km for AR2, and 9.7 km for AR3 (see Fig. 1 and Table 1).

### *Event AR1*

The horizontal peak ground velocity plots (Fig. 3) show that ground-motions are primarily controlled by the source mechanism. As expected, the synthetics show the simplest waveforms for the 1D model, longer coda for the 1D+3D model, and more complex waveforms and longest coda for the 3D models. Overall, timing of the P- and S-wave arrivals are well modeled by all three models, however, the best results are obtained by the 3D model synthetics. Synthetics for the 1D, 1D+3D, and 3D models result in similar maximum amplitudes (see Fig. 8, pages 17-27). Results for all stations show that synthetics from all models over predict the observed maximum amplitude and duration of shaking. The same is true for the high-resolution simulation results (see Fig. 8, bottom two rows).

### *Event AR2*

The source depth of the event AR2 was shallower than that for AR1. The horizontal peak ground velocity plots (Fig. 4) for the two 3D models show a band of stronger ground motions in the NE and SW directions from the epicenter, along the ME axis. The synthetics fit the observations well, in particular the results obtained with the 3D model (see Fig. 8, pages 28-37). Stations close to the source (e.g., LPAR, Fig. 8) as well as more distant stations within the ME (e.g., PENM, Fig. 8) are modeled well with the 3D model. This is true for amplitudes and coda duration. The timing of the P- and S-wave arrivals is best fit with the 3D model. The high-resolution results also show significantly better fit than in the case of the event AR1.

### *Event AR3*

The source depth of the AR3 event was 9.7 km, which is the shallowest of the three AR events. The horizontal peak ground velocity plots (Fig. 5) show a strong influence of the ME on the shaking. The 3D and 3DHR model simulations both show that the basin velocity structure, and not the source mechanism, controls the ground motions. Overall the synthetics obtained with the 3D model fit the observations well (amplitude and coda duration; see Fig. 8, pages 38-48). This is true for the nearby stations (e.g., GNAR, Fig. 8) as well as distant stations (e.g., PARM, HENM, UTMT, Fig. 8). Stations GLAT and HICK, located in the NE part of the ME, are

the two stations for which the synthetics over predict the amplitudes and coda duration. The timing of the P- and S-wave arrivals is again best fit by the 3D model.

#### *Event BDWL*

The Bardwell event had a similar magnitude and mechanism as the three AR events, only that it was located further to the NE and at significantly shallower depth of 2.6 km (see Fig. 1 and Table 1). The event was most challenging to model and despite testing different event depths we were not able to fit the observations well. The horizontal peak ground velocity plots (Fig. 6) show that the simulated motions are controlled primarily by the source mechanism, however some influence of the ME structure can be observed to the south. The oscillating pattern seen in Figure 6 suggests that artificial reflections within the model grid could have been generated. However, tests with different grid setups that varied in the depth of the grid refinement did not affect the results. The waveforms show good agreement in the timing of the P- and S-wave arrivals, but the amplitudes are not modeled well (see Fig. 8, pages 49-58). Overall the synthetics obtained with 3D and 3DHR models significantly over predict the amplitudes and the coda duration. Observations at only a few stations are modeled reasonably well (e.g., HENM, Fig. 8). Also, observations at some of the stations (e.g., GNAR, PENM, PVMO, UTMT, Fig. 8) show very long coda duration that is not well modeled by the 3D model synthetics. We tested different event depths as well as different grid refinement schemes to check if setup of our model/event could be the reason for the disagreement between synthetics and observations, but have so far not been able to find an explanation. It is possible that strong lateral velocity variations and extremely narrow basin in the hypocenter region of the CUSVM v1 3D model contribute to large amplitudes obtained with the 3D and 3DHR models (see 5-km-depth section in Fig. 2 at X=250 and Y=150 km). Note that for this event the 1D and 1D+3D models fit the observations better than the 3D models. Our results suggest that in this region the current CUSVM 3D model needs further testing and possible refinement.

#### *Event IL*

The Mt. Carmel event was much stronger ( $M_w$ 5.2) than the other four events that we modeled. It was also located well outside of the ME and therefore the seismic waves entered the ME from the north. Note that in this case a larger model was used for the simulations (see Fig. 1). Also, longer waveforms (130 sec) were modeled. The horizontal peak ground velocity plots show that the velocity structure of the ME plays an important factor (Fig. 7). The simulated waveforms for the 3D model fit the observations well (see Fig. 8, pages 59-70). This is true for the nearby strong-motion stations (e.g., WVIL, HAIL, Fig. 8) as well as more distant stations (e.g., HENM, PARM, Fig. 8). The amplitudes, coda duration, and the time of the P- and S-wave arrivals were best modeled by the 3D model synthetics. The amplification of the ground motions within the ME was also well modeled by the 3D model (e.g., HICK, HENM, HALT, GLAT, Fig. 8). Due to the spurious arrivals after 130 sec (e.g., WVIL, Fig. 8), which were likely generated by the numerical instabilities along the model boundaries, we were not able to model longer waveforms. It is likely that model variations along the model edges and/or different boundary conditions could resolve this issue.

#### **Conclusions**

Waveforms obtained with the CUSVM v1 3D velocity fit the observations better than the synthetics obtained with the 1D and 1D+3D model. This is true for the waveform amplitudes, coda duration, and the arrival times of the P- and S-waves. The 3D model simulations confirmed that the ME significantly affects the ground motions. This is particularly true for the events AR2 and AR3 that occurred in the 10-15 km depth range. Modeling results for the Bardwell event showed that further testing and possible refinement of the 3D model in this region are needed to better fit the observations. The stronger Mt. Carmel event provided an important validation of the model since the event was located outside of the ME and the seismic waves enter the ME from the north. Good agreement between the synthetics and the observations (arrival times, maximum amplitudes, and coda duration) showed that the 3D CUSVM model will provide an important tool for modeling larger events in the region.

Additional simulations using the 3D models that included attenuation are needed before any conclusions are drawn about the importance to include attenuation ground motion simulations in the ME.

## Acknowledgments

We thank L. Ramirez-Guzman, R. A. Williams, O. Boyd, and S. Hartzell for sharing their preliminary CUSVM 3D velocity model with us. This work was carried out in part using computer resources at the University of Minnesota Supercomputing Institute.

## Peer-Reviewed Reporting of Results

Dolenc and Horton are preparing a manuscript for submission to Bulletin of the Seismological Society of America. It will describe modeling results presented in this report. Also included will be results obtained with the revised CUSVM velocity model that is currently in preparation as well as results of the simulations that will include attenuation.

## References

- Aagaard, B. T., T. M. Brocher, D. Dolenc, D. Dreger, R. W. Graves, S. Harmsen, S. Hartzell, S. Larsen, K. McCandless, S. Nilsson, N. A. Petersson, A. Rodgers, B. Sjoegreen, and M. L. Zoback (2008). Ground-motion modeling of the 1906 San Francisco Earthquake, Part II: Ground-motion estimates for the 1906 Earthquake and scenario events, *Bull. Seism. Soc. Am.*, 98, 1012-1046.
- Al-Shukri, H. and B. Mitchell (1990). Three-dimensional attenuation structure in and around the New Madrid seismic zone, *Bull. Seism. Soc. Am.*, 80, 615-632.
- Al-Shukri, H., B. Mitchell, and H. A. A. Ghalib (1988). Attenuation of seismic waves in the New Madrid seismic zone, *Seism. Res. Lett.*, 59, 133-140.
- Anderson, J. G., P. Bodin, J. N. Brune, J. Prince, S. K. Singh, R. Quaas, and M. Onate (1986). Strong ground motion from the Michoacan, Mexico, earthquake, *Science*, 233, 1043-1049.
- Atkinson, G. M. and I. A. Beresnev (2002). Ground motions at Memphis and St. Louis from M 7.5-8.0 earthquakes in the New Madrid Seismic Zone, *Bull. Seism. Soc. Am.*, 92, 1015-1024.
- Brocher, T. M. (2005). Empirical relations between elastic wavespeeds and density in the Earth's crust, *Bull. Seism. Soc. Am.*, 95, 2081-2092.
- Chen, K.-C., J.-M. Chiu, and Y.-T. Yang (1994).  $Q_p$ - $Q_s$  relations in the sedimentary basin of the Mississippi embayment using converted phases, *Bull. Seism. Soc. Am.*, 84, 1861-1868.
- Gomberg, J., B. Waldron, E. Schweig, H. Hwang, A. Webbers, R. VanArsdale, K. Tucker, R. Williams, R. Street, P. Mayne, W. Stephenson, J. Odum, C. Cramer, R. Updike, S. Hutson, and M. Bradley (2003). Lithology and shear-wave velocity in Memphis, Tennessee, *Bull. Seism. Soc. Am.*, 93, 986-997.
- Horton, S. P., W.-Y. Kim, and M. Withers (2005). The 6 June 2003 Bardwell, Kentucky, earthquake sequence: Evidence for a locally perturbed stress field in the Mississippi embayment, *Bull. Seism. Soc. Am.*, 95, 431-445.
- Hough, S. E. (2004). Scientific overview and historical context of the 1811-1812 New Madrid earthquake sequence, *Annals of Geophysics*, 47, 523-537.
- Kawase, H. (1996). The cause of the damage belt in Kobe: "The basin edge effect", constructive interference of the direct S-wave with the basin-induced diffracted/Rayleigh waves, *Seism. Res. Lett.*, 67, 25-34.
- Langston, C. A. (2003a). Local earthquake wave propagation through Mississippi embayment sediments, Part II: Influence of local site velocity structure on  $Q_p$ - $Q_s$  determinations, *Bull. Seism. Soc. Am.*, 93, 2685-2702.
- Langston, C. A. (2003b). Local earthquake wave propagation through Mississippi embayment sediments, Part I: Body-wave phases and local site responses, *Bull. Seism. Soc. Am.*, 93, 2664-2684.
- Langston, C. A., P. Bodin, C. Powell, M. Withers, S. Horton, and W. Mooney (2005). Bulk sediment  $Q_p$  and  $Q_s$  in the Mississippi embayment, Central United States, *Bull. Seism. Soc. Am.*, 95, 2162-2179.
- Liu, Z., M. E. Wuenschel, and R. B. Herrmann (1994). Attenuation of body waves in the central New Madrid seismic zone, *Bull. Seism. Soc. Am.*, 84, 1112-1122.

- Nilsson, S., N. A. Peterson, B. Sjoegreen, and H.-O. Kreiss (2007). Stable difference approximations for the elastic wave equation in second order formulation, *SIAM J. Numer. Anal.*, 45, 1902-1936.
- Pitarka, A., K. Irikura, T. Iwata, and T. Kagawa (1996). Basin structure effects in the Kobe are inferred from the modeling of ground motions from two aftershocks of the January 17, 1995, Hyogo-ken Nanbu earthquake, *J. Phys. Earth*, 44, 563-576.
- Rodgers, A. N., A. Petersson, S. Nilsson, B. Sjoegreen, and K. McCandless (2008a). Broadband waveform modeling of moderate earthquakes in the San Francisco Bay Area and preliminary assessment of the USGS 3D Seismic Velocity Model, *Bull. Seism. Soc. Am.*, 98, 969-988.
- Rodgers, A. and X.-B. Xie (2008b). Ground motion modeling of recent moderate (M4-5) and large (M>6.5) scenario earthquakes on the Hayward fault, *Seism. Res. Lett.*, 79, 342.
- Saikia, C. K., A. Pitarka, and G. A. Ichinose (2006). Effects of irregular structure of the Mississippi Embayment on ground-motion amplification, *Bull. Seism. Soc. Am.*, 96, 1448-1473.
- Saikia, C. K. and P. G. Somerville (1997). Simulated hard-rock motions in Saint Louis, Missouri, from Large New Madrid earthquakes (Mw >= 6.5), *Bull. Seism. Soc. Am.*, 87, 123-139.
- Singh, S. K., J. Lermo, T. Dominguez, M. Ordaz, J. M. Espinosa, E. Mena, and R. Quass (1988). The Mexico earthquake of September 19, 1985 – A study of amplification of seismic waves in the Valley of Mexico with respect to a hill zone site, *Earthquake Spectra*, 4, 653-673.
- Stearns, R. G. (1957). Cretaceous, Paleocene, and lower Eocene geologic history of the northern Mississippi embayment, *Geol. Soc. Am. Bull.*, 68, 1077-1100.
- Stearns, R. G. and M. V. Marcher (1962). Late Cretaceous and subsequent structural development of the northern Mississippi embayment area, *Geol. Soc. Am. Bull.*, 73, 1387-1394.
- Tuttle, M. P. and E. S. Schweig (1996). Archaeological and pedological evidence for large prehistoric earthquakes in the New Madrid seismic zone, Central United States, *Geology*, 23, 253-256.
- Tuttle, M. P., E. S. Schweig, J. D. Sims, R. H. Cafferty, L. W. Wolf, and M. L. Haynes (2002). The earthquake potential of the New Madrid seismic zone, *Bull. Seism. Soc. Am.*, 92, 2080-2089.

Table 1. Source parameters for the recent well-recorded events located in the Mississippi Embayment (events 1-4) and in the Illinois basin (event 5) that were included in our modeling. Note a wide range of focal depths for the events located in the ME.

Event	Date	Time (UTC)	Lat (N)	Lon (W)	Depth (km)	M <sub>w</sub>	Focal Mechanism (Strike/Dip/Rake)
AR 1	2003/04/30	04:56:22	35.92	89.92	23.8	4.0	140/75/-20
AR 2	2005/02/10	14:04:54	35.76	90.25	15.5	4.1	55/80/-165
AR 3	2005/05/01	12:37:32	35.83	90.15	9.7	4.2	214/73/148
BDWL	2003/06/06	12:29:34	36.87	88.98	2.6	4.02	165/85/15
IL	2008/04/18	09:37:00	38.45	87.89	11.6	5.2	25/90/-175

Table 2. The 1D velocity model from Horton et al. (2005). We determined the density values using the Nafe-Drake equation (Brocher, 2005).

Depth Range (km)	v <sub>P</sub> (km/s)	v <sub>S</sub> (km/s)	ρ (g/cm <sup>3</sup> )
0 – 0.34	1.8	0.6	1.81
0.34 – 2.5	6.02	3.56	2.72
2.5 – 5	4.83	3.2	2.51
5 – 17	6.17	3.57	2.75
17 - 27	6.6	3.82	2.86
27 - 50	7.3	4.22	3.06

Table 3. Memory requirements for the simulations using different velocity models. Note that the use of attenuation in WPP code more than doubles the memory requirements from the purely elastic case.

Small Model (354 x 225 x 50 km)		Large Model (500 x 225 x 50 km)	
Low Resolution (f < 0.5 Hz)		High Resolution (f < 1 Hz)	
No Attenuation	With Attenuation	No Attenuation	No Attenuation
19 GB	46 GB	110 GB	28 GB
			163 GB

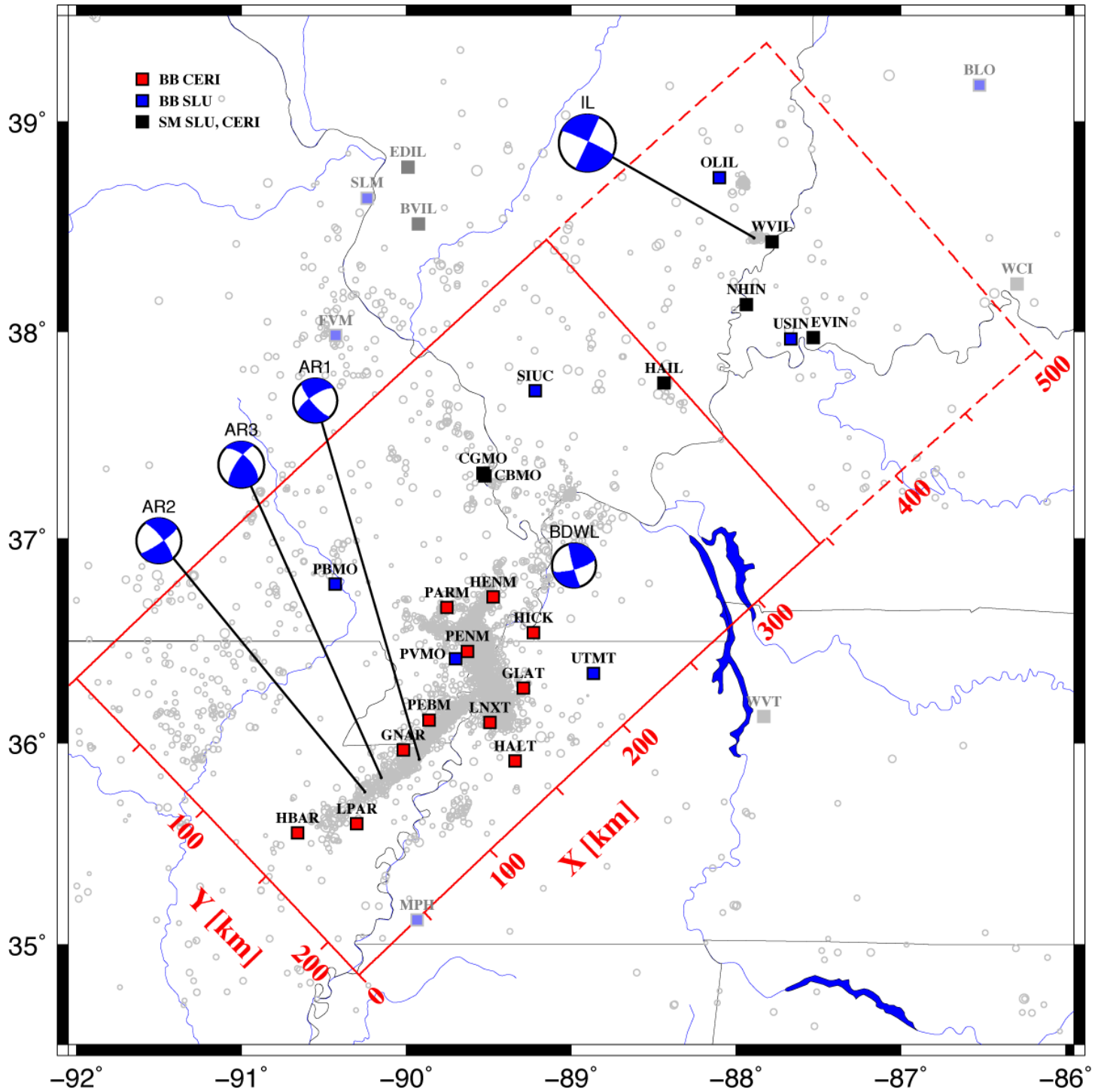


Figure 1. Map showing the size of the velocity models used in finite-difference simulations for the 4 events in the ME (red, solid) and in the Illinois basin (red, dashed). Red and blue squares are broadband seismometers. Black squares are strong motion stations.

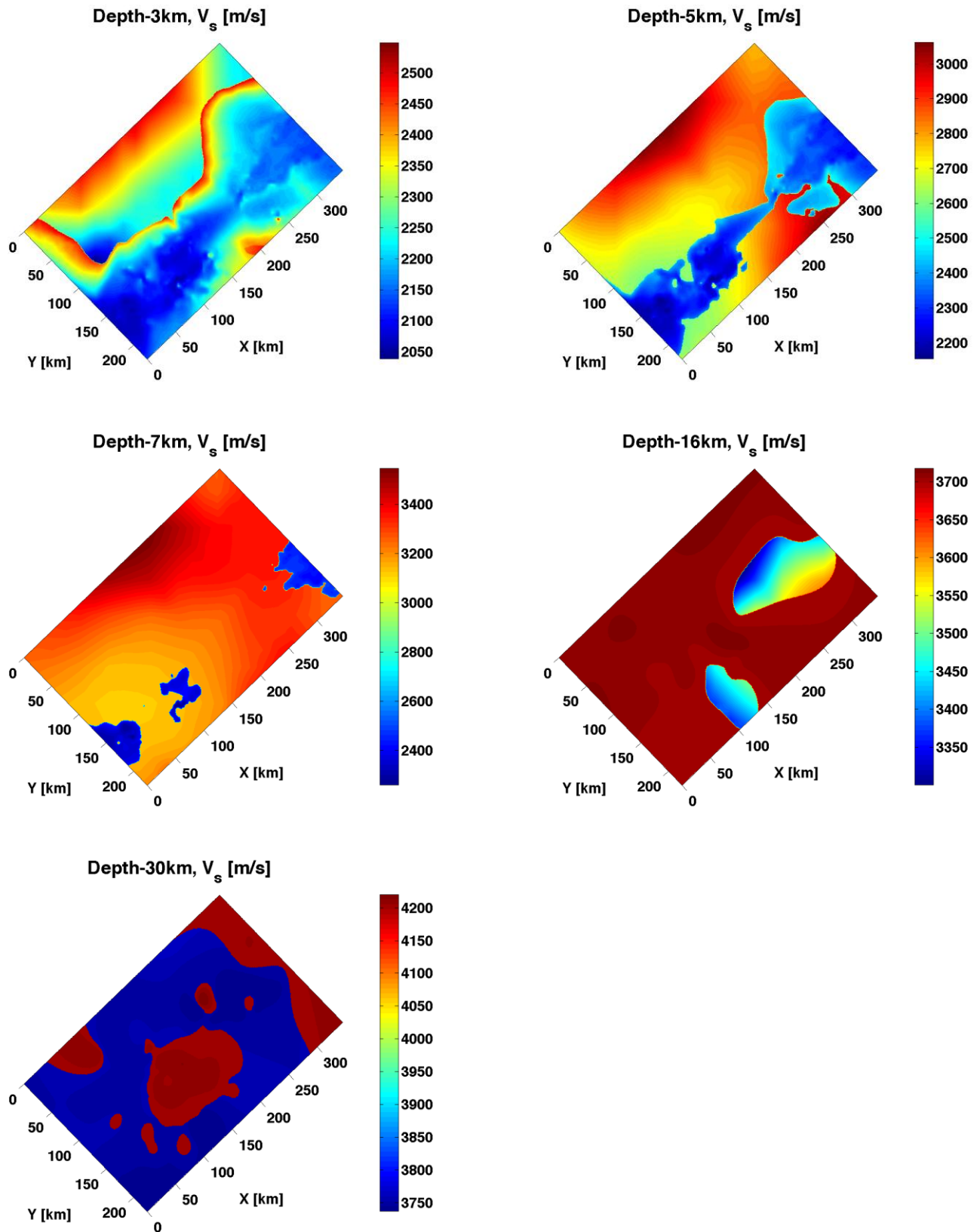


Figure 2. S-wave velocity cross-sections at 3, 5, 7, 16, and 30 km depth from the CUSVM v1 3D velocity model. The thin structure seen at 3 km depth along the entire embayment is an artifact and will be revised in the next model release (L. Guzman, personal communication).

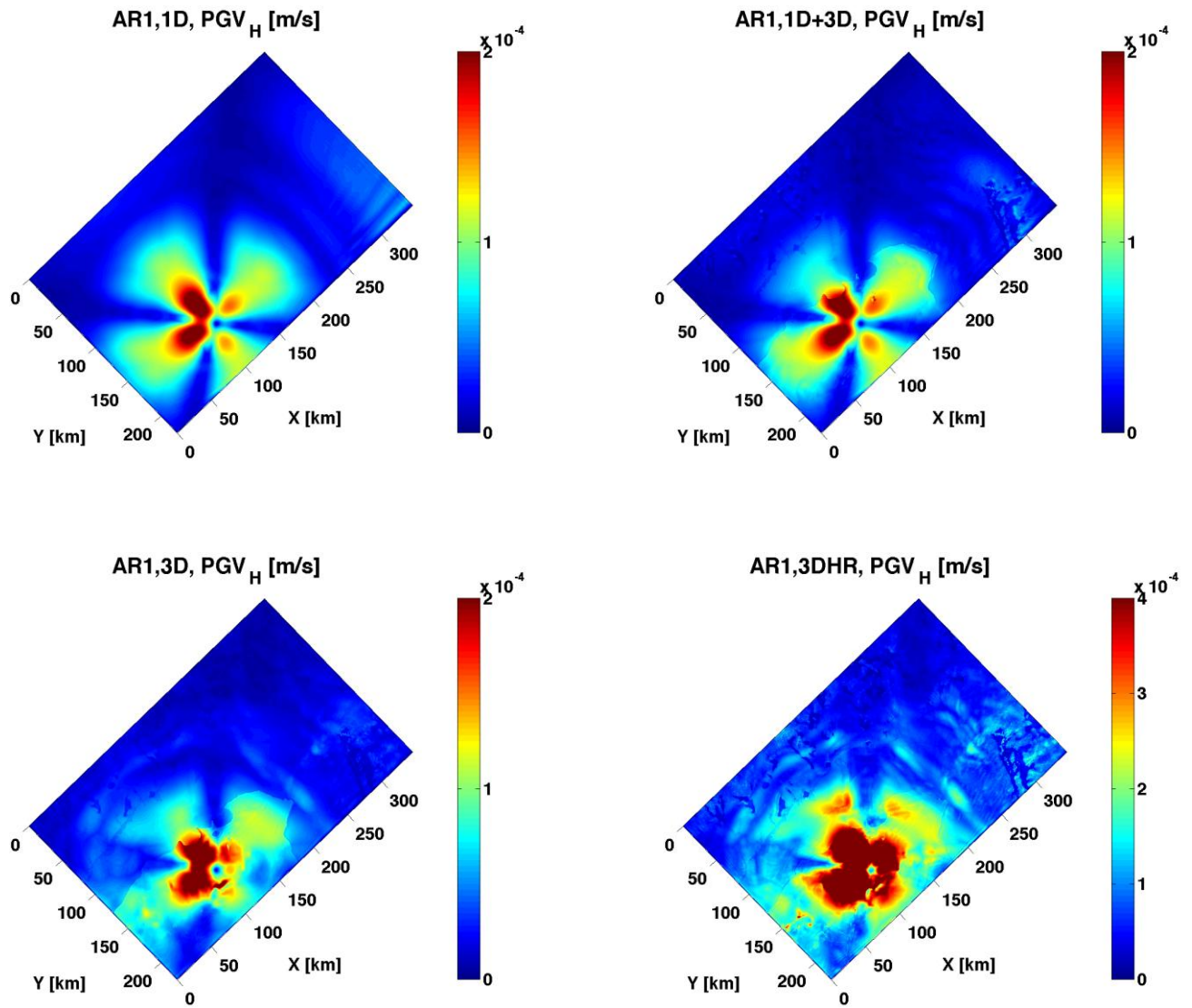


Figure 3. Horizontal peak ground velocity for the AR1 event (see Fig. 1 and Table 1). Results obtained with the 1D velocity model (1D), the 1D velocity model with 3D shallow (above 340 m) structure (1D+3D), and the 3D velocity model (3D) are shown. Also shown is the result for the higher-resolution simulation with the 3D velocity model (3DHR).

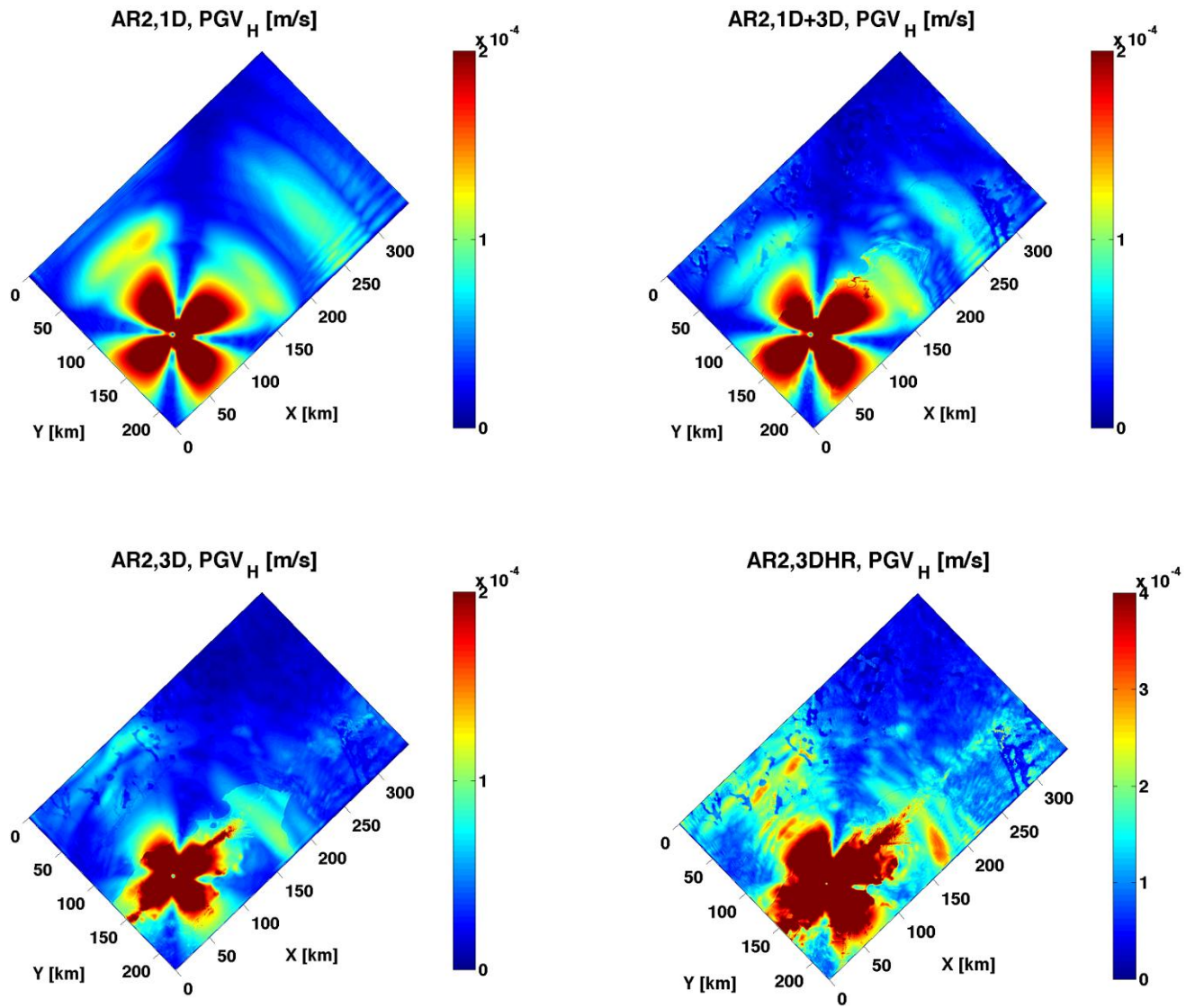


Figure 4. Same as Figure 3, only for the AR2 event (see Fig. 1 and Table 1).

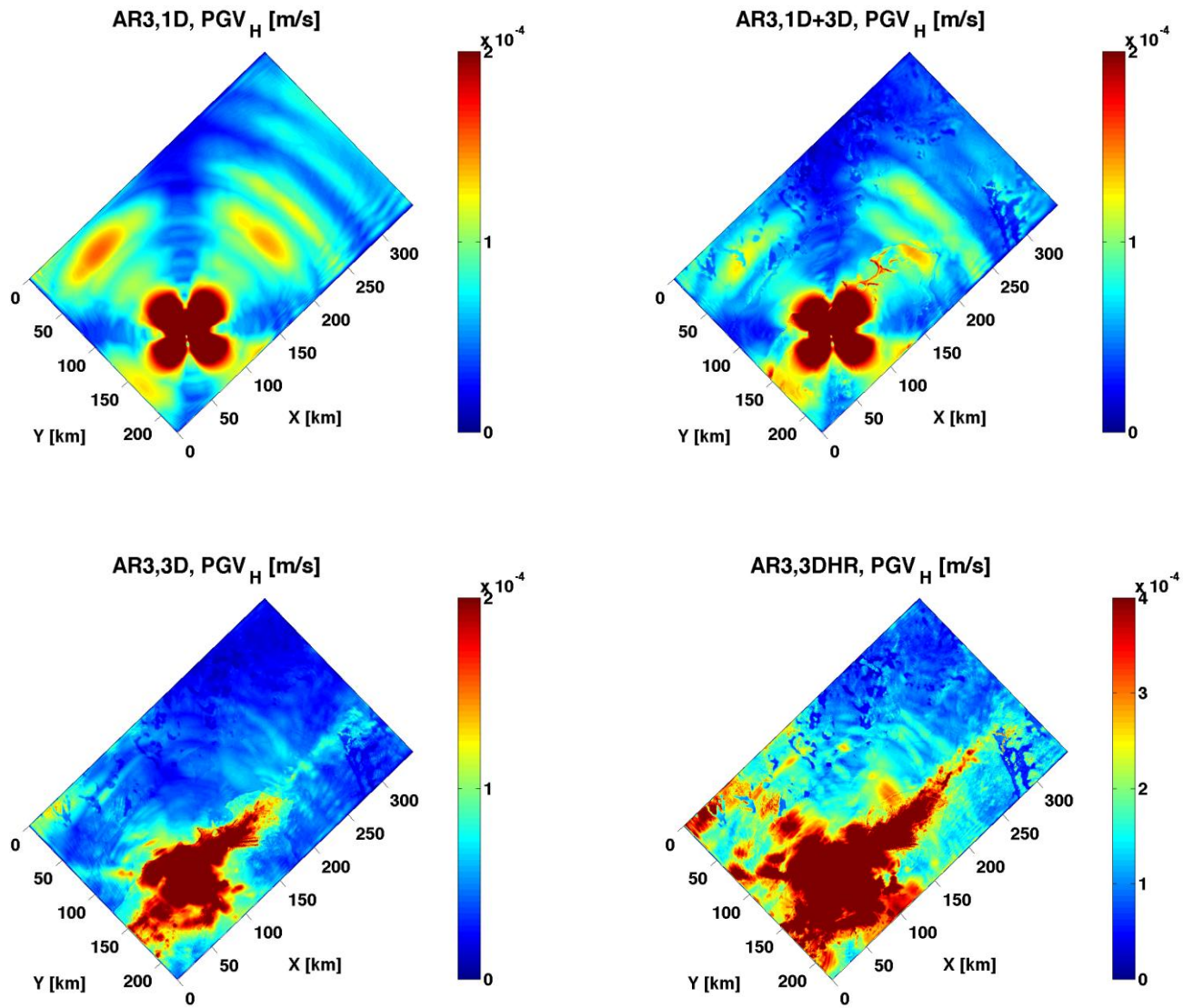


Figure 5. Same as Figure 3, only for the AR3 event (see Fig. 1 and Table 1).

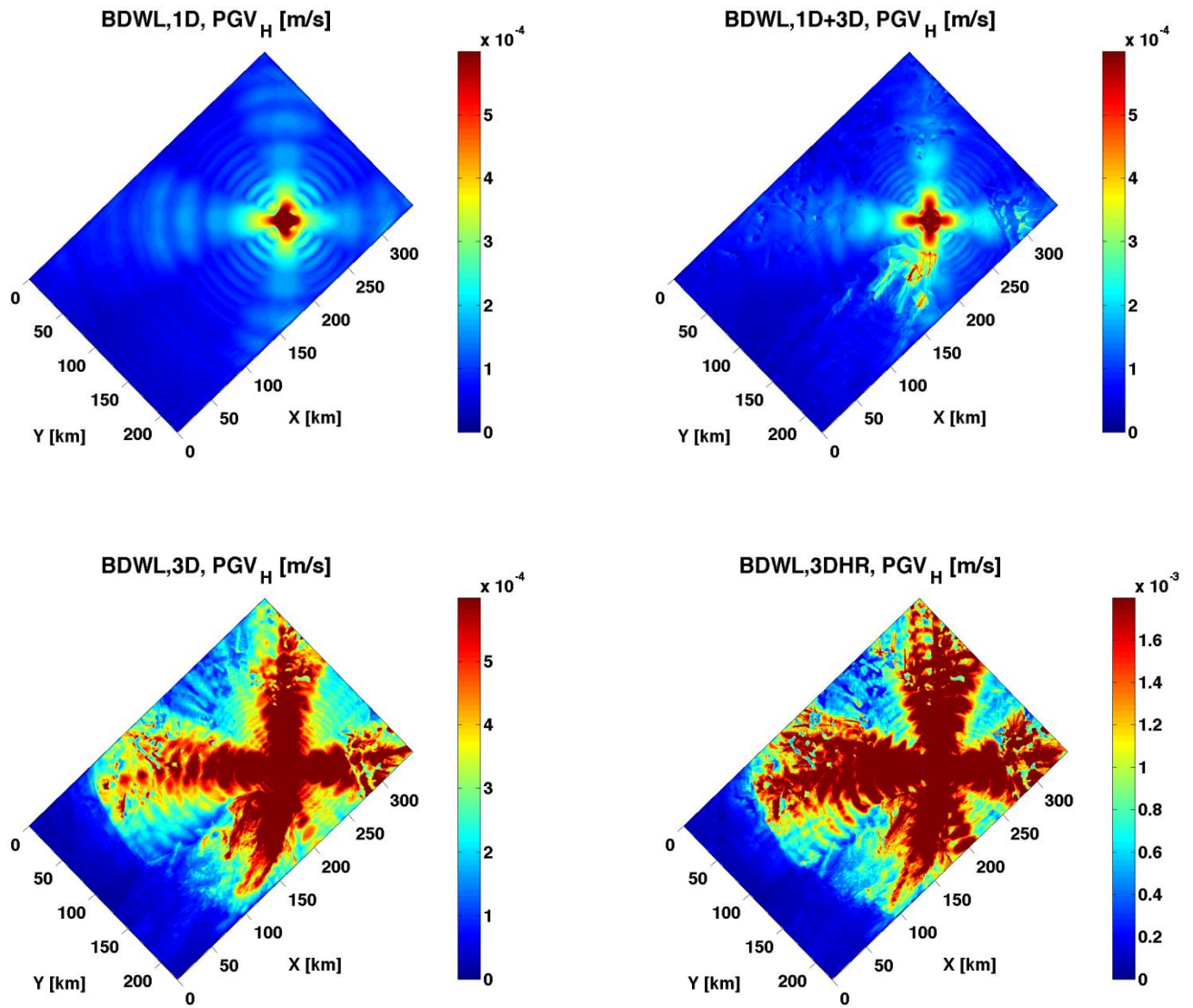


Figure 6. Same as Figure 3, only for the Bardwell (BDWL) event (see Fig. 1 and Table 1).

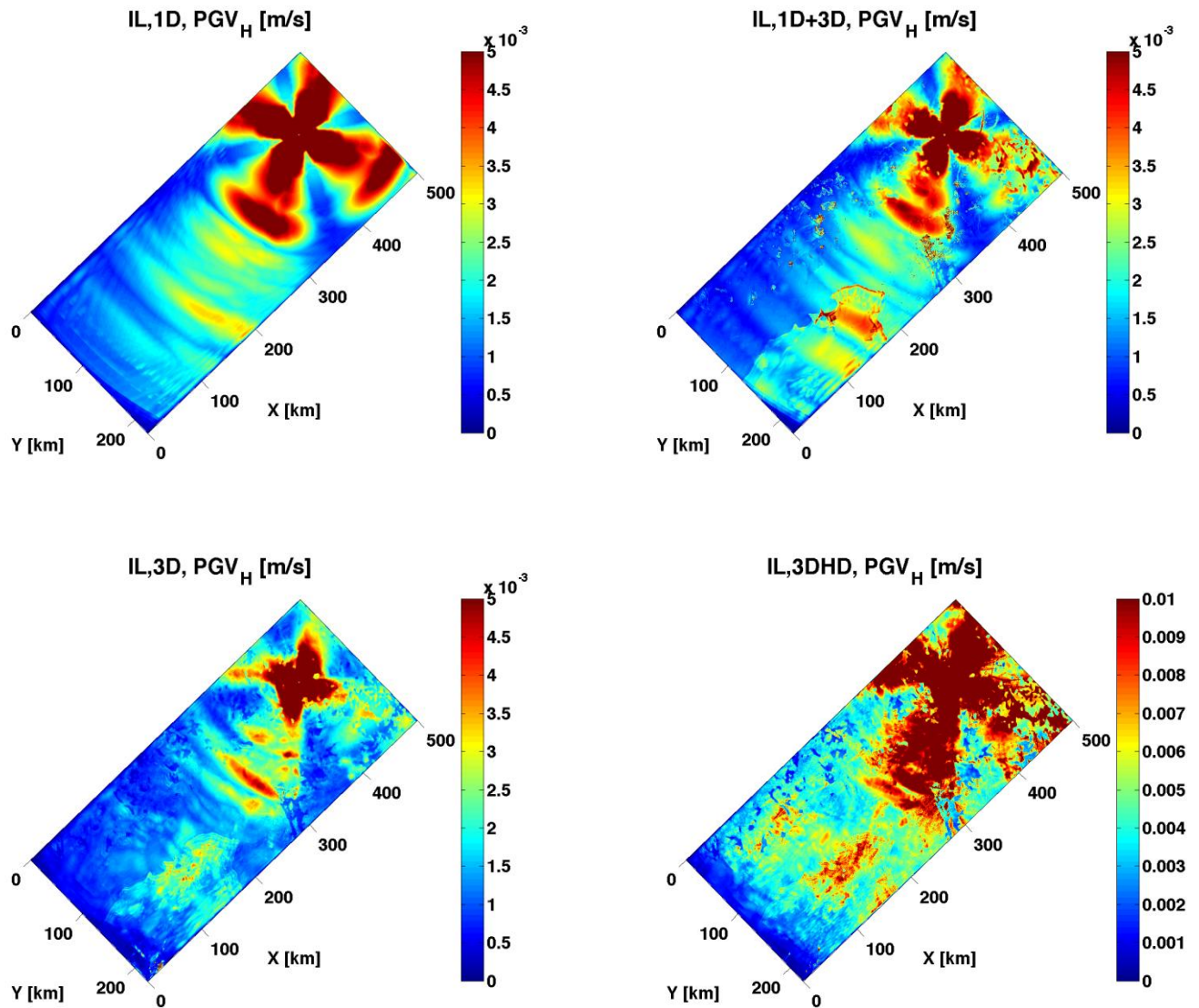
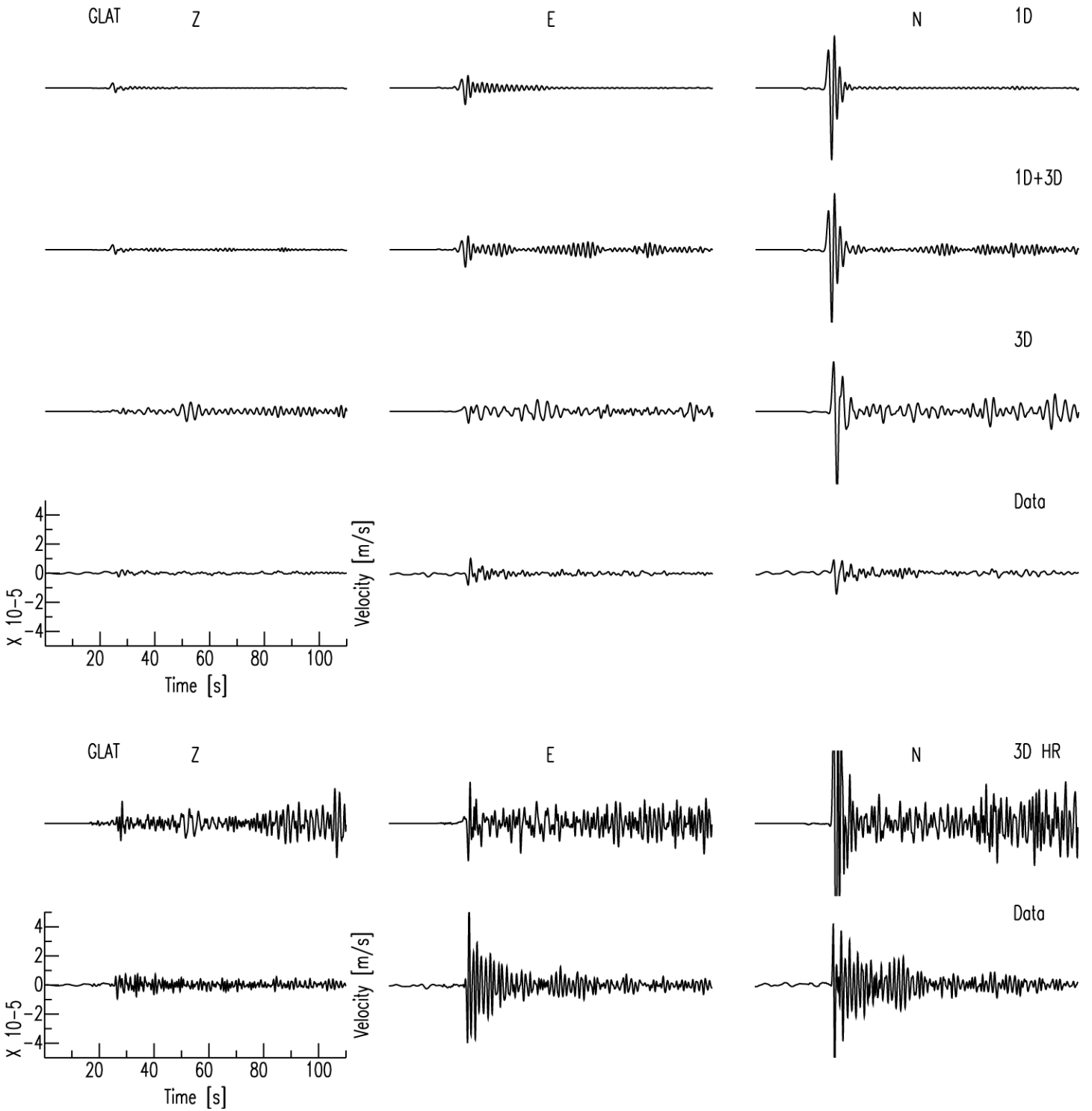
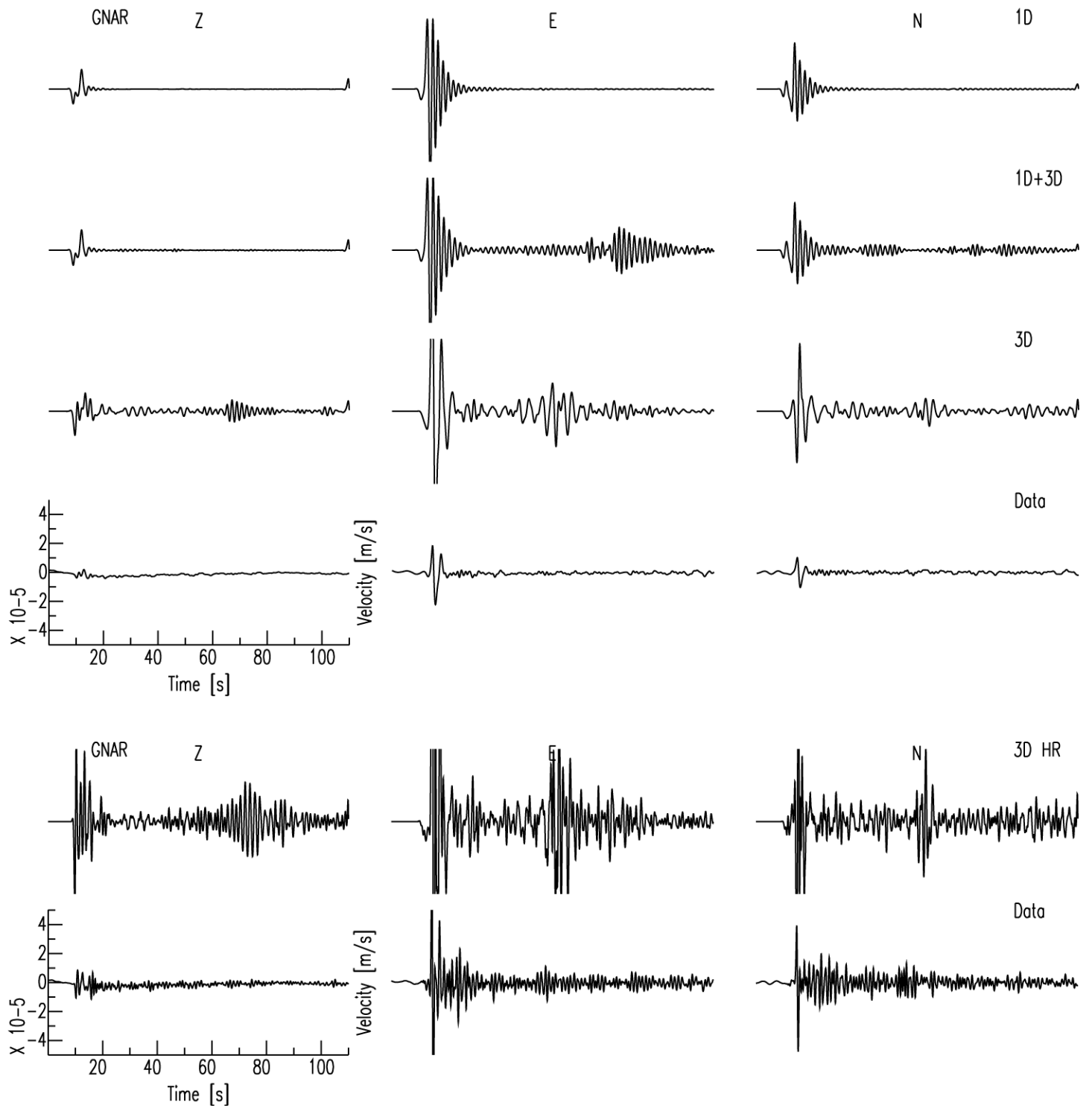


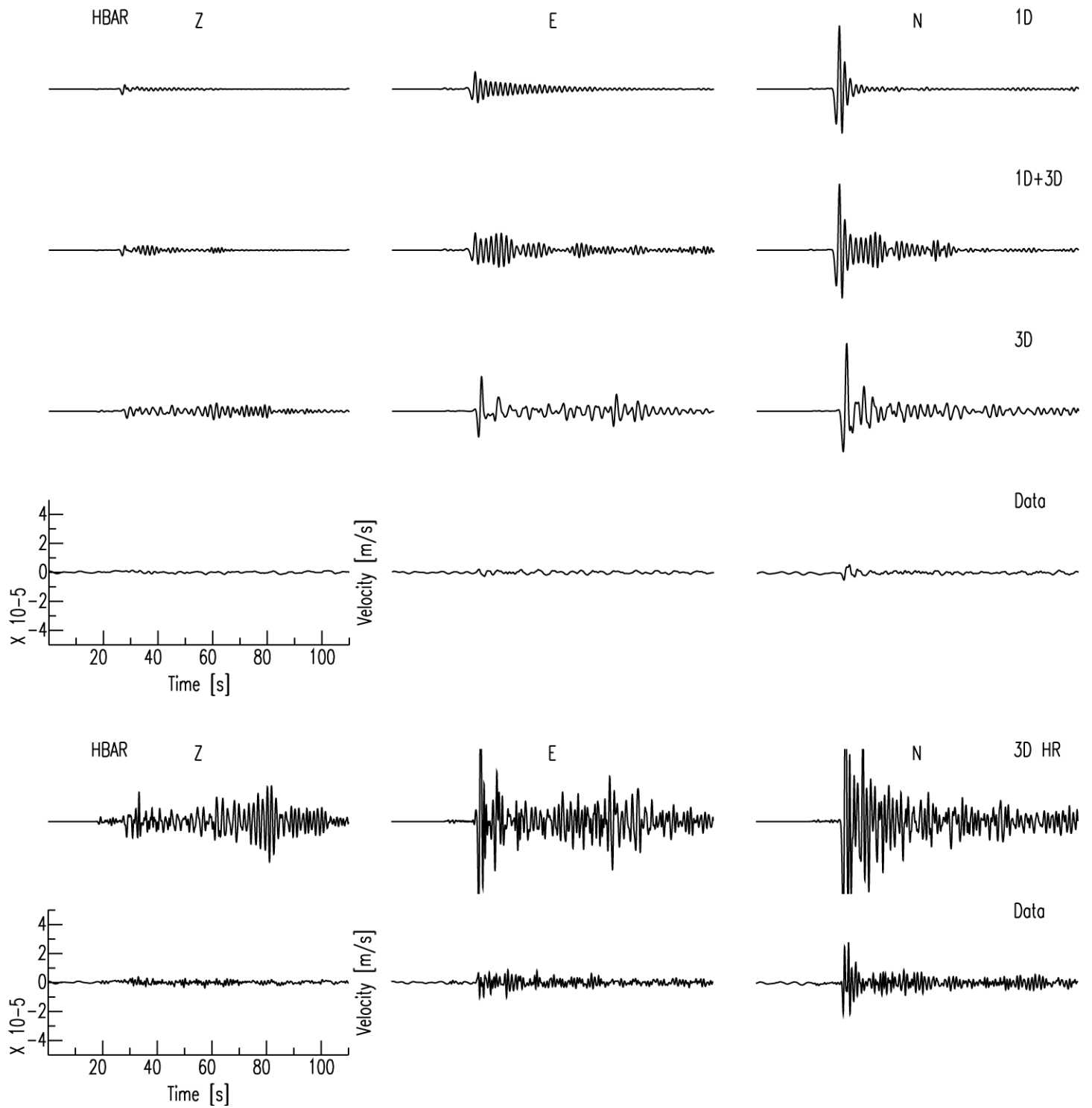
Figure 7. Same as Figure 3, only for the Mt. Carmel (IL) event (see Fig. 1 and Table 1). Note that a larger velocity model was used for this event (see Fig. 1).

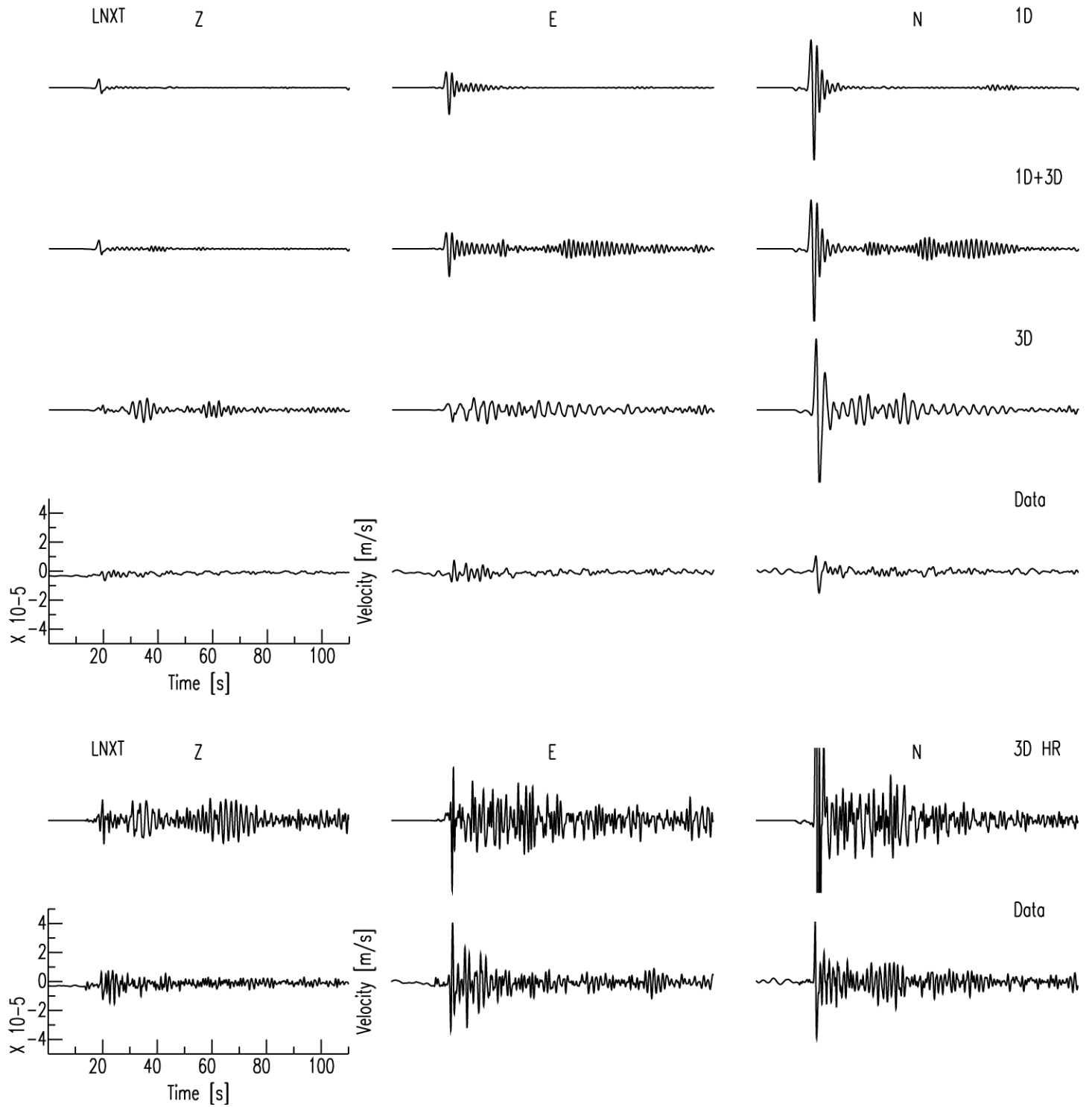
Figure 8 (next pages). Simulated and observed waveforms for the events AR1 (pages X-Y), AR2 (pages ), AR3 (pages ), BDWL (pages ), and IL (pages ). Columns show results for the vertical and the two horizontal components. Top three rows show results obtained with the 1D, 1D+3D, and 3D models (see section “Velocity Models” for details). The fourth row shows observations. Waveforms in top four rows were low-pass filtered at 0.5 Hz. The same scale was used for the top four rows for all three AR events to enable direct comparison of the waveforms. Bottom two rows show synthetics obtained with the higher-resolution 3D model (3DHR) and observations. Waveforms in bottom two rows were low-pass filtered at 1 Hz.

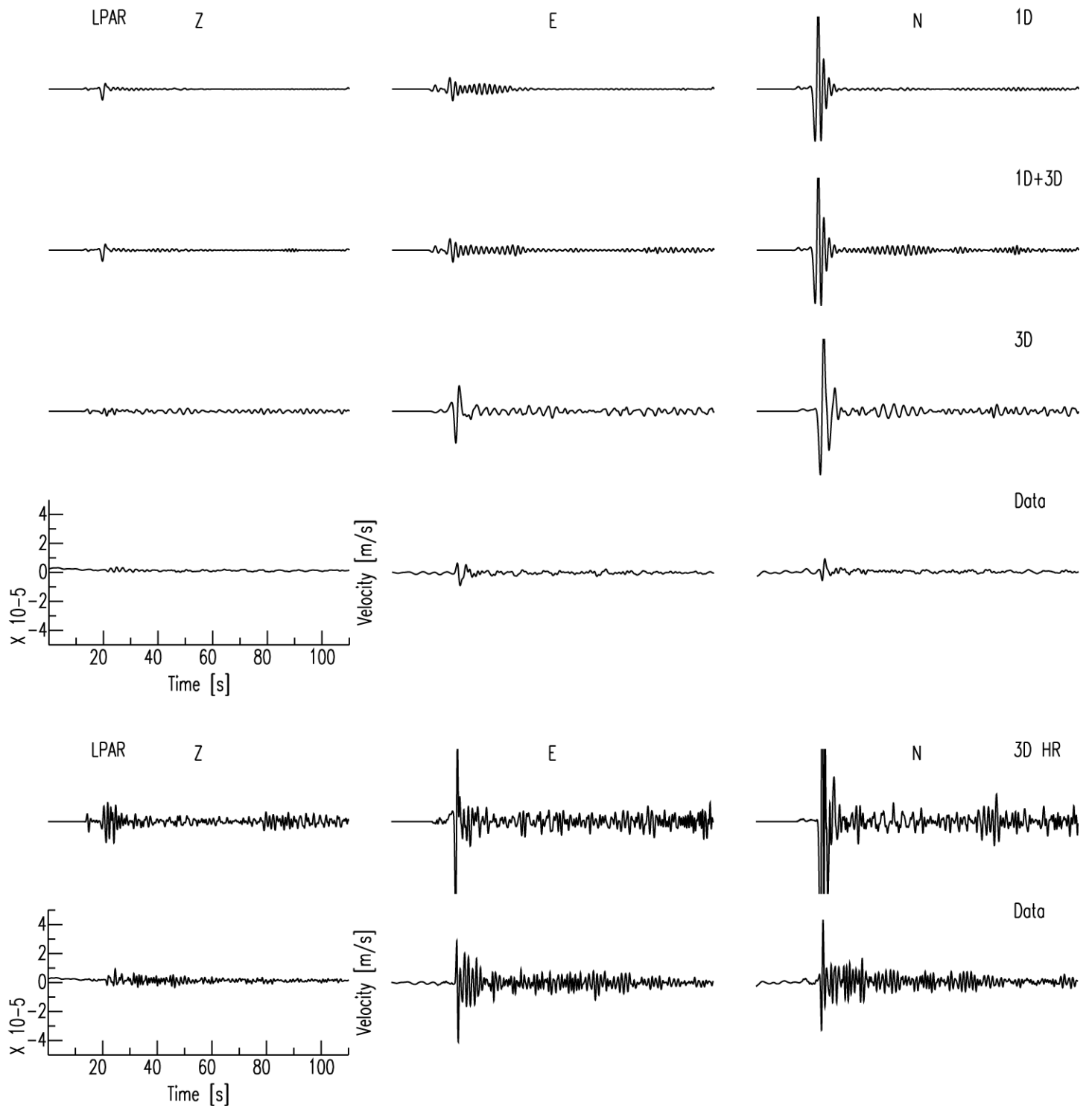




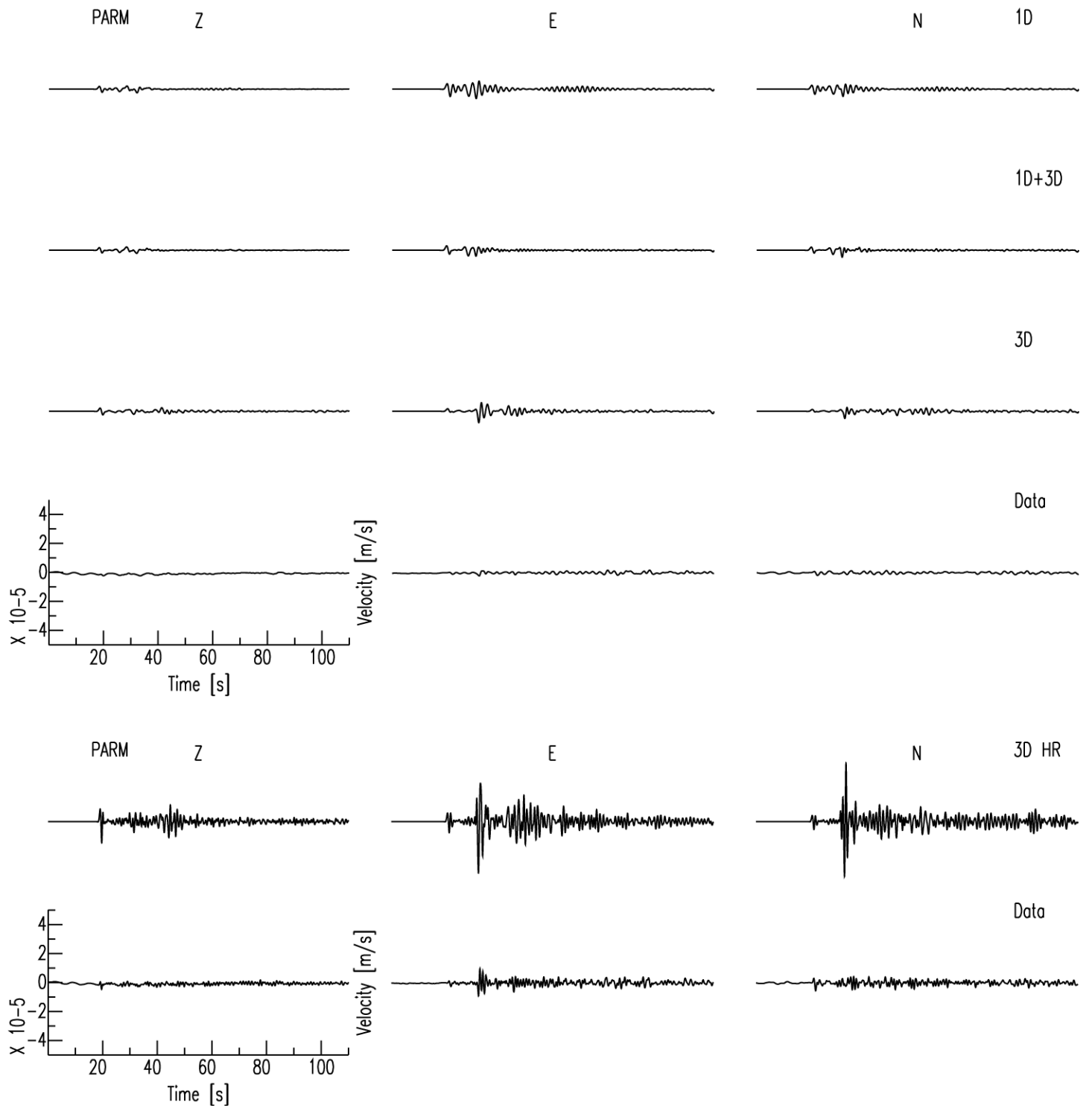
AR1

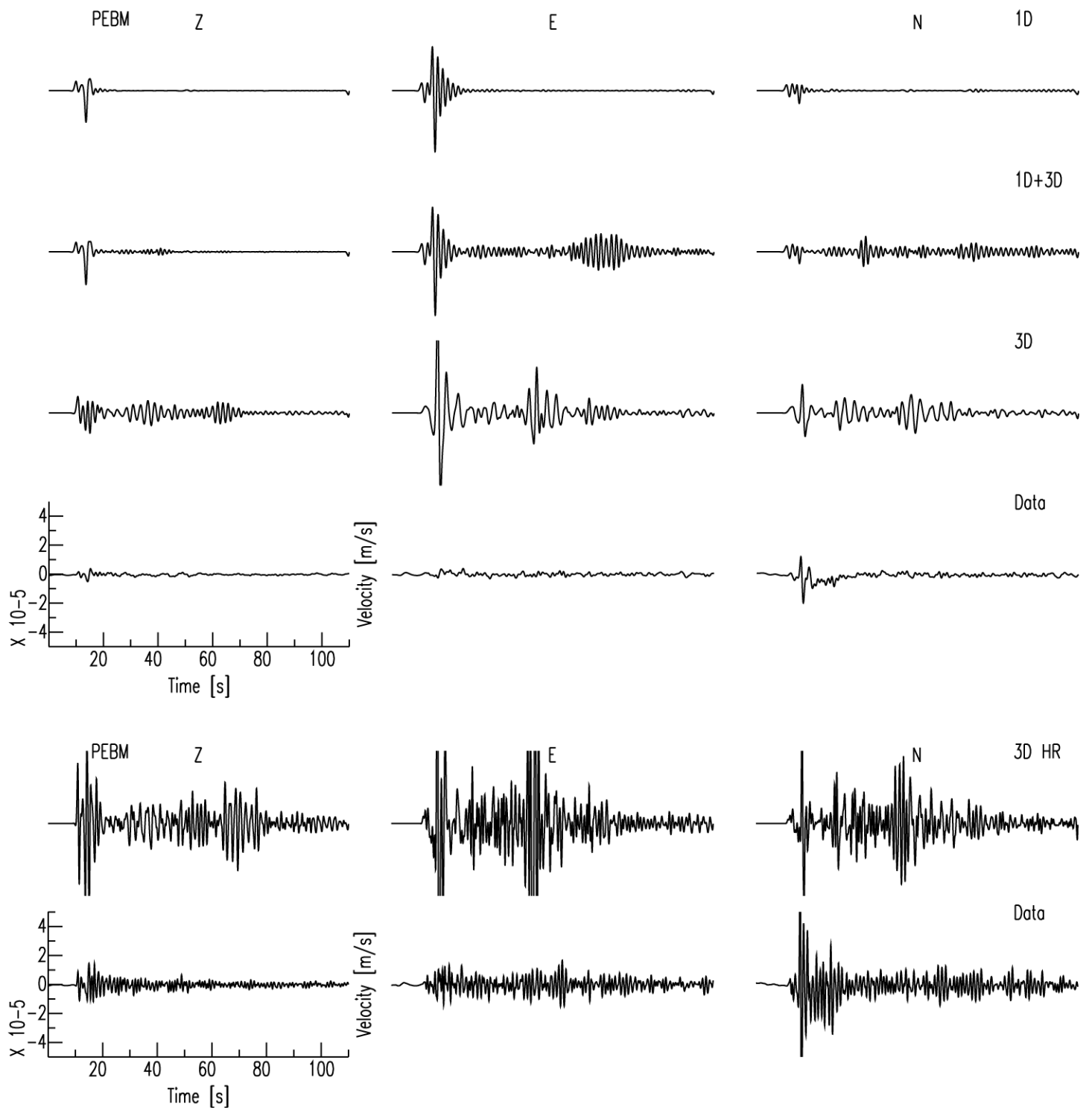




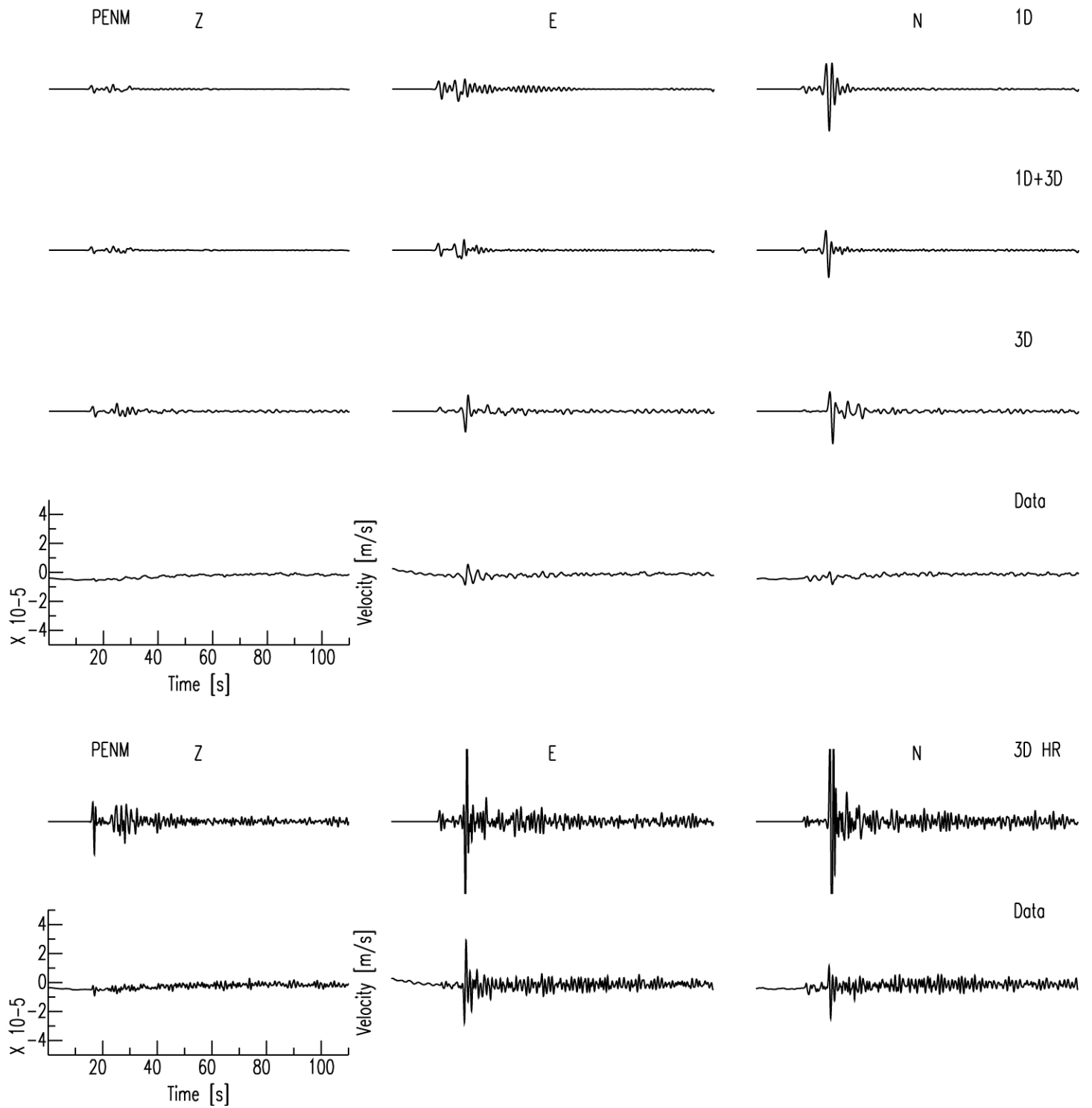


AR1

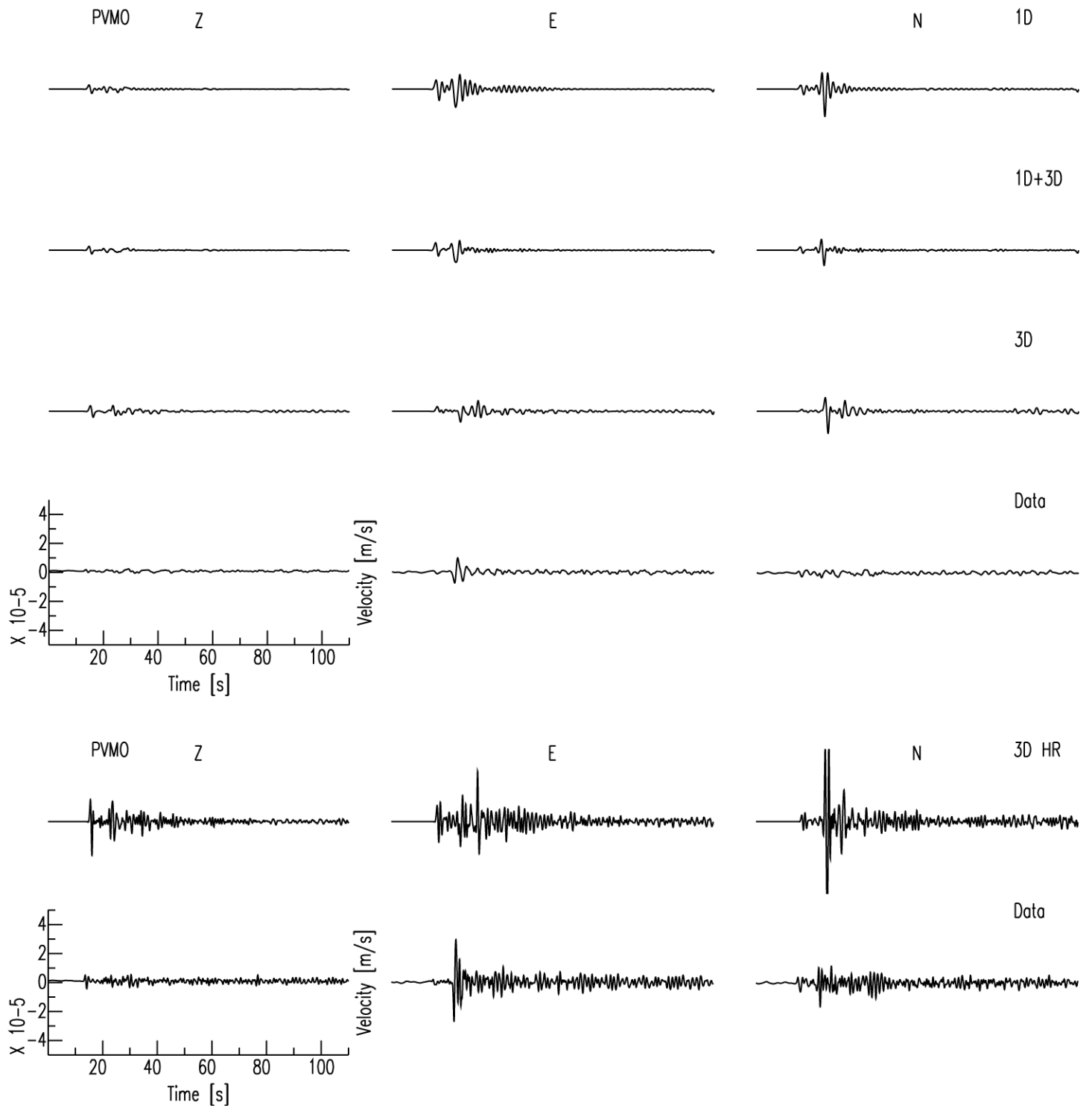




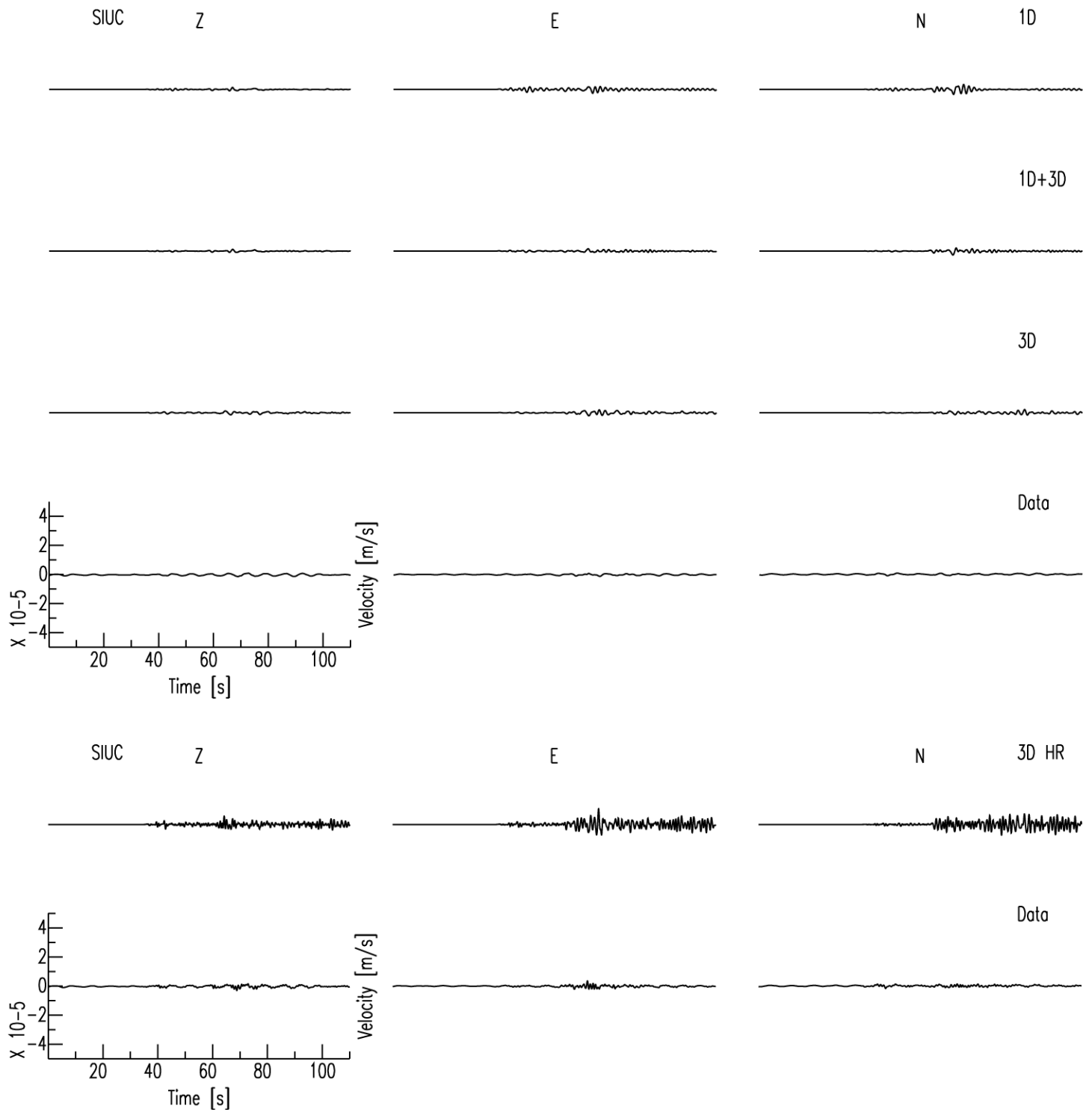
AR1

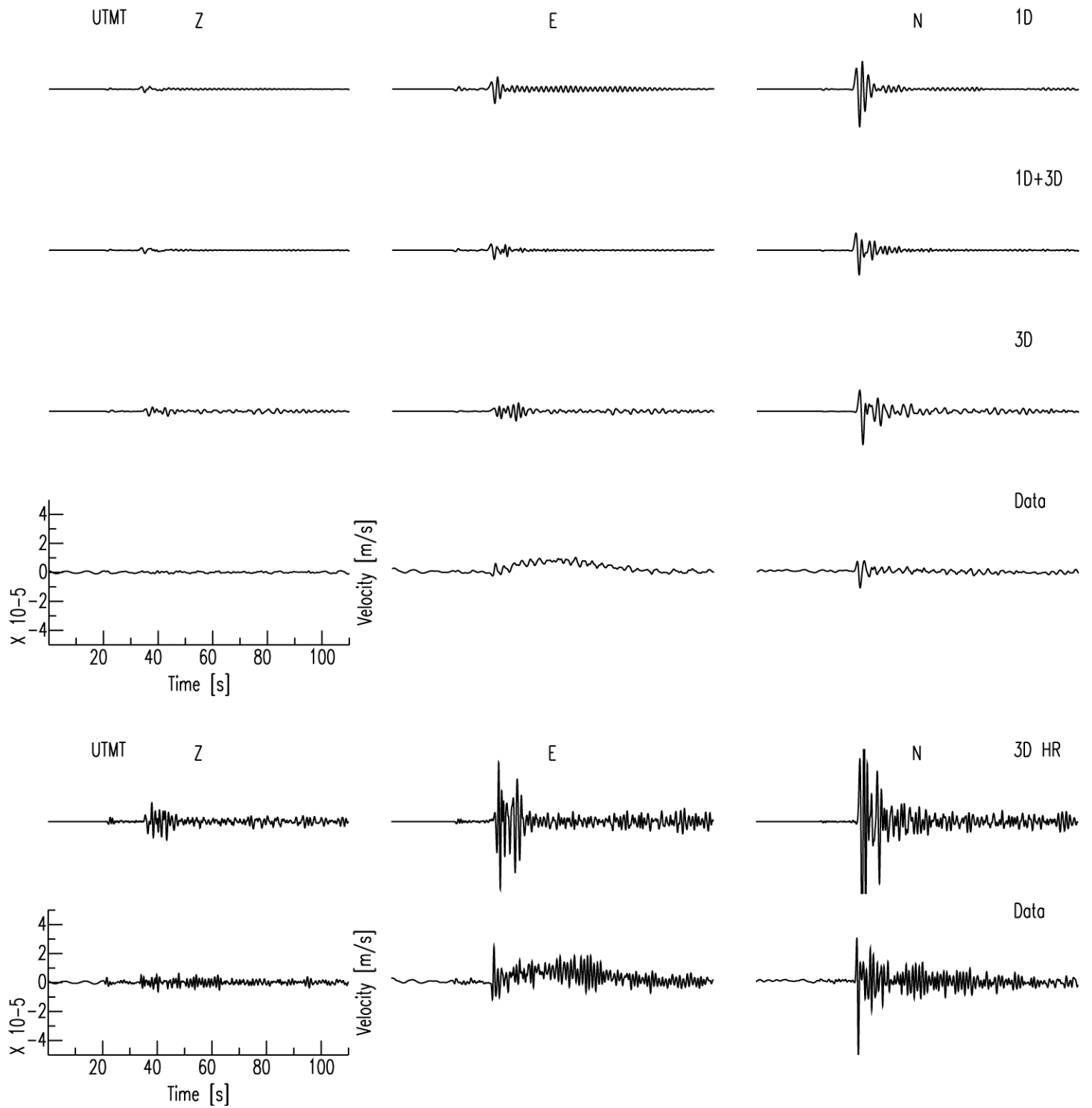


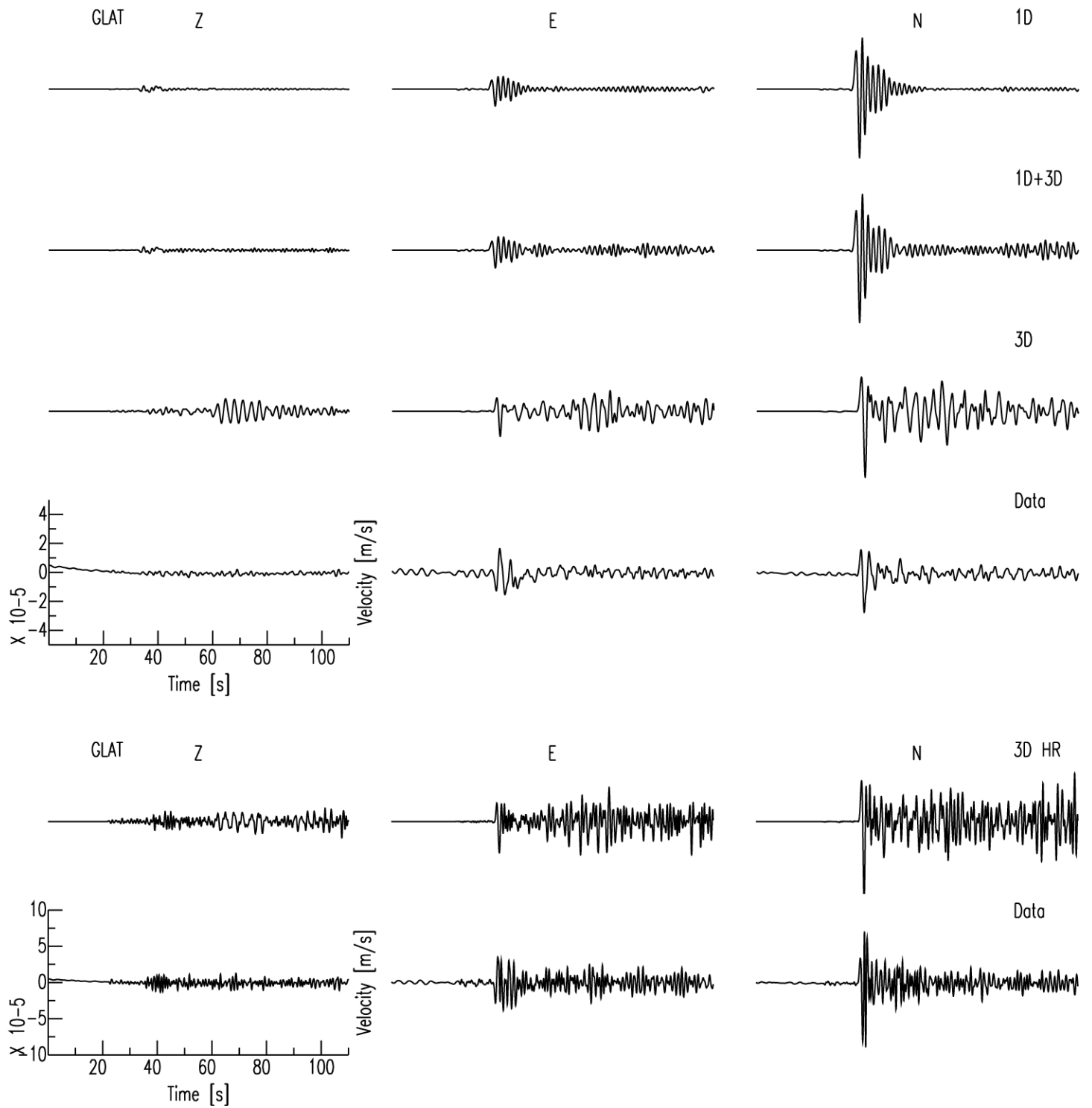
AR1

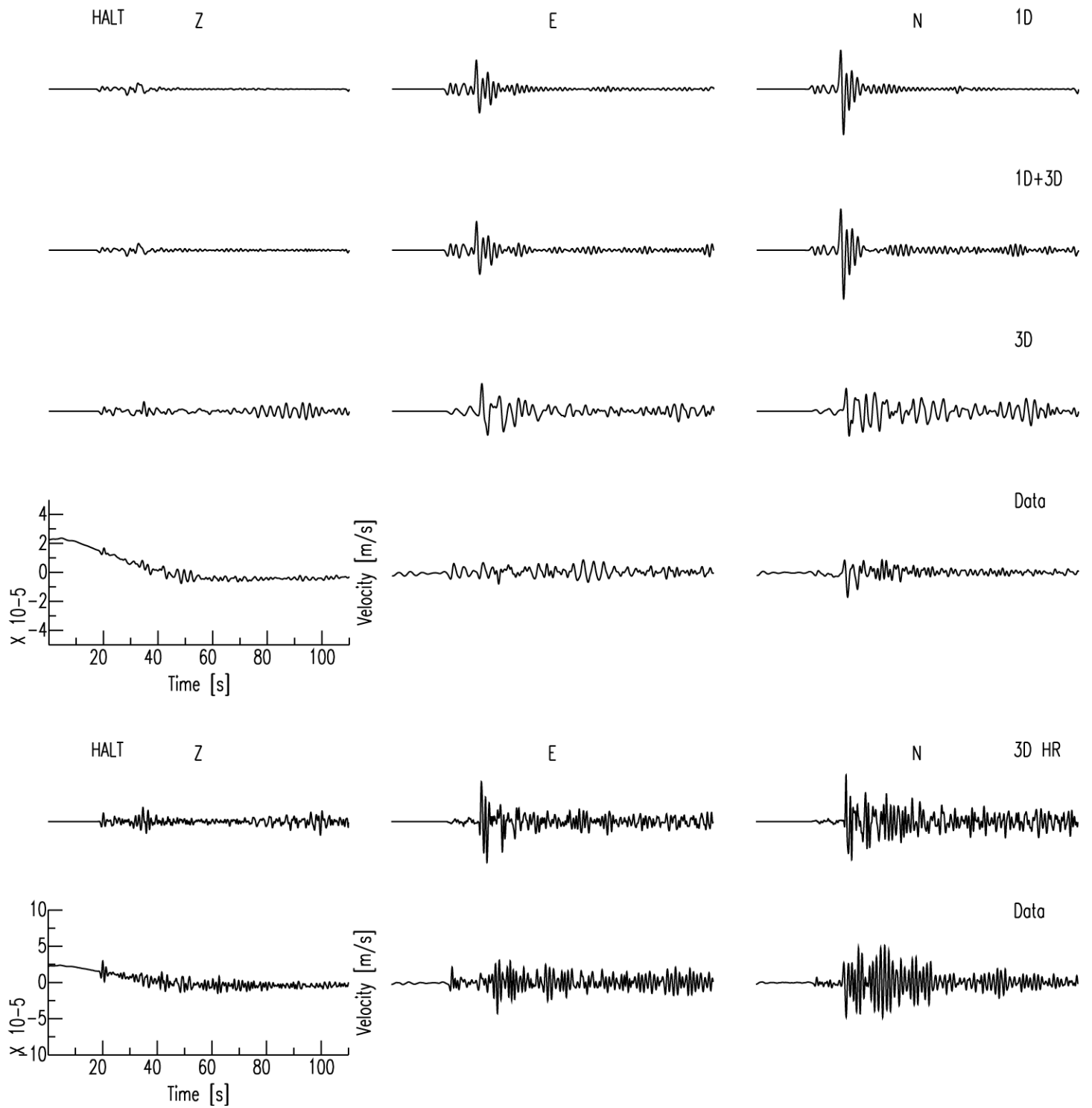


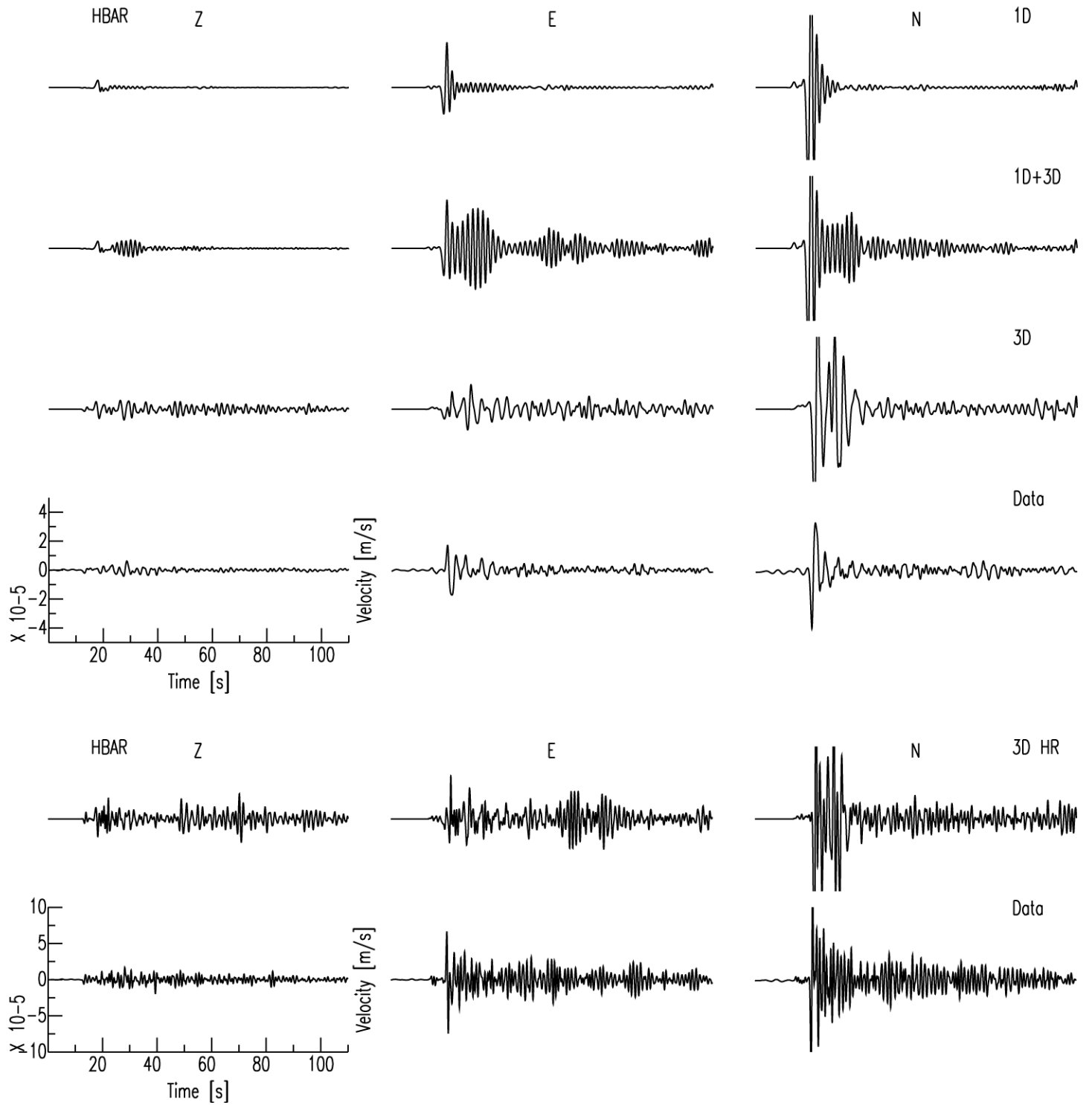
AR1

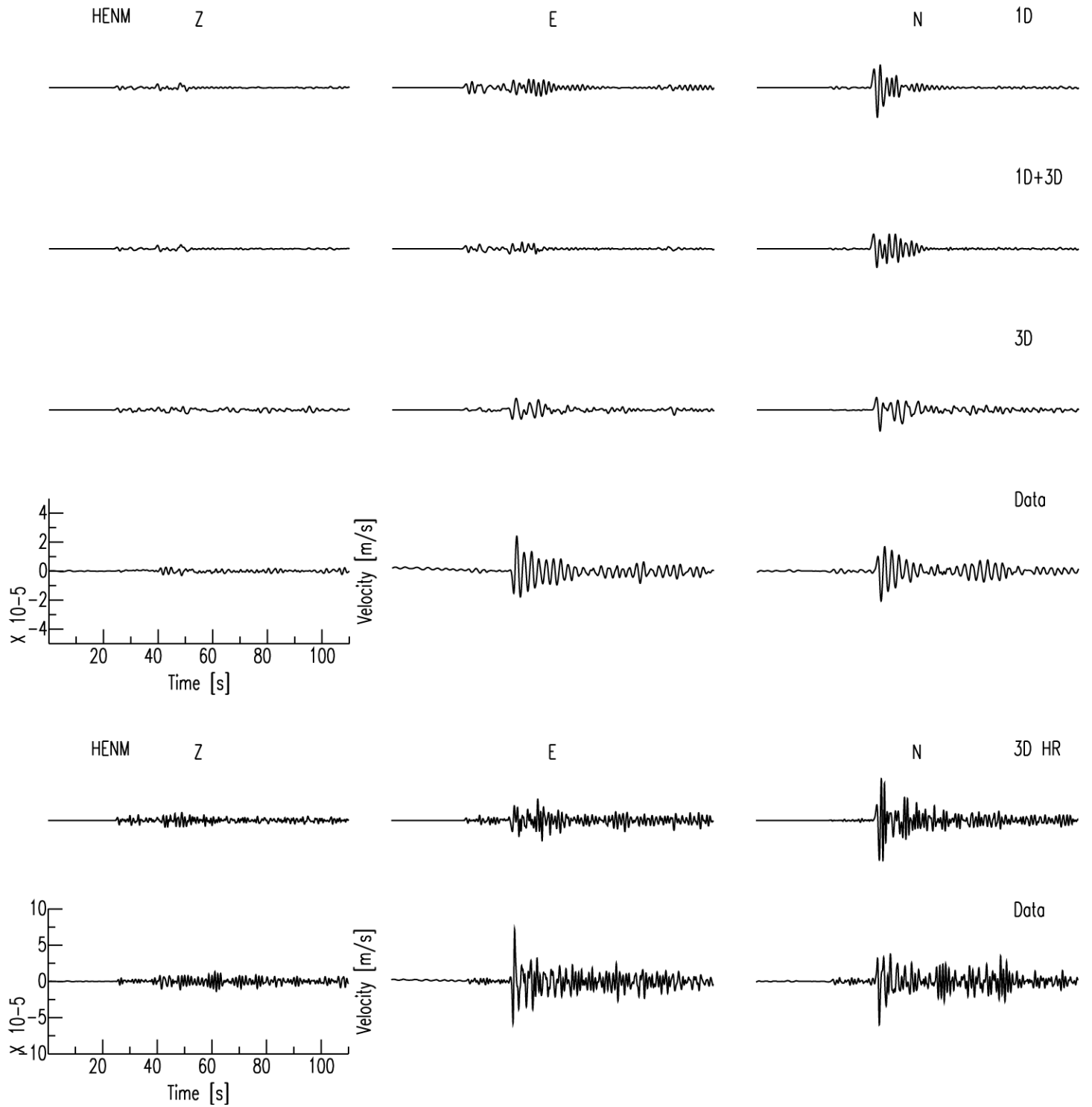


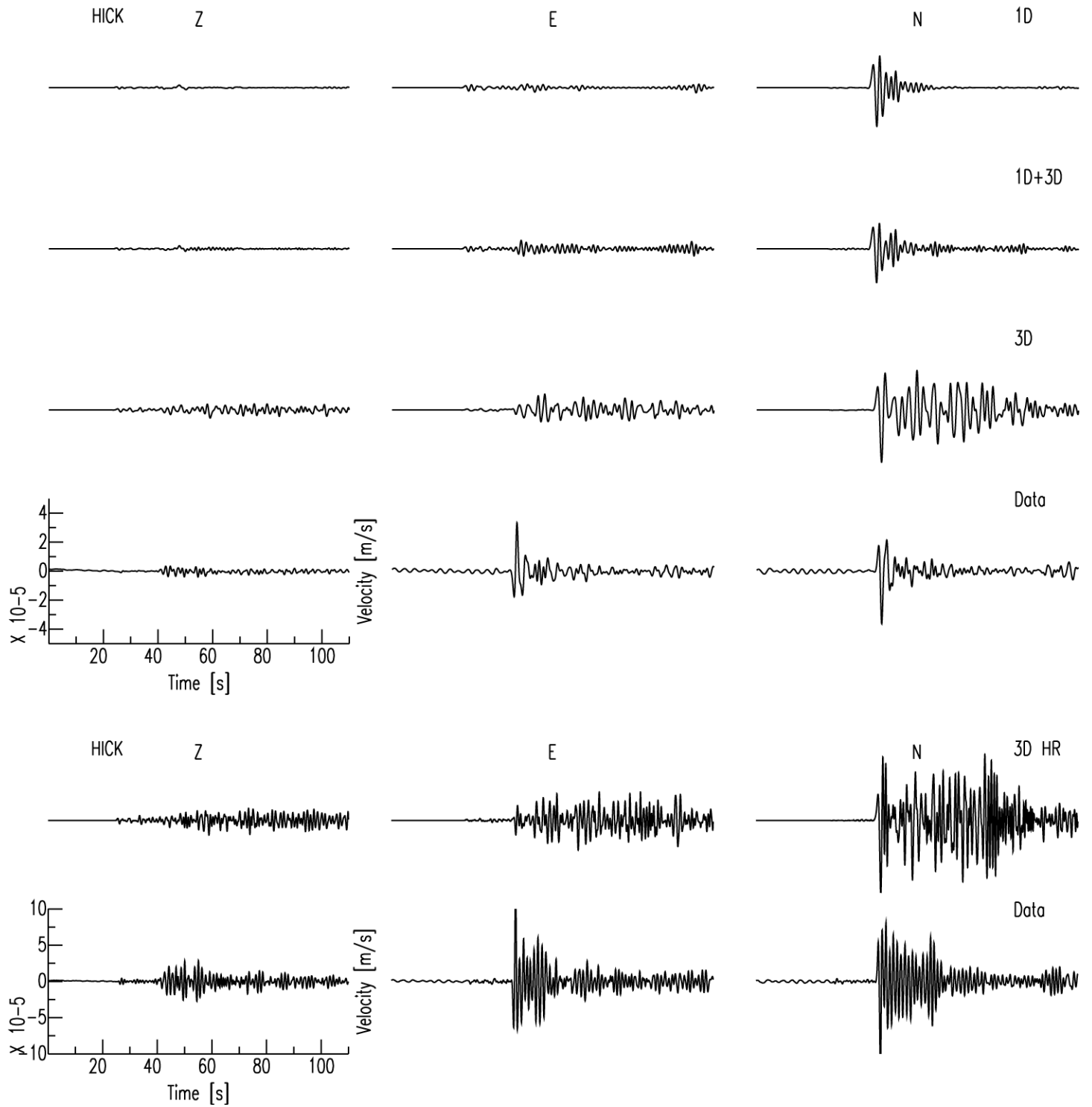


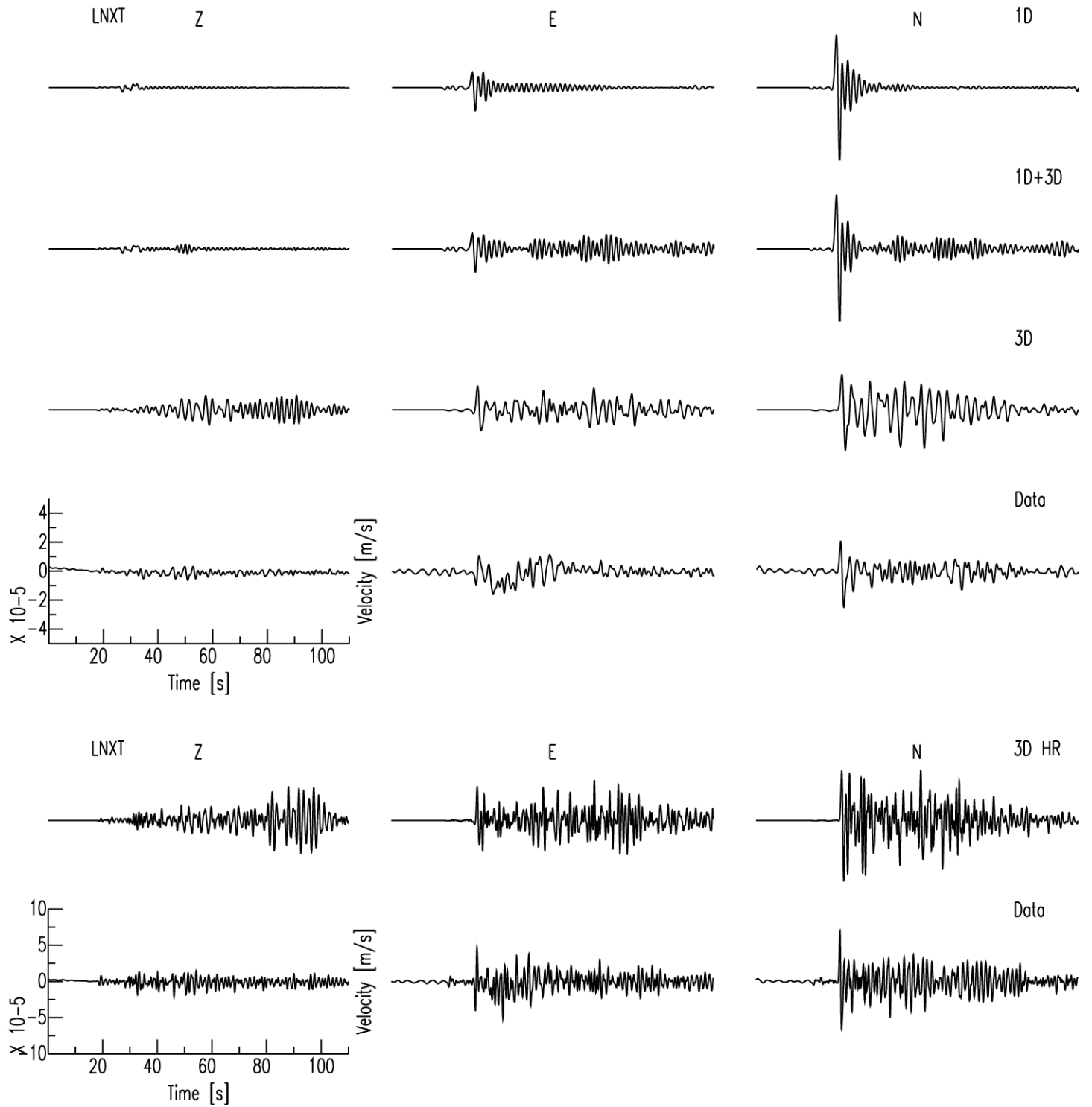


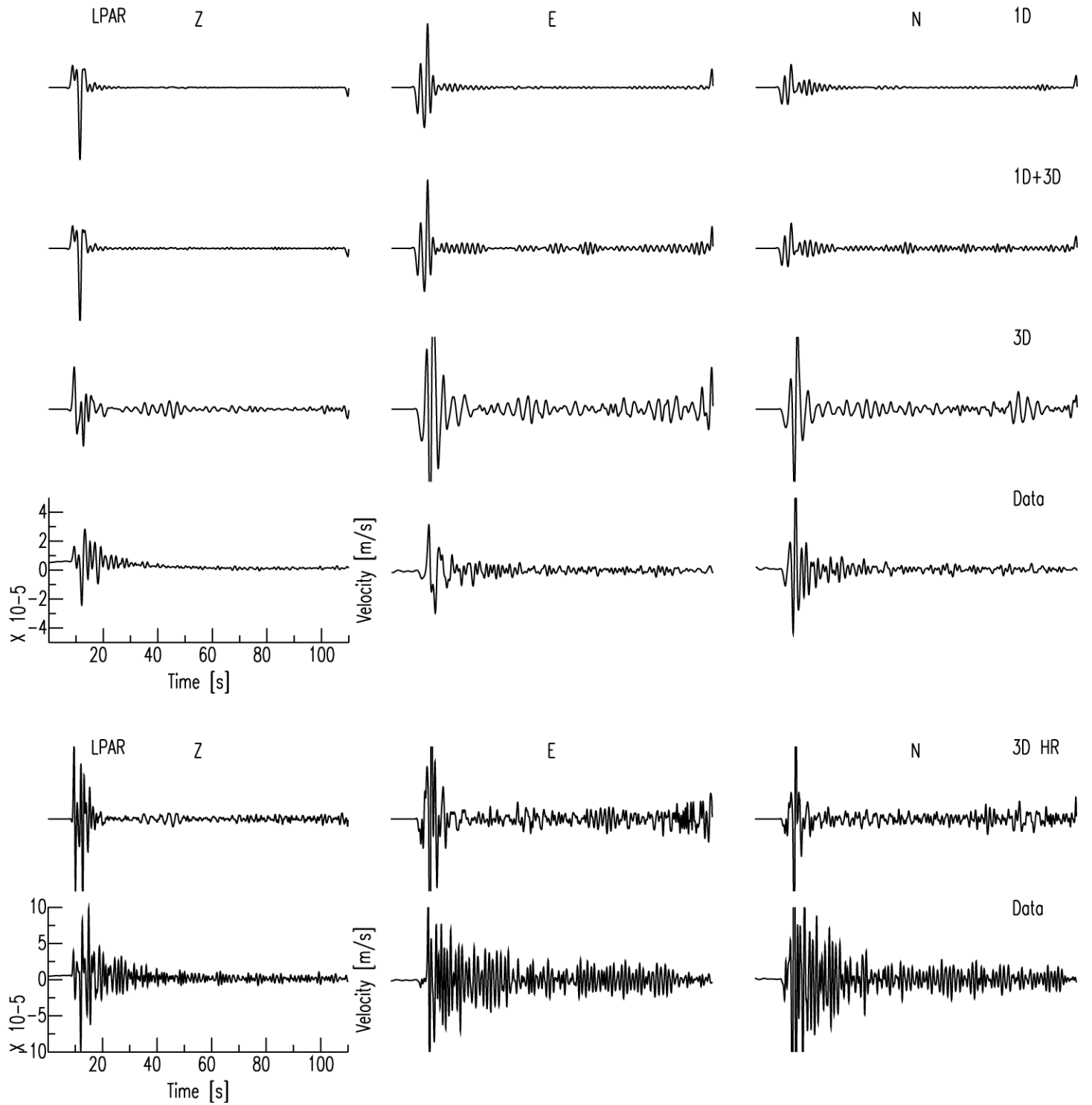


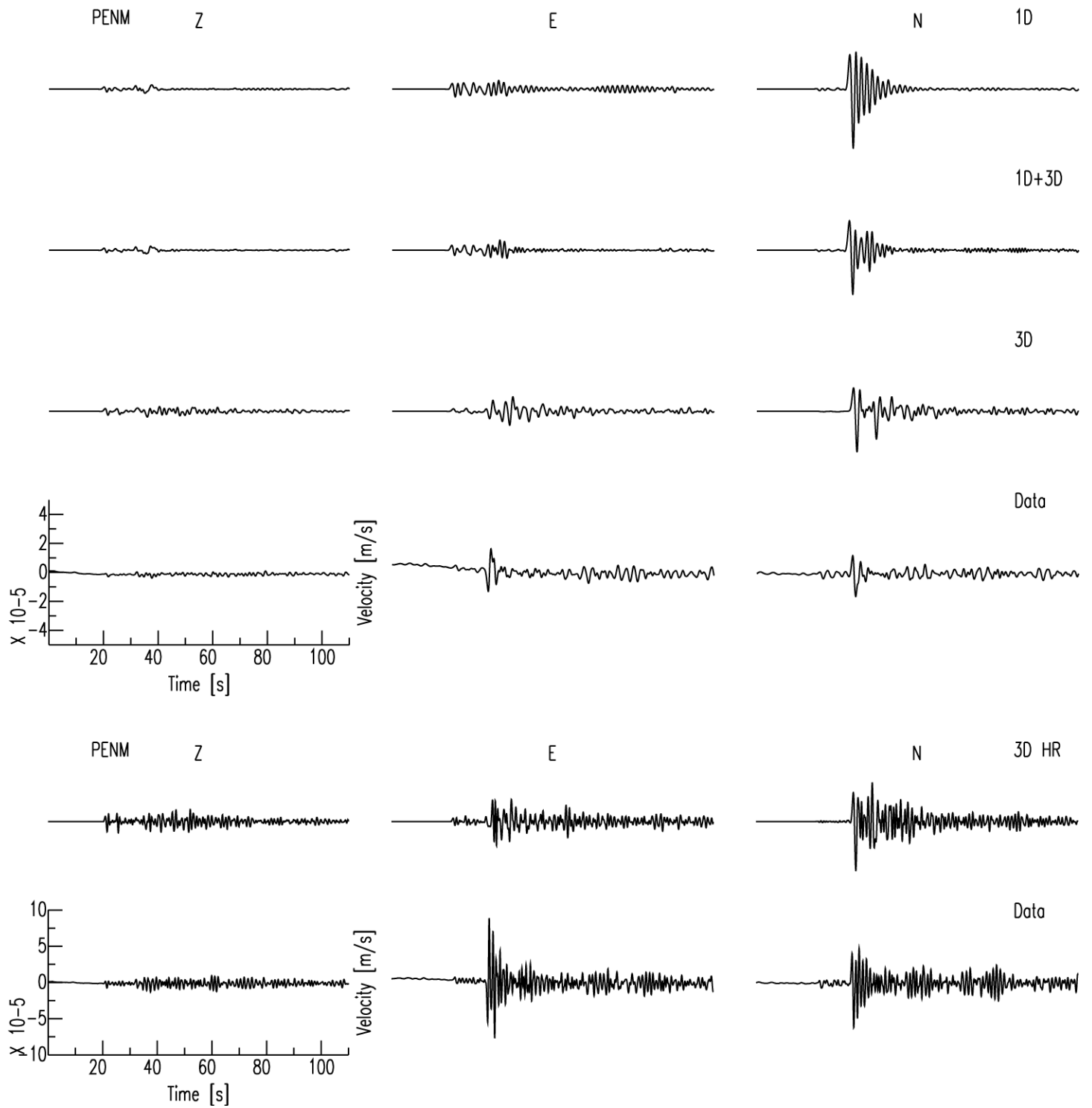


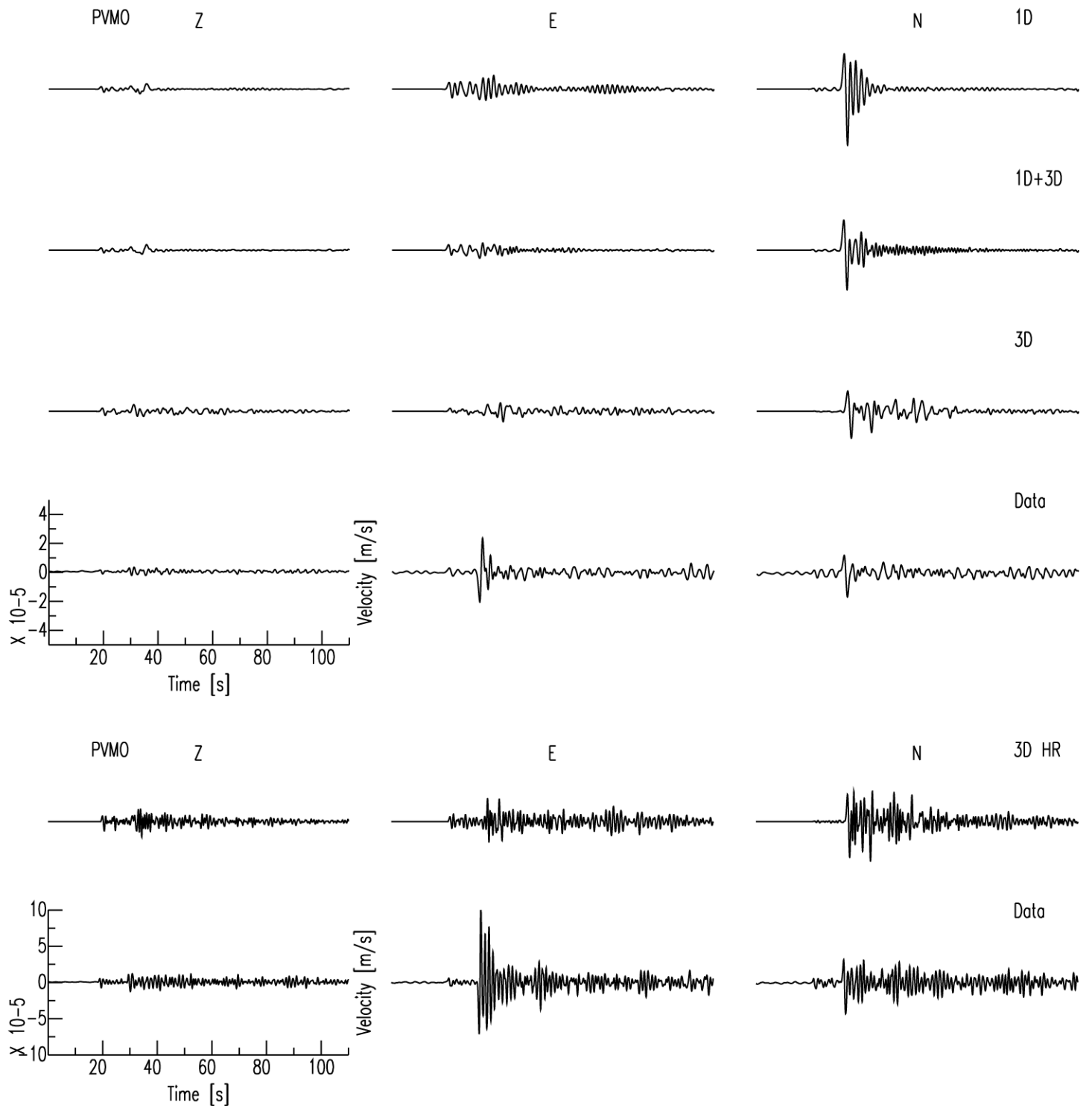


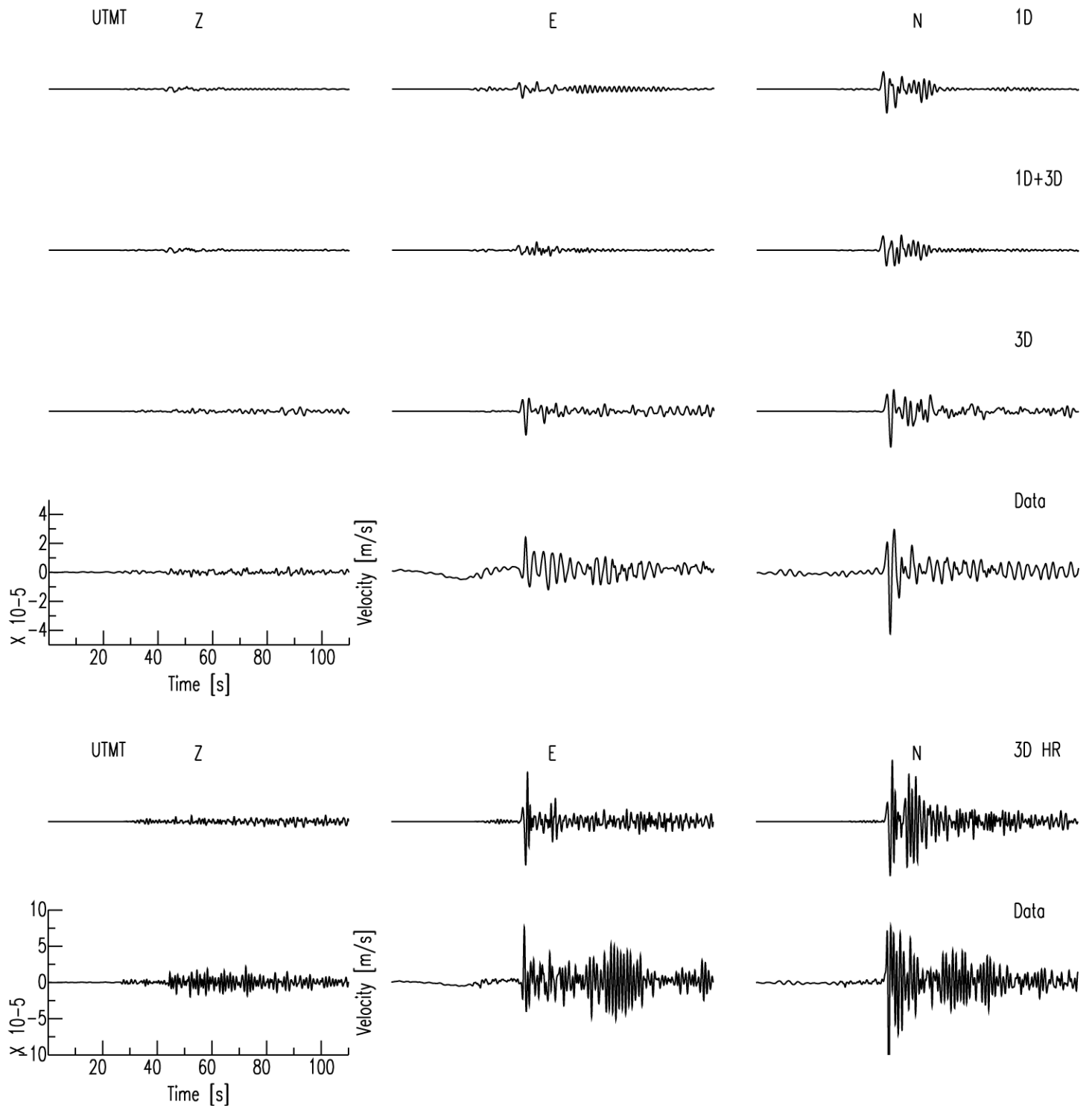


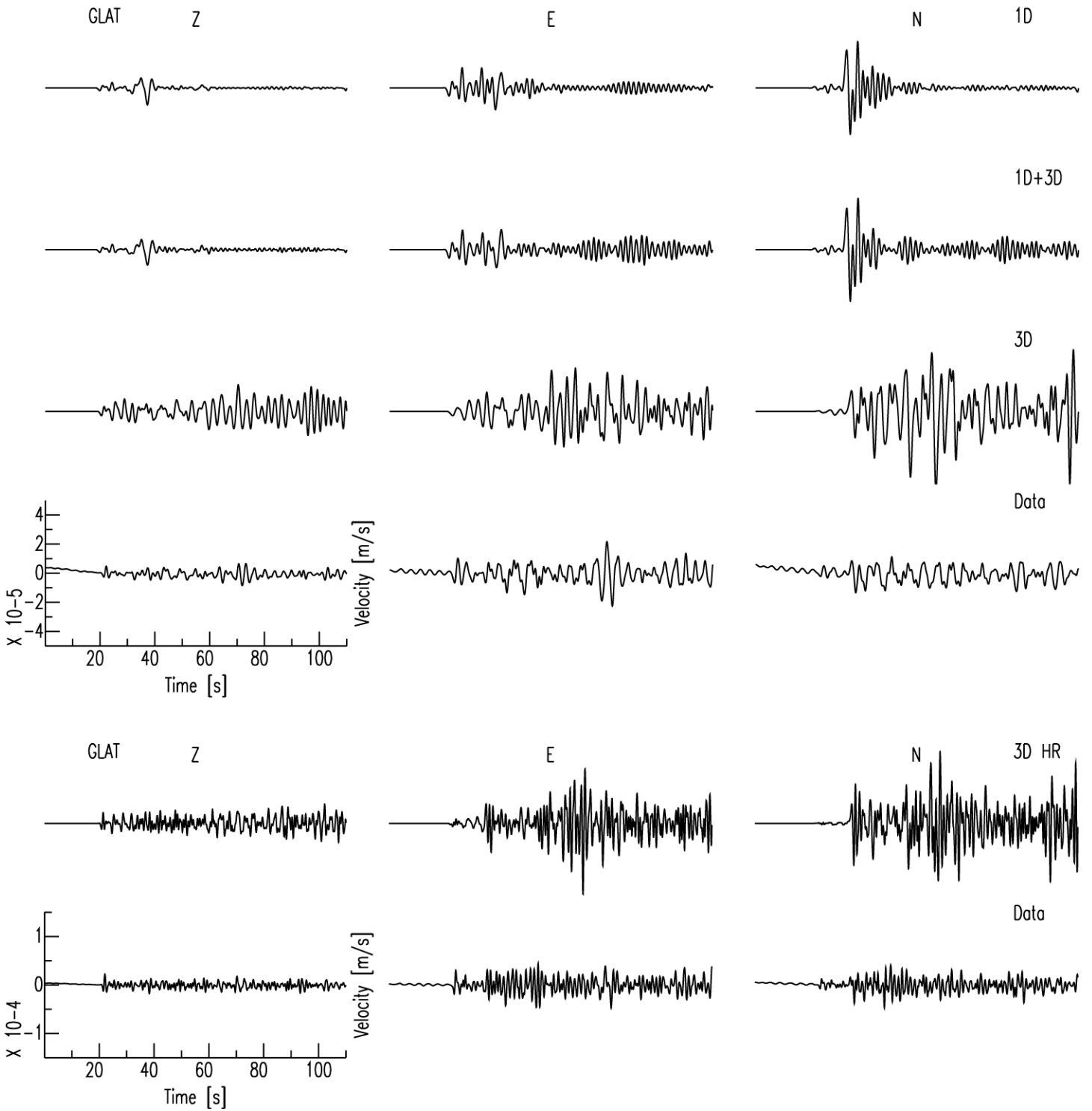


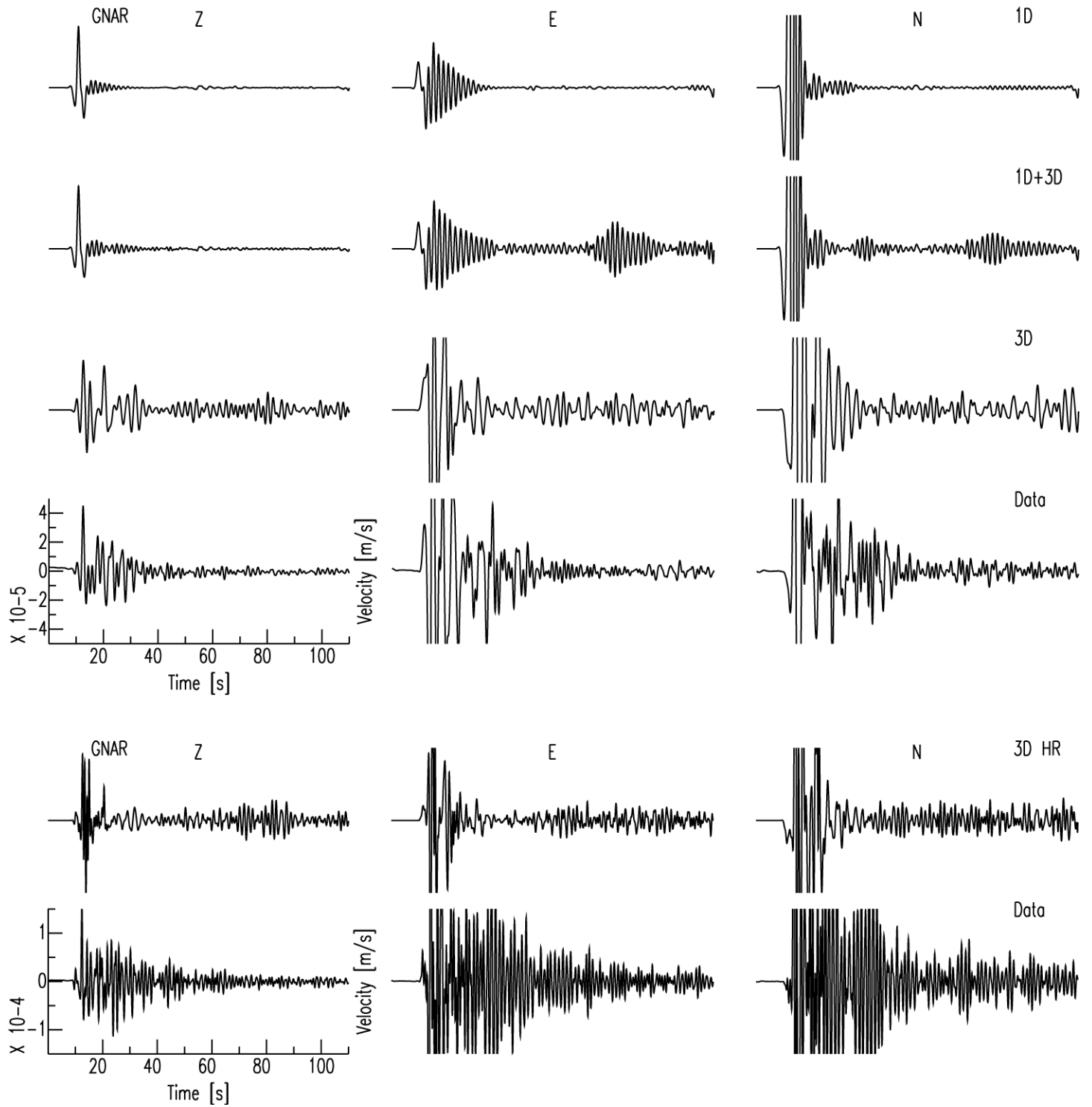


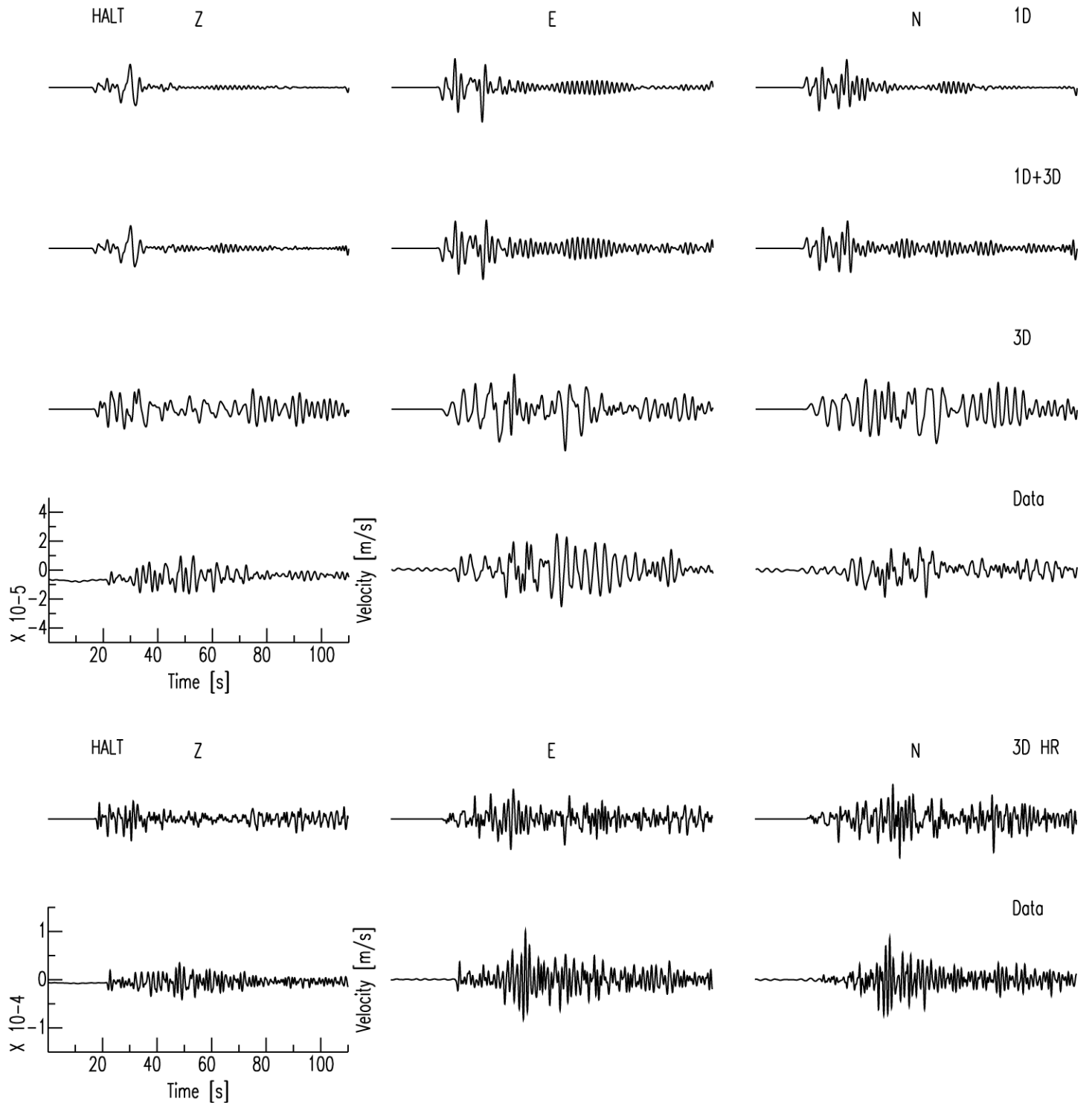


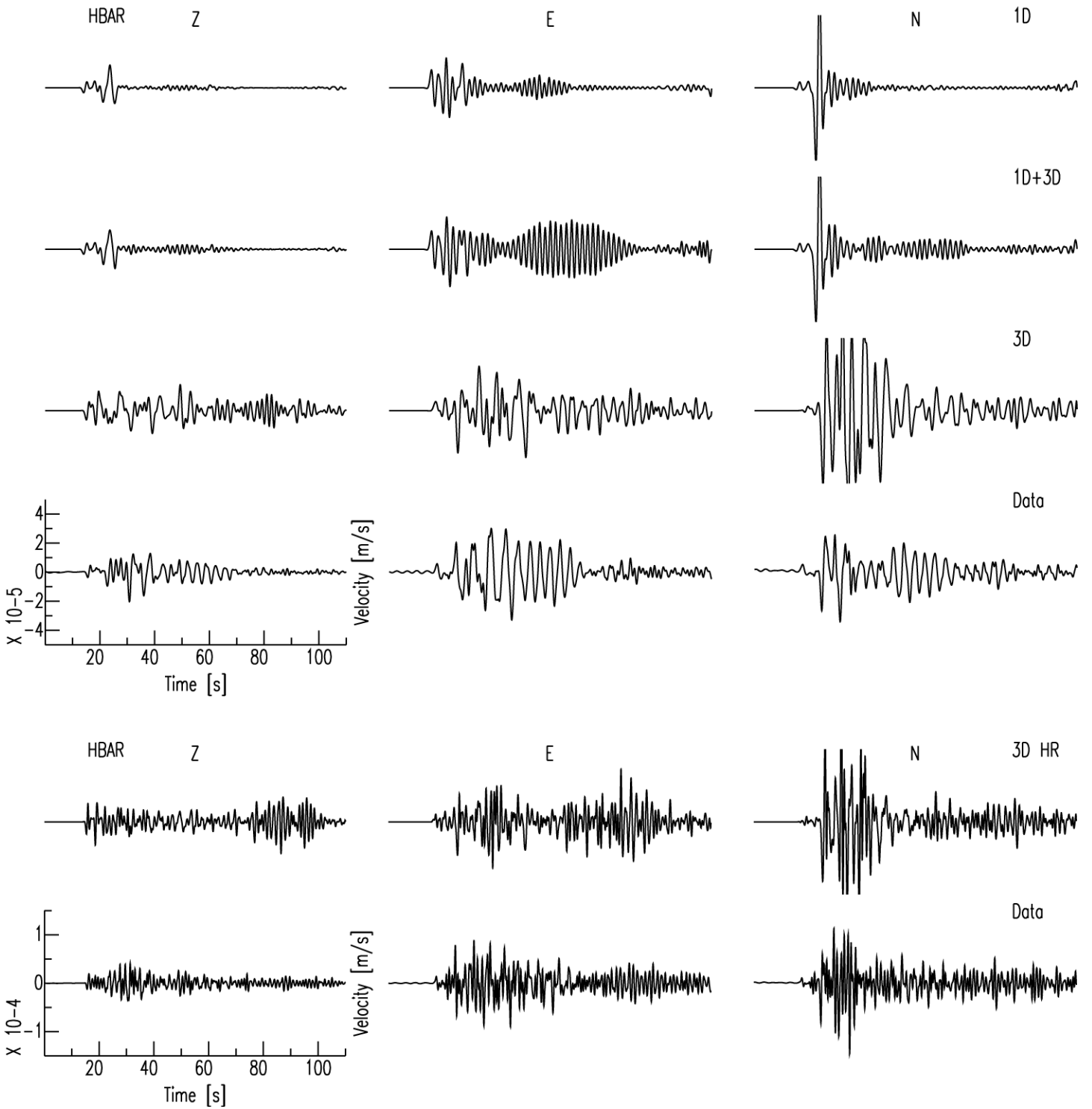


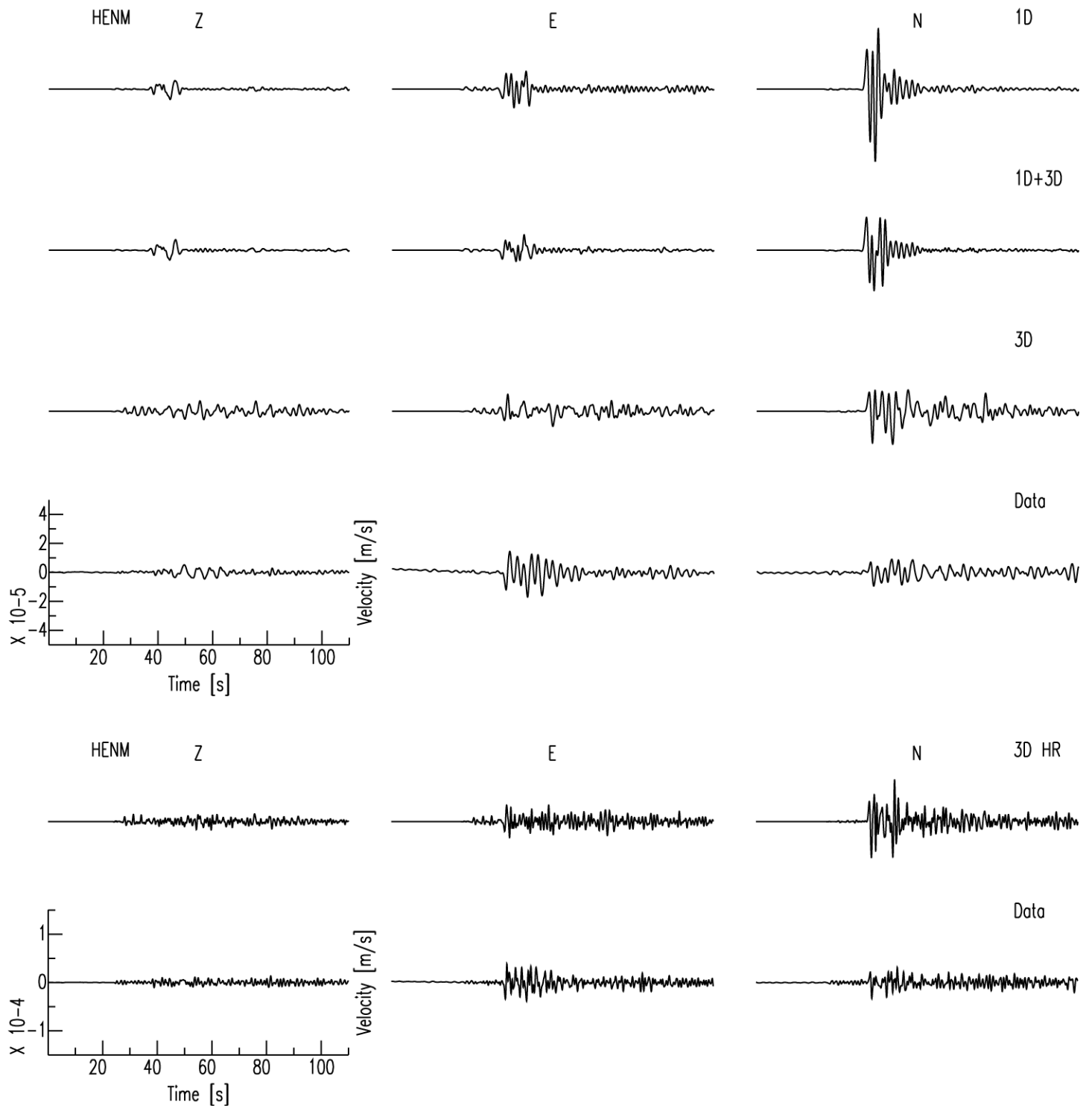


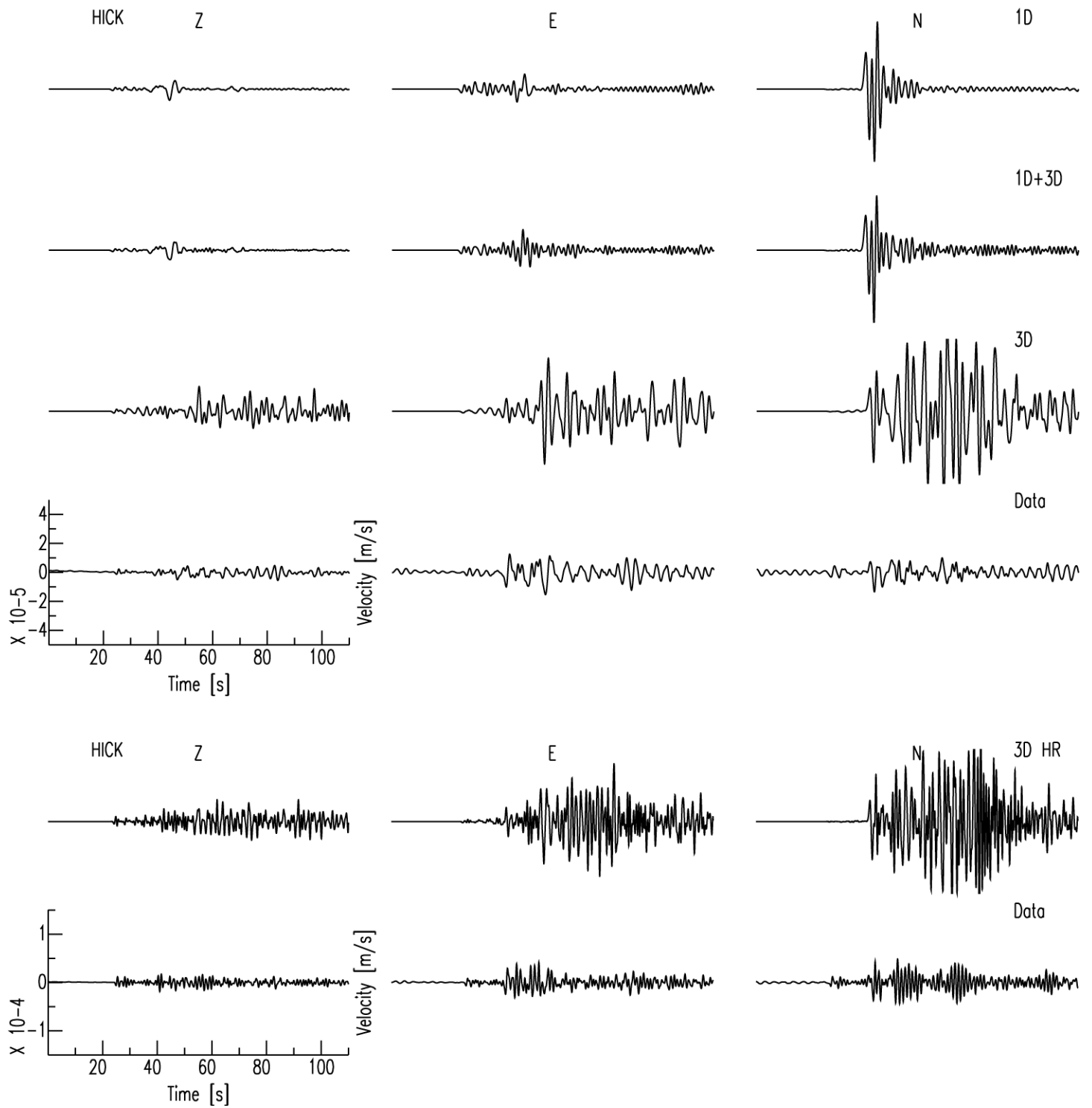


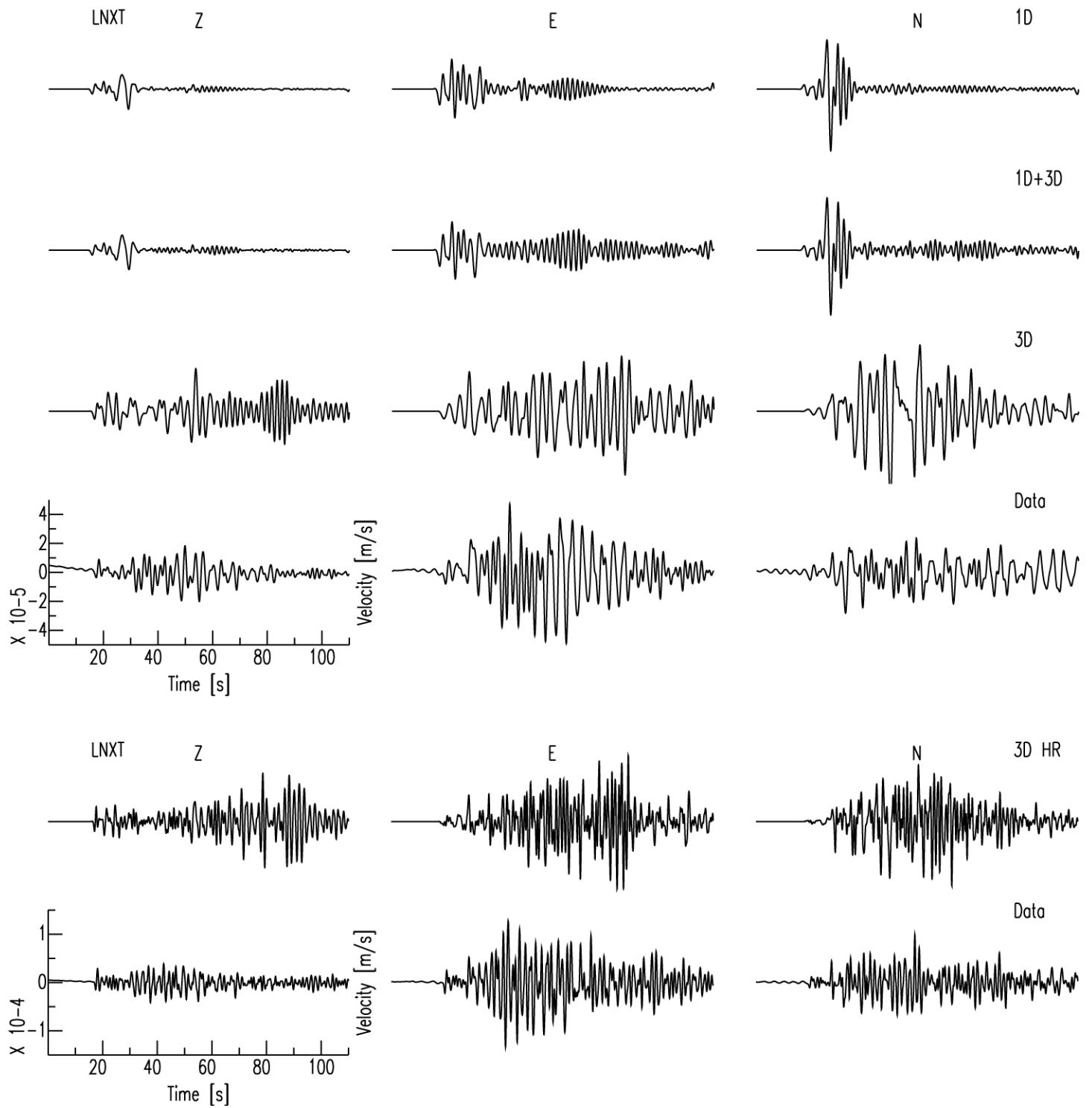


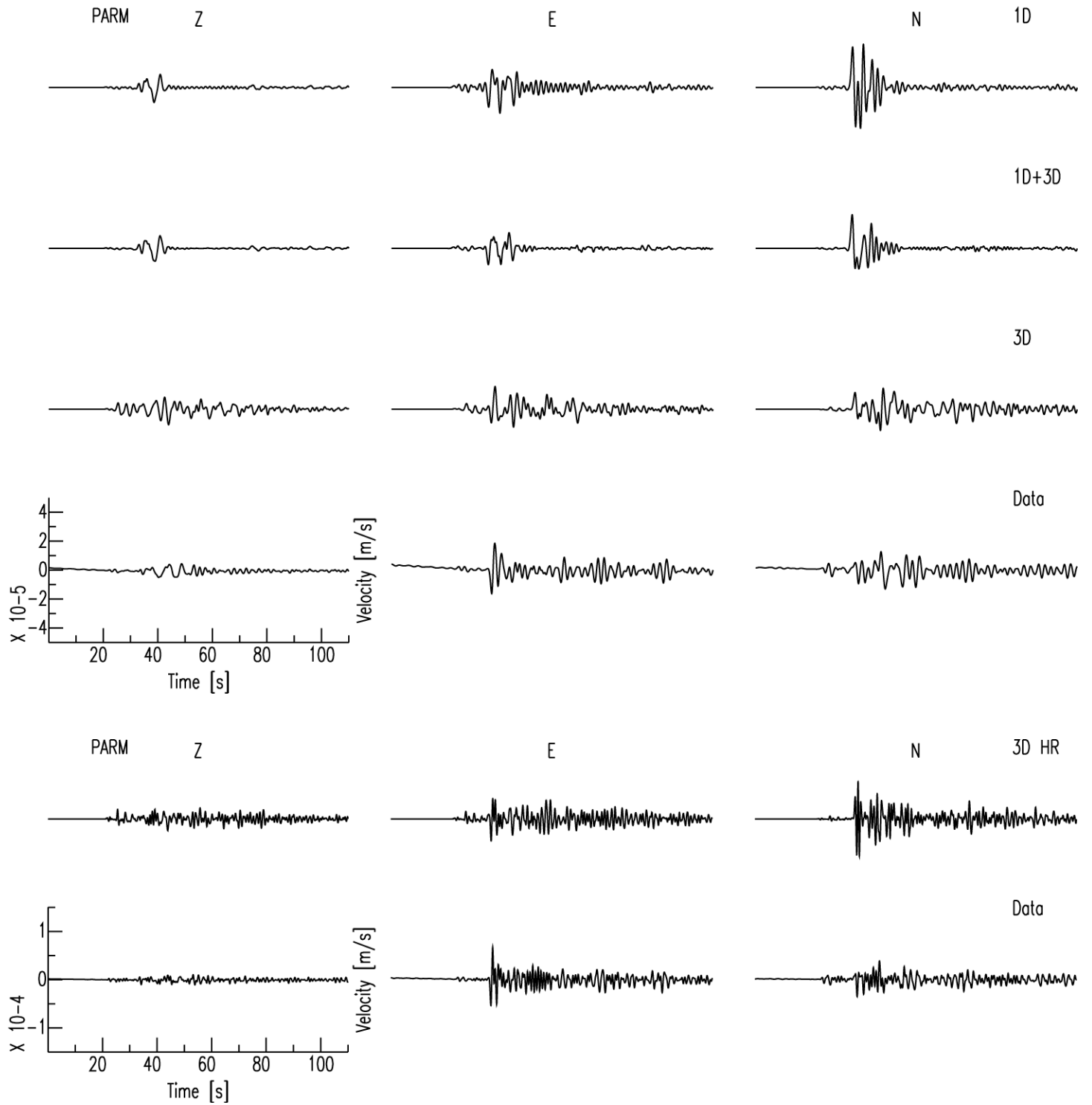


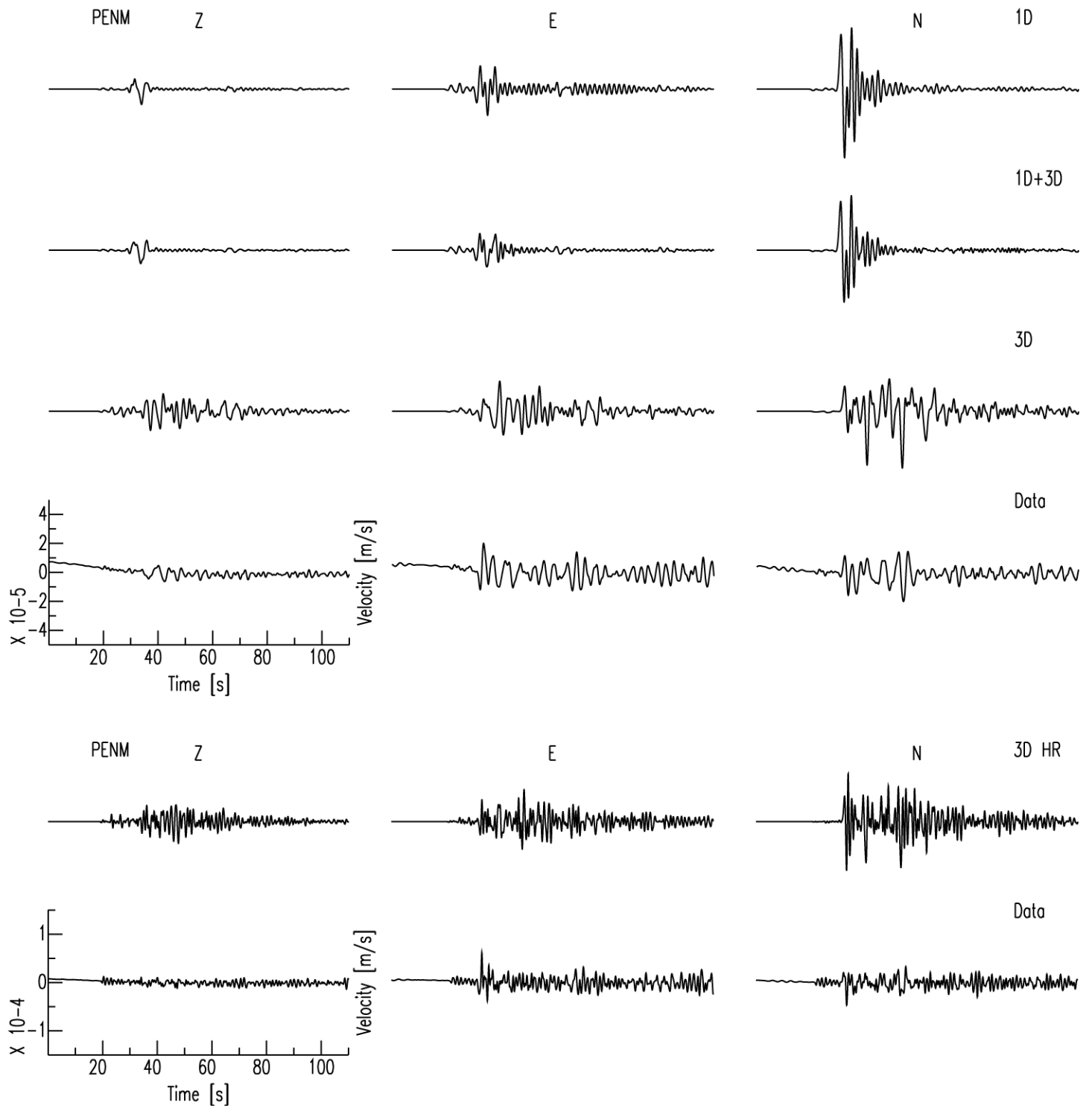


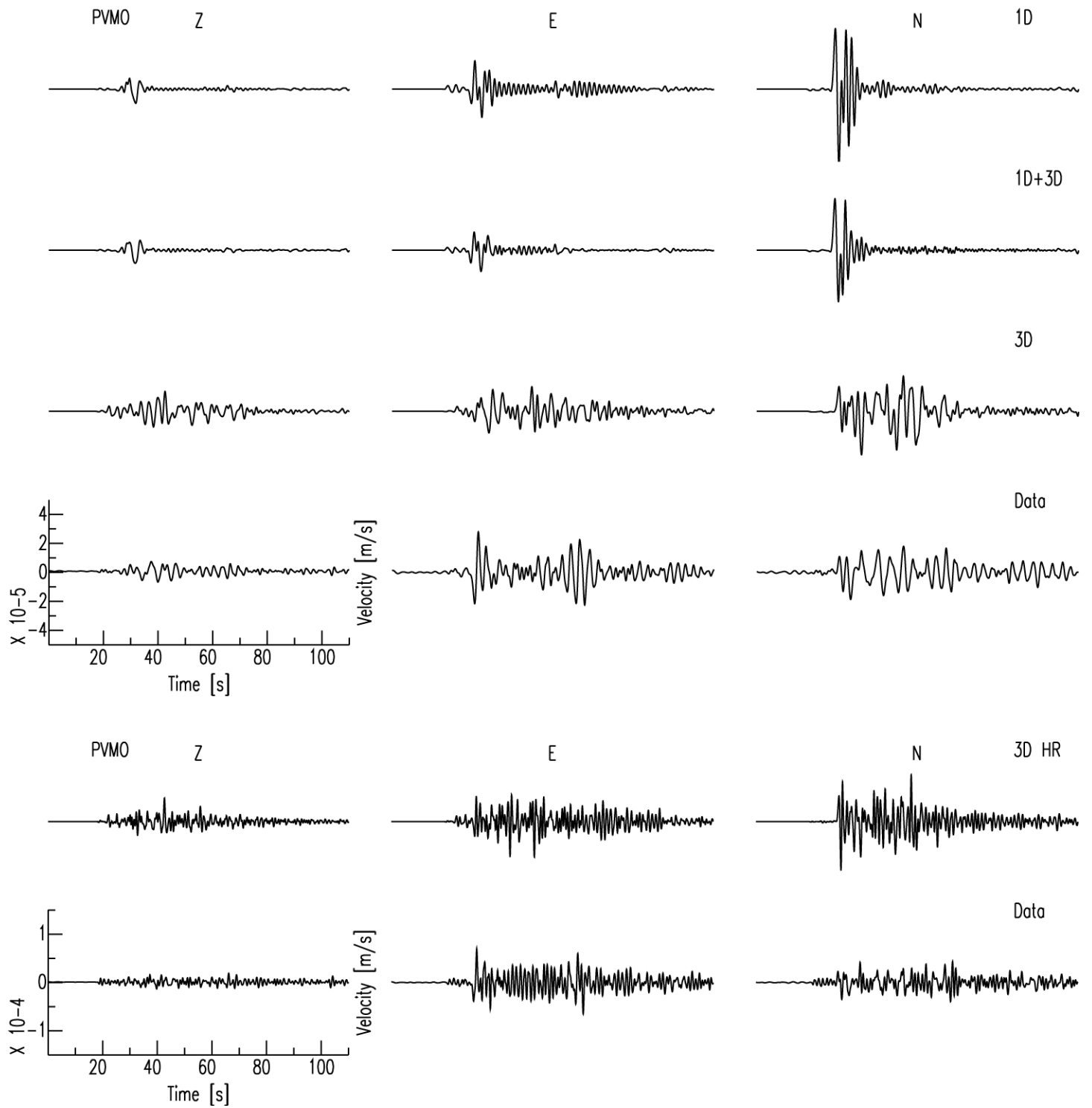


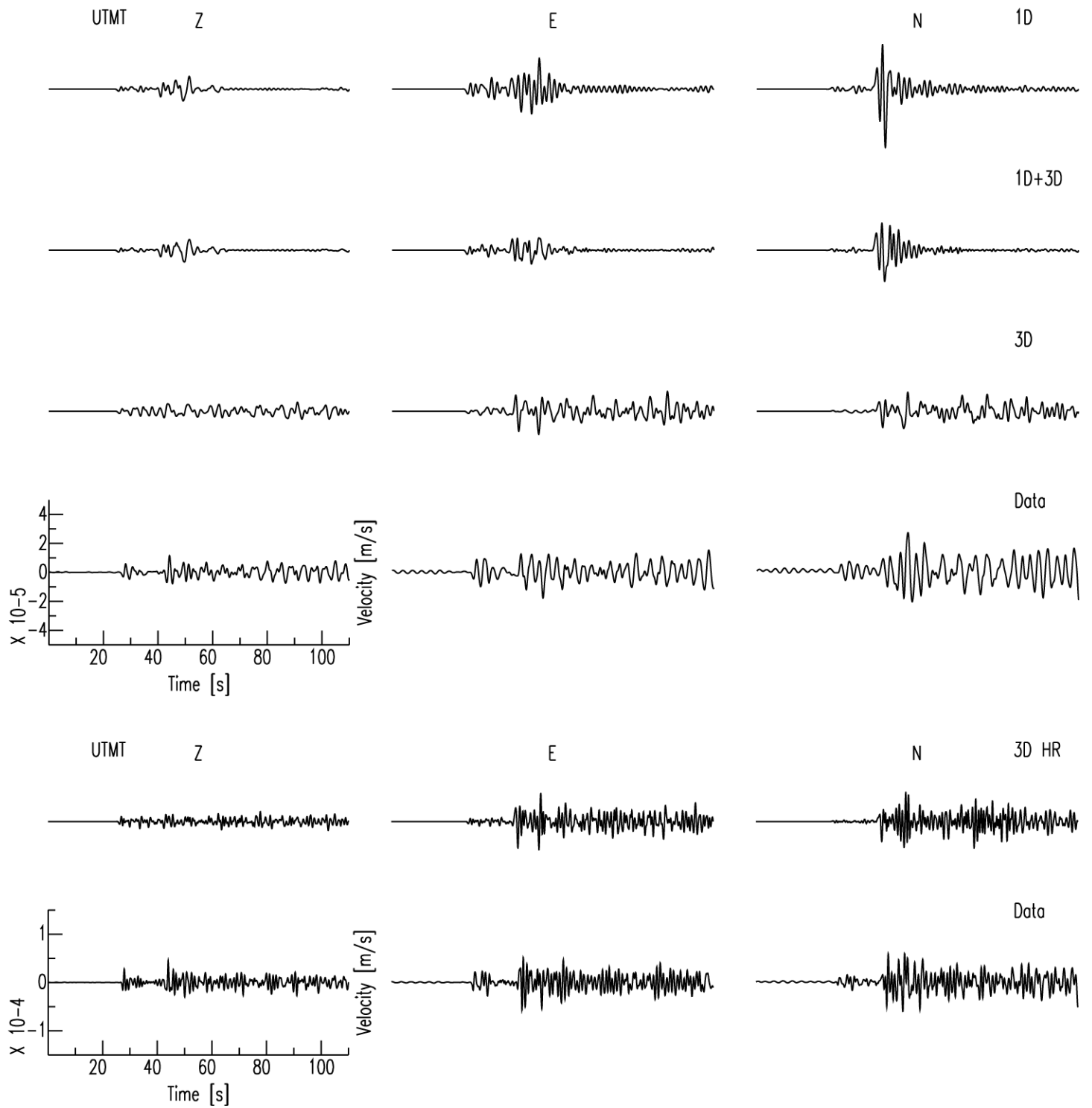




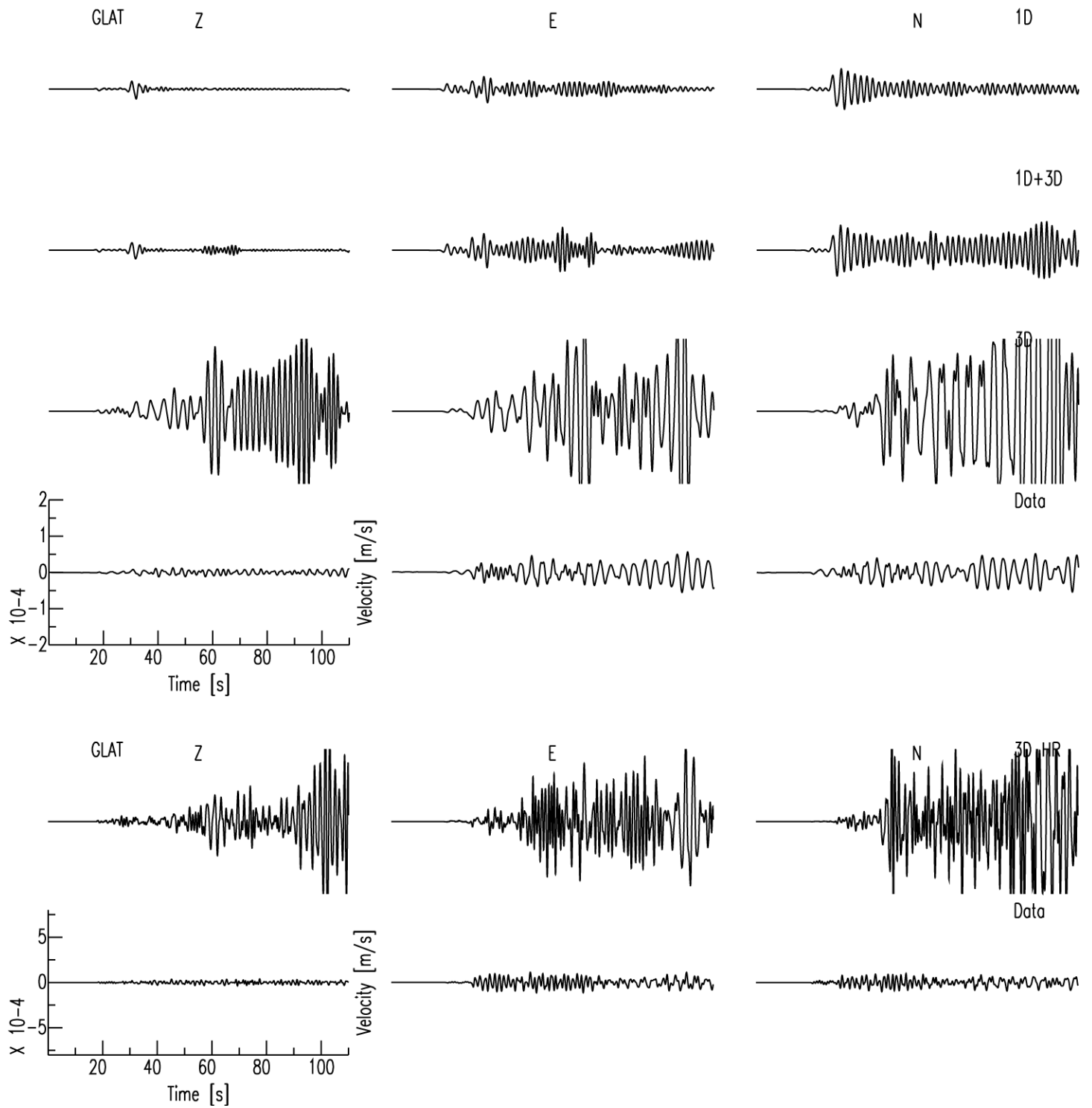




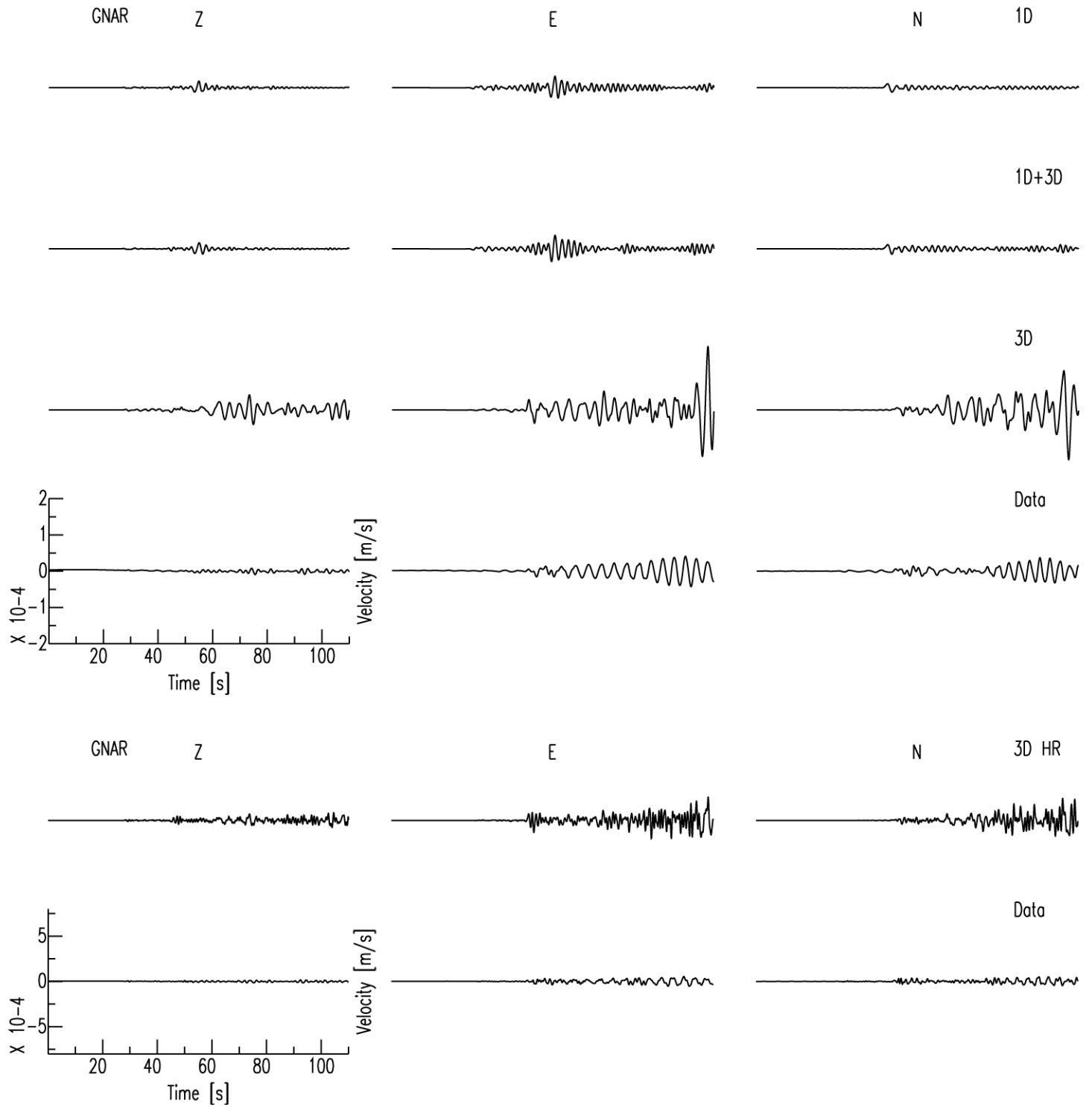




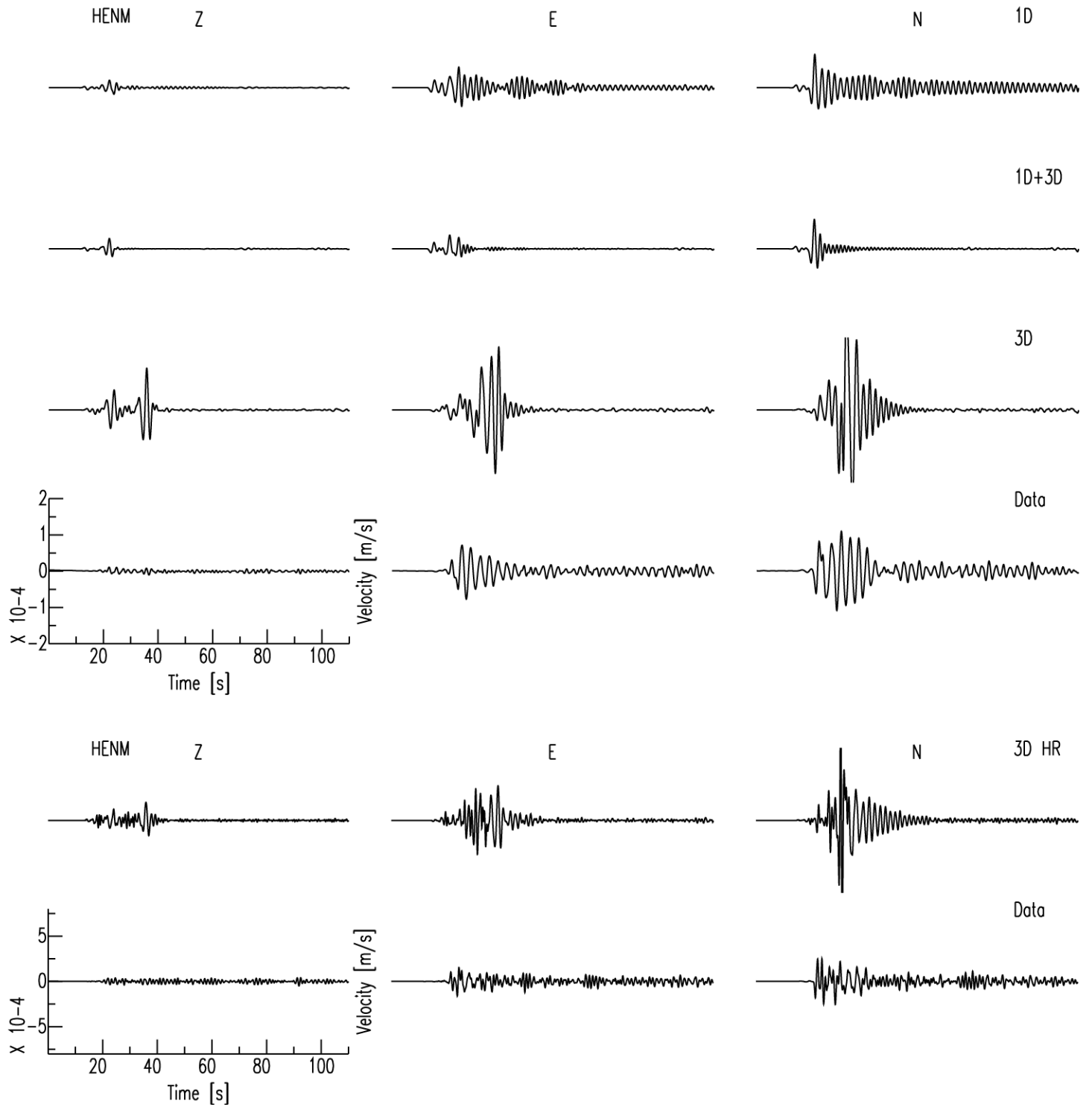
BDWL



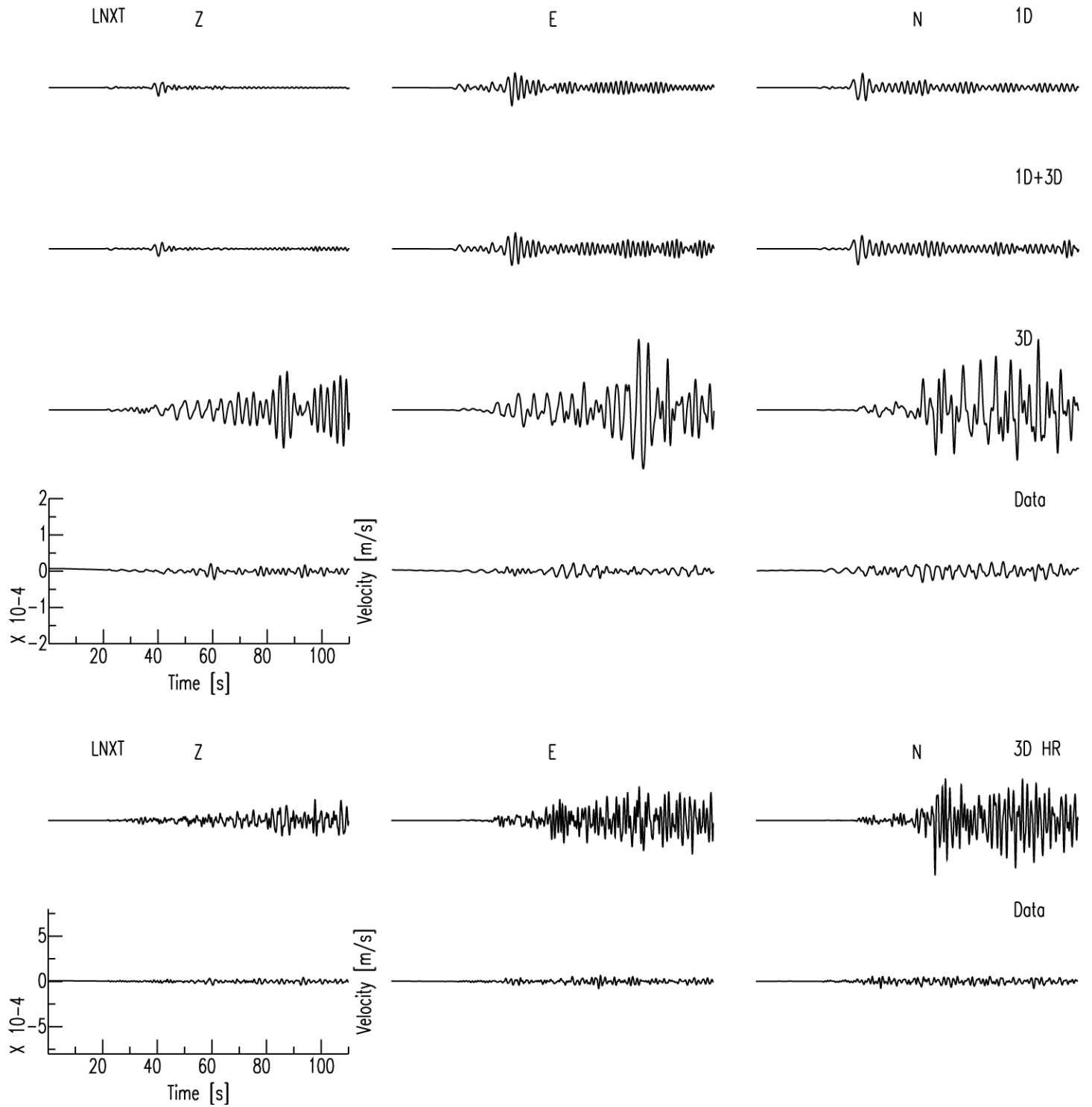
BDWL



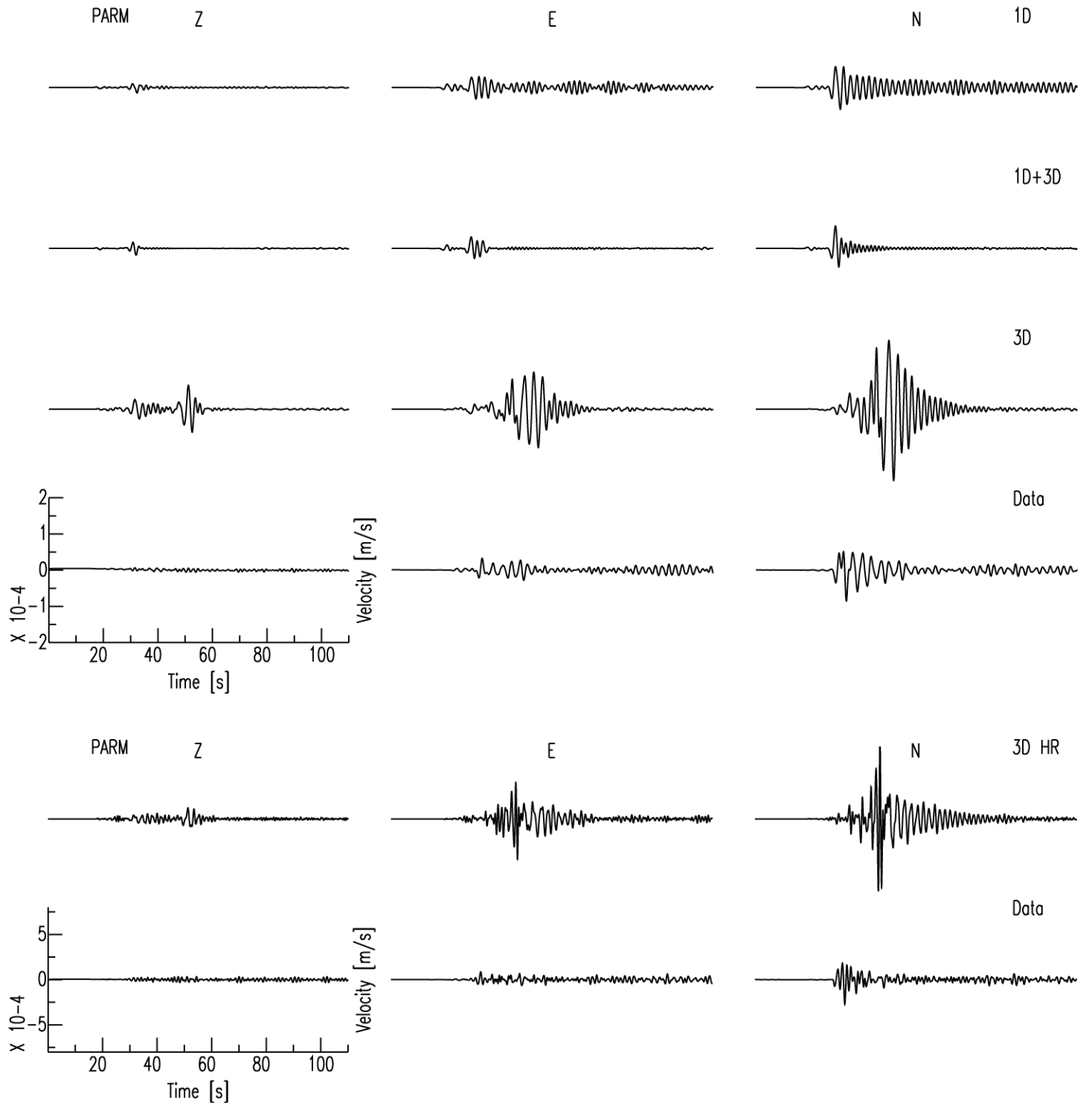
BDWL



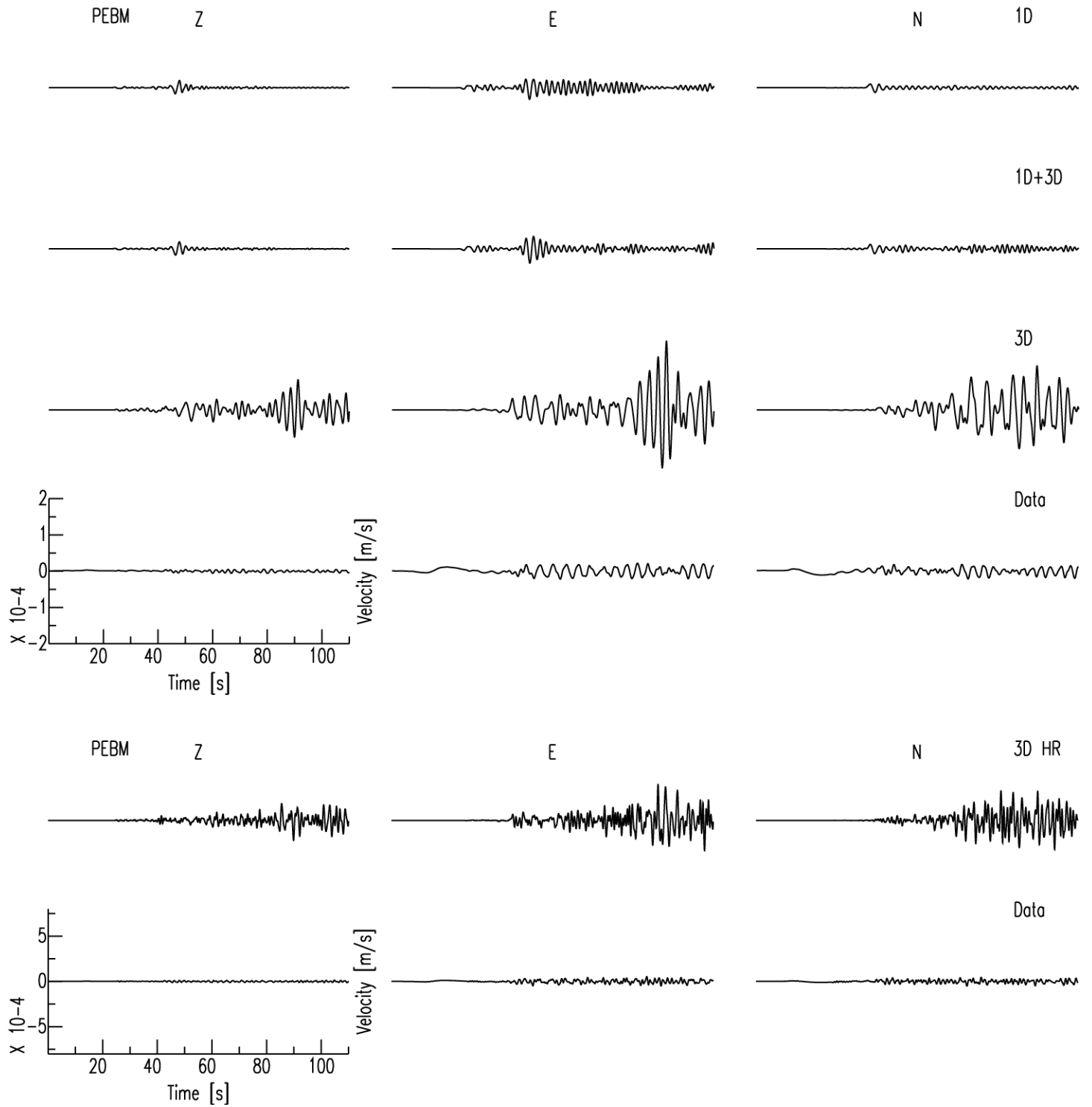
# BDWL



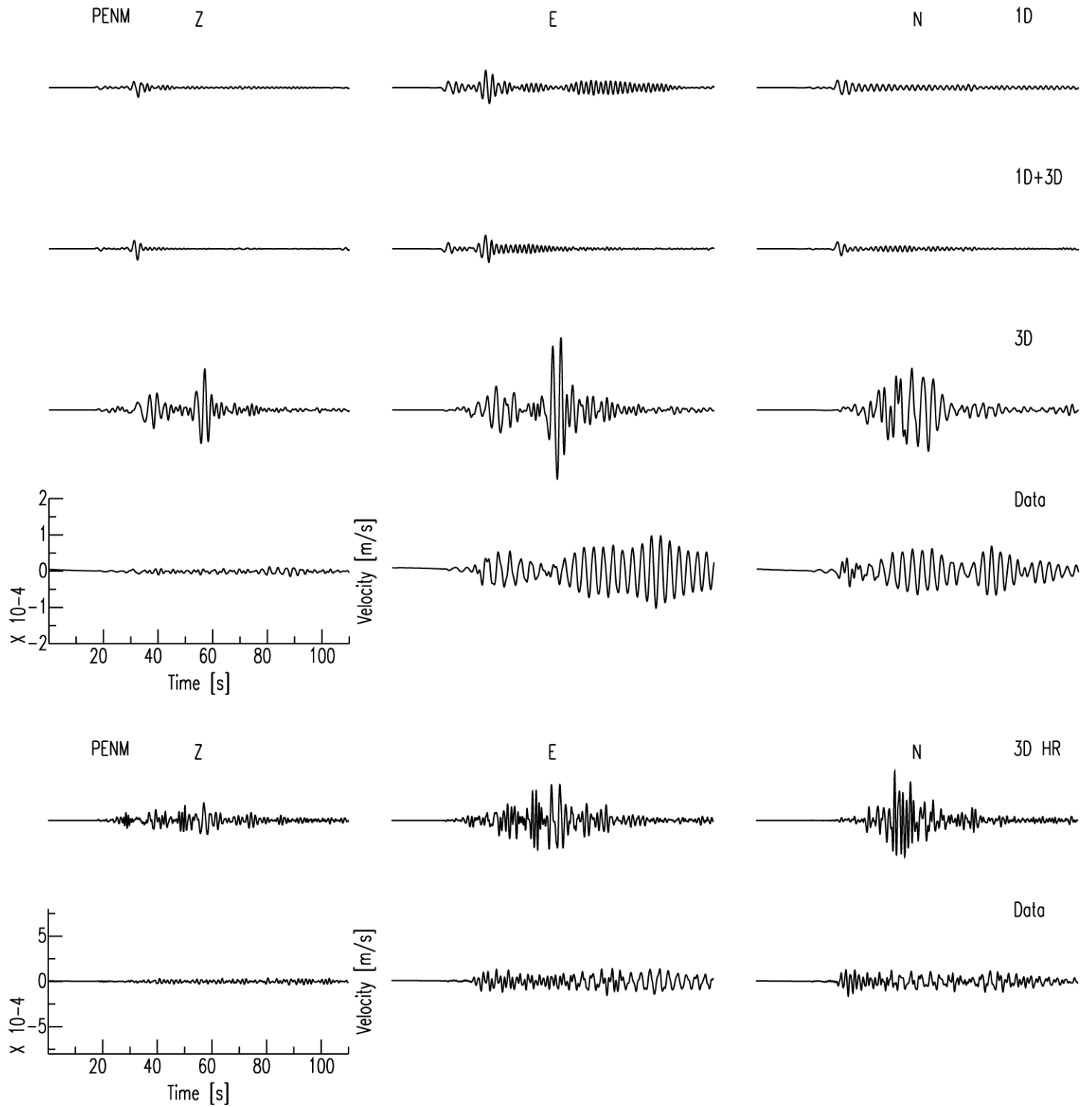
BDWL



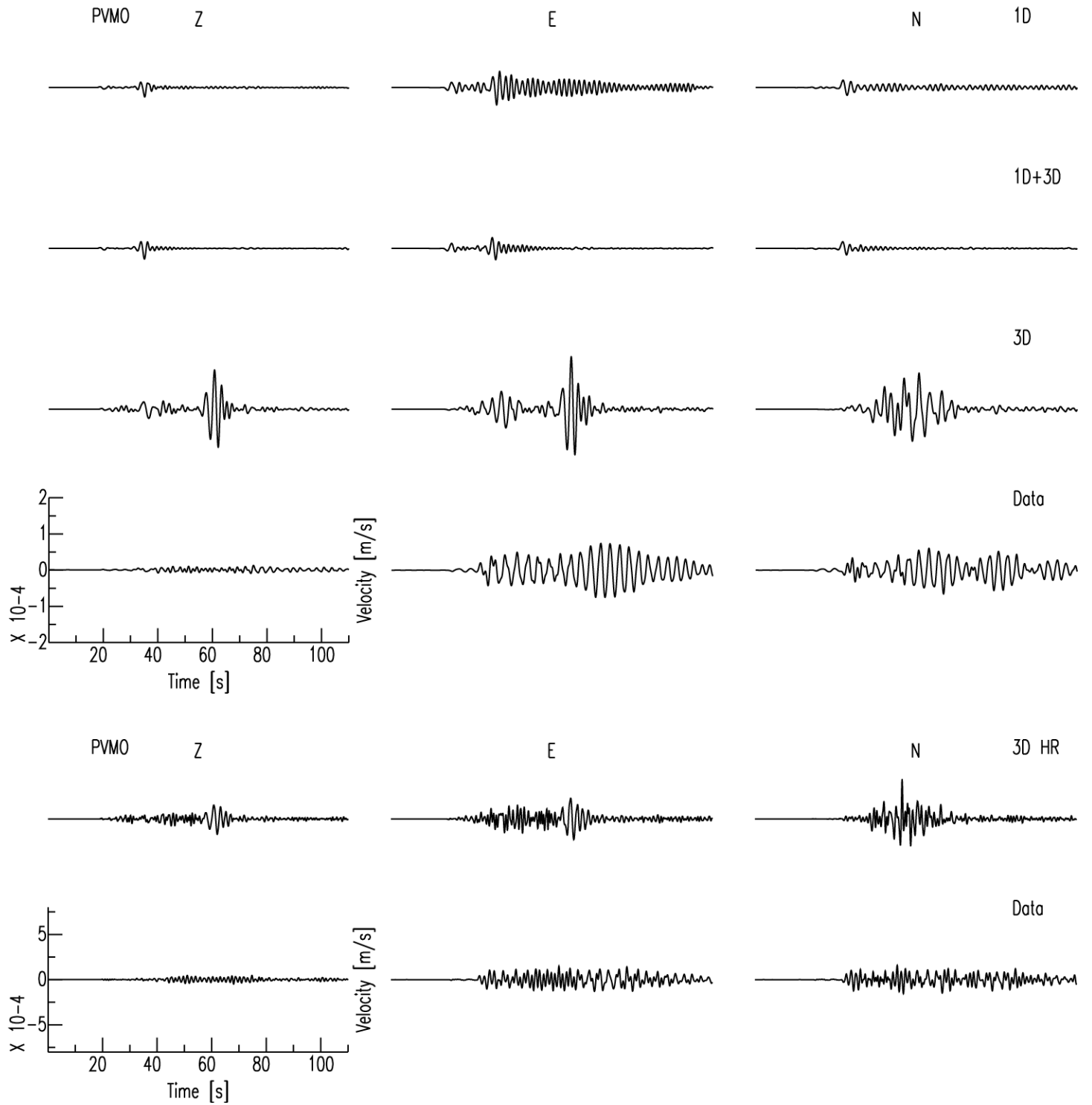
BDWL



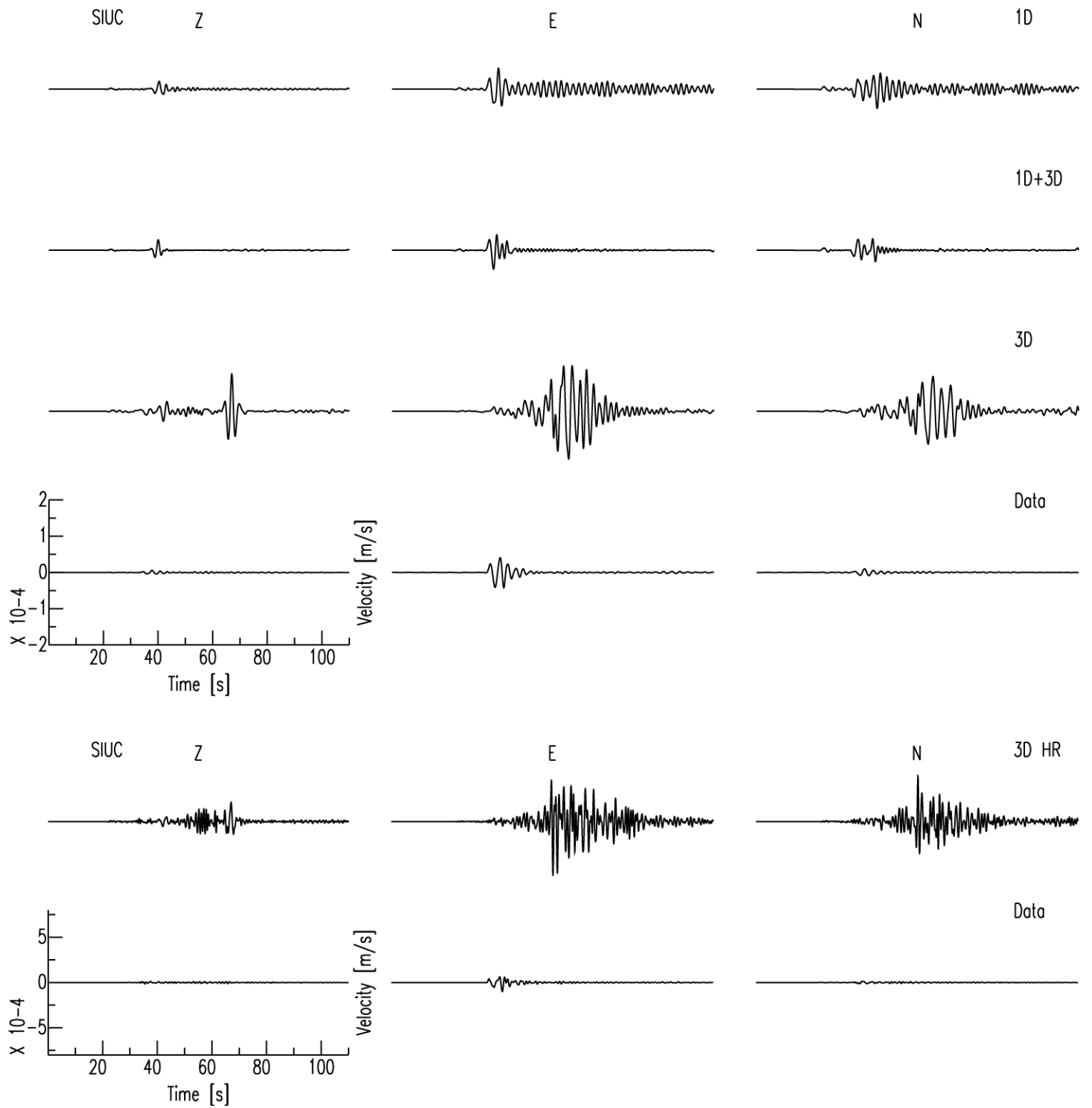
BDWL



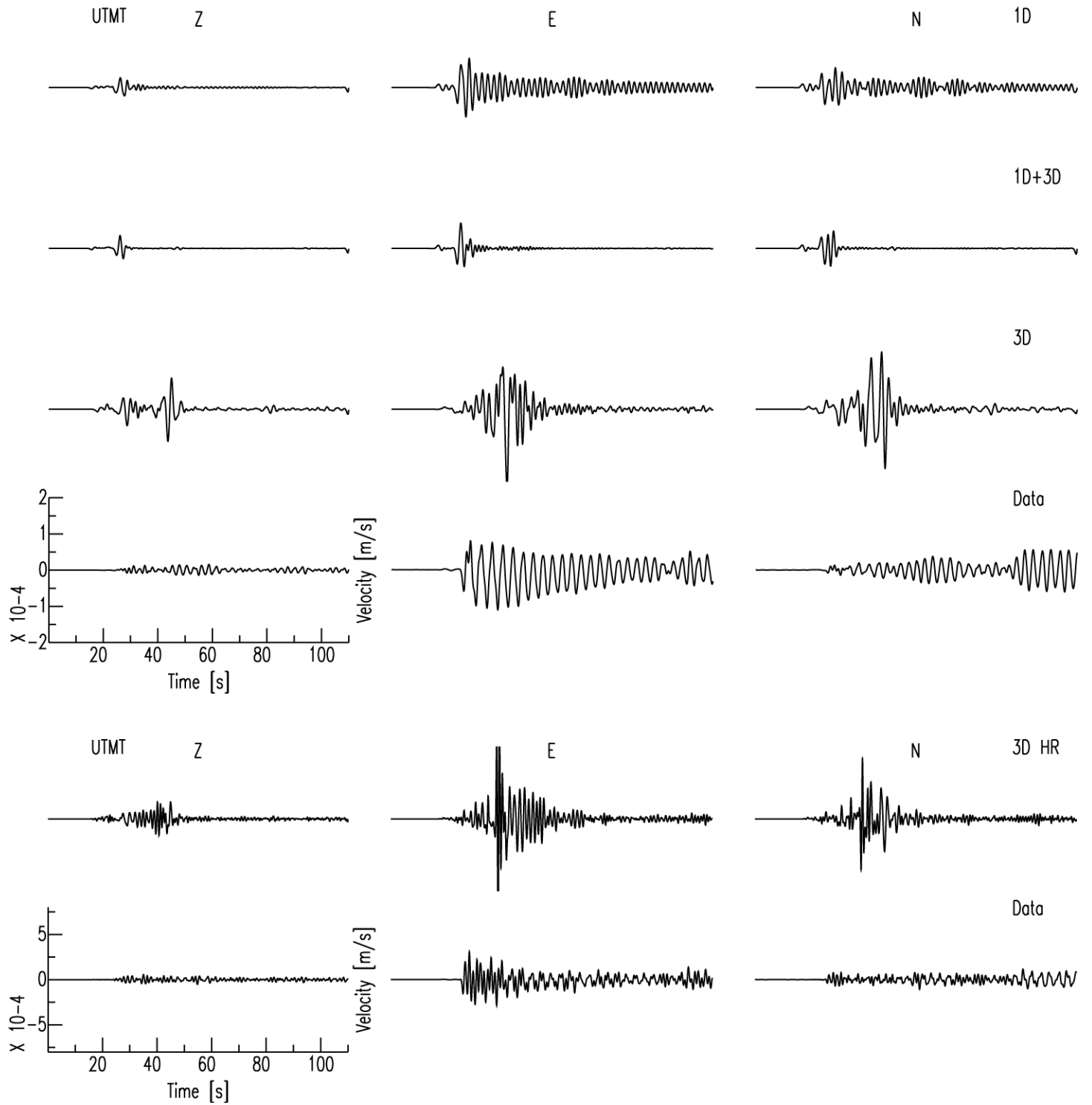
BDWL



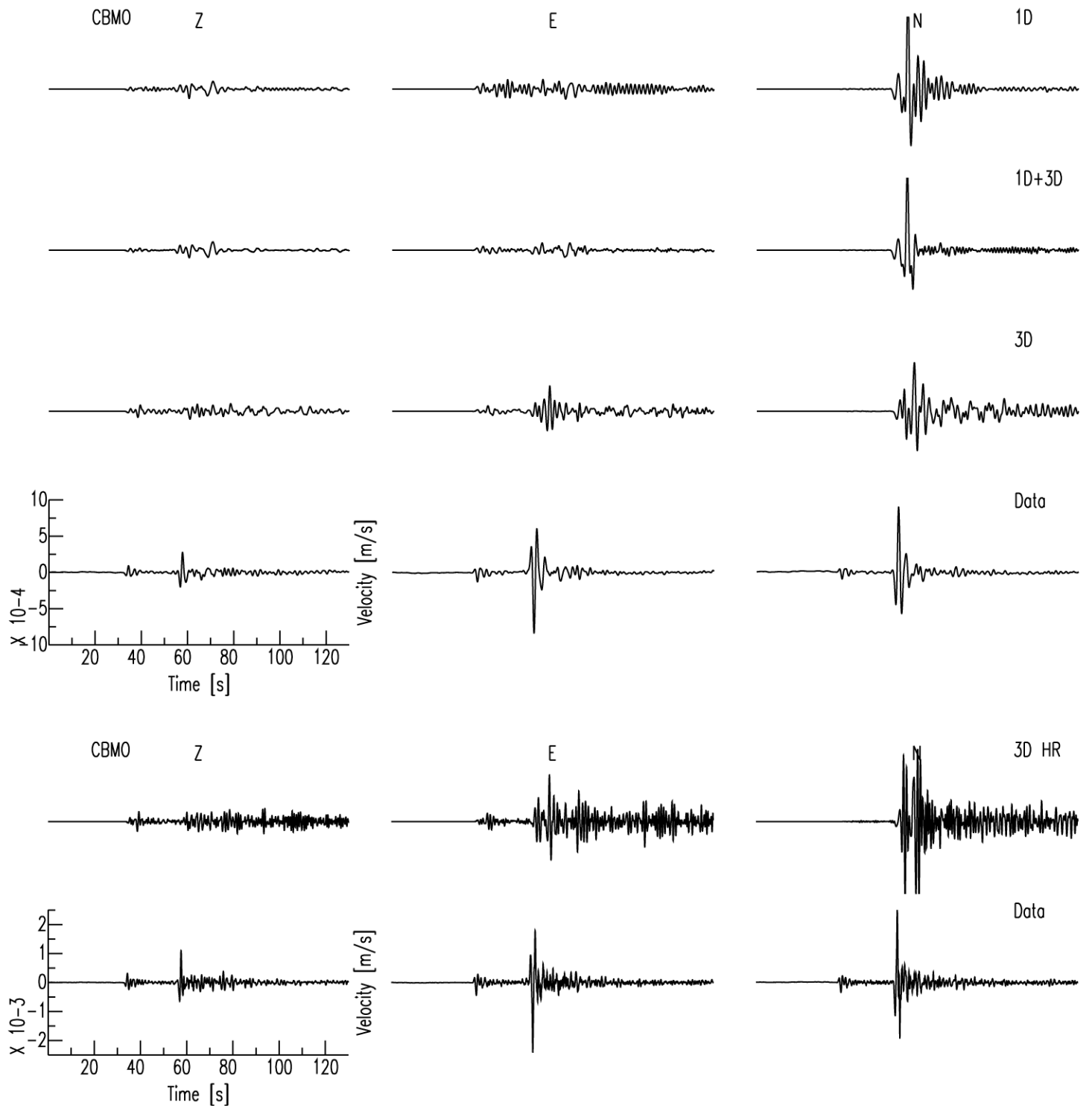
BDWL



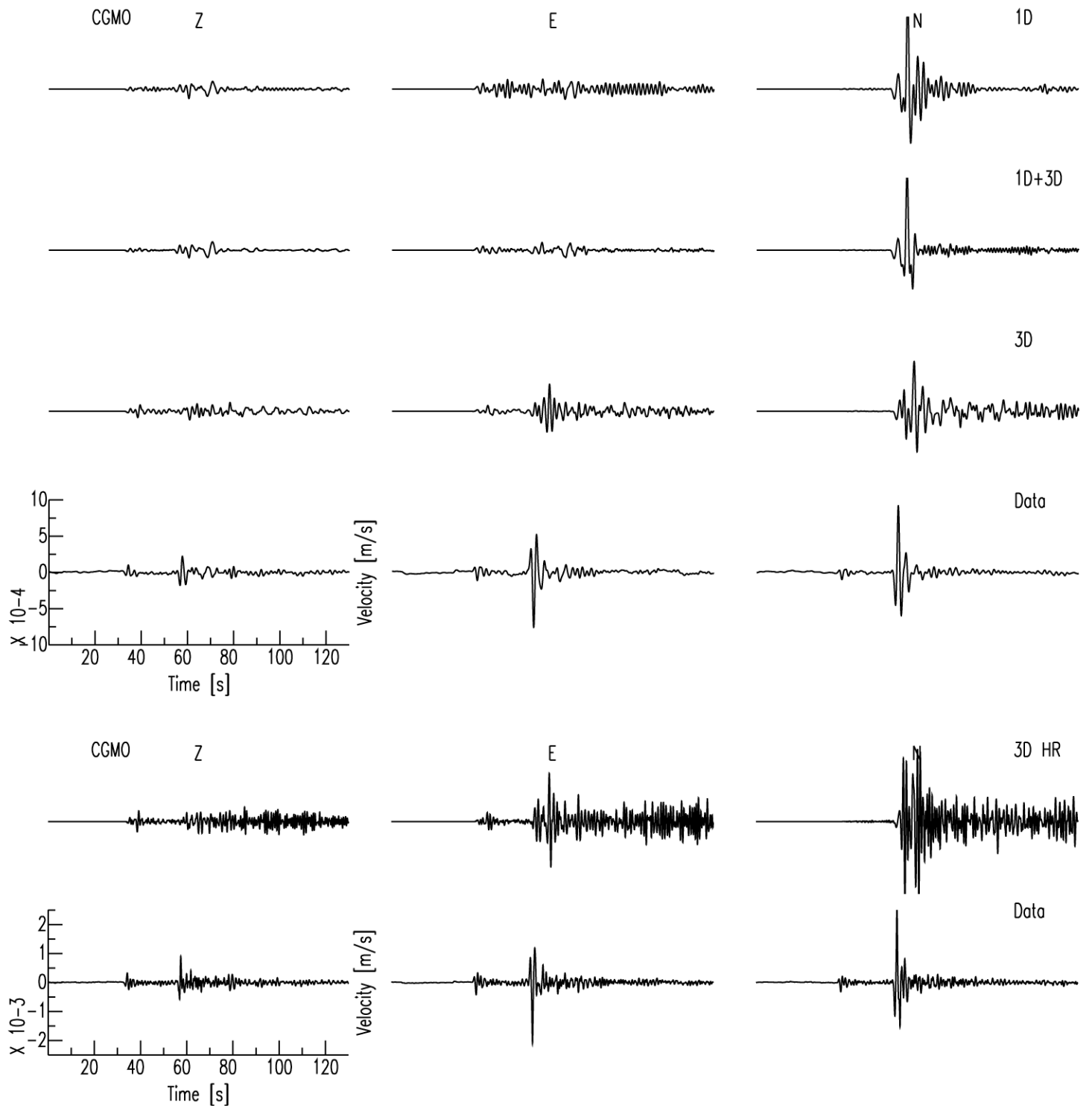
BDWL

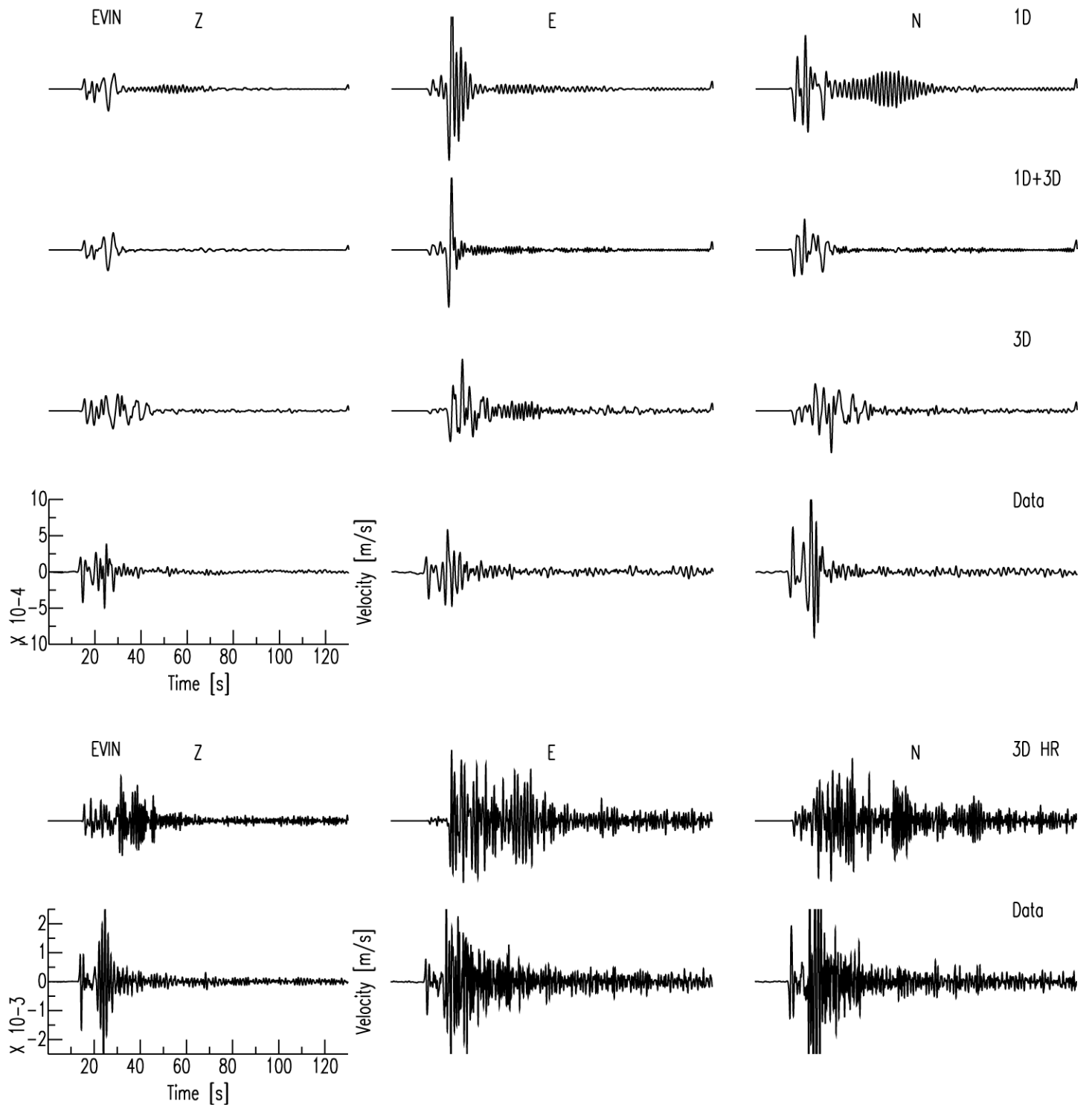


IL

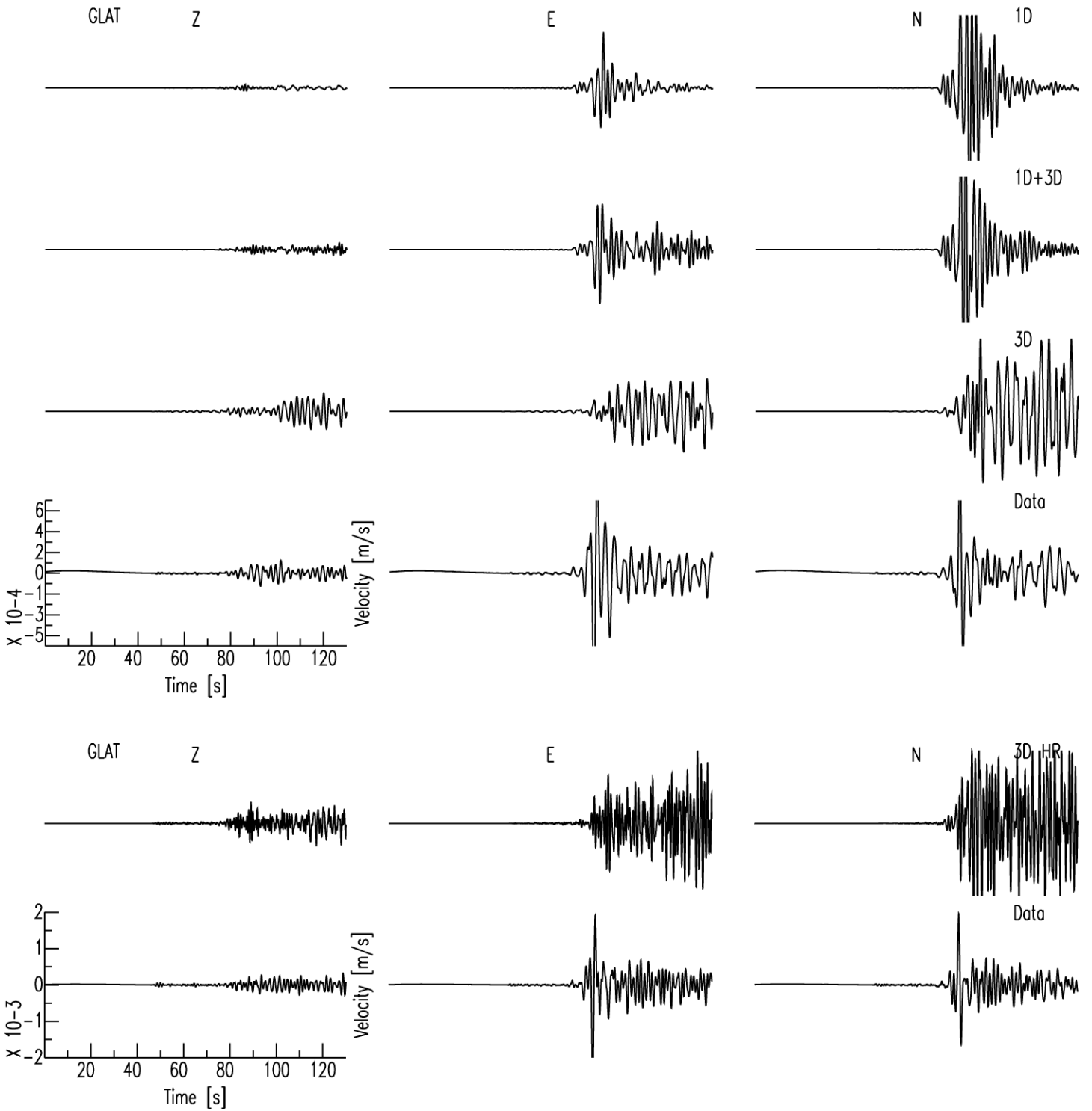


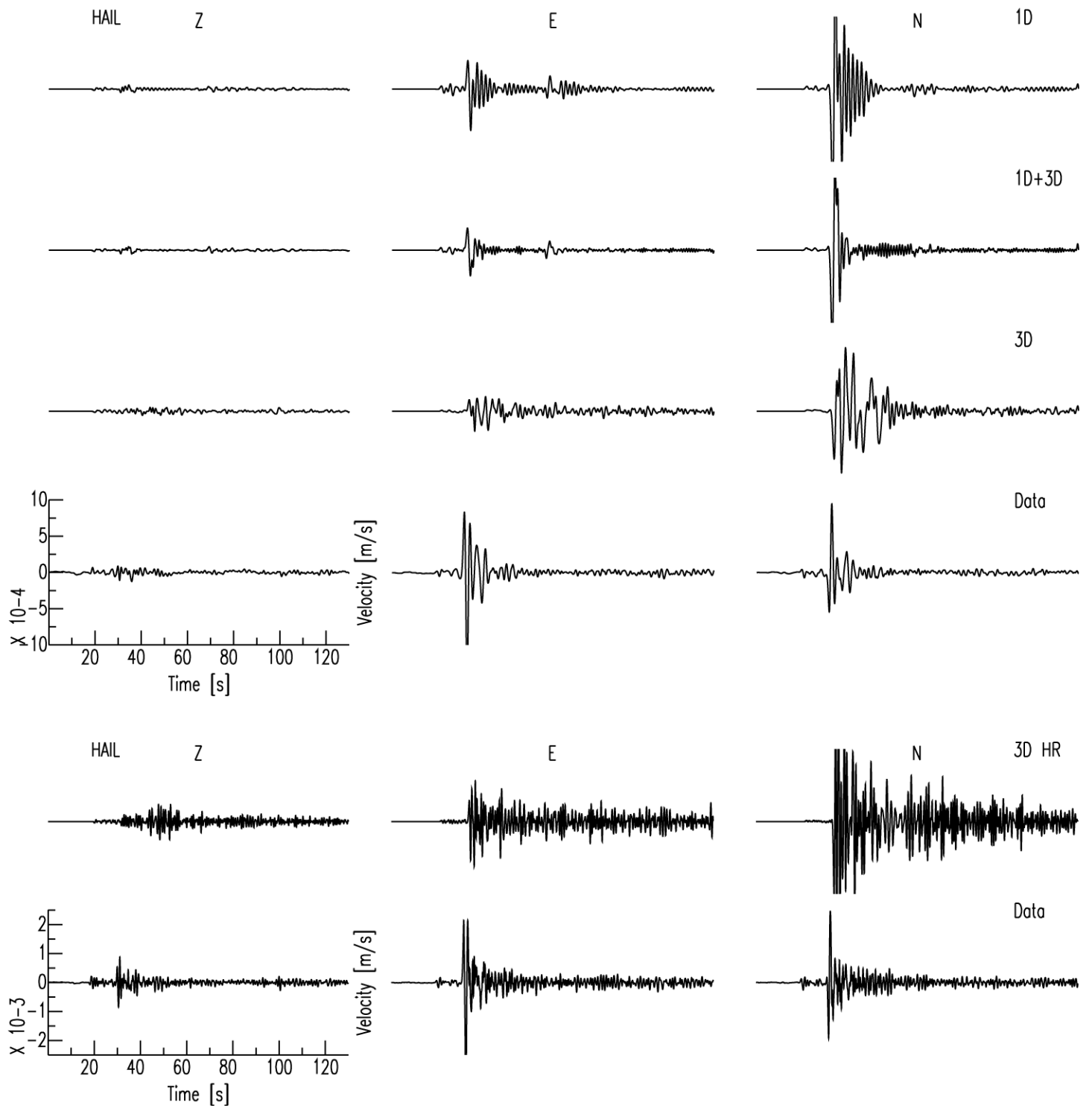
IL



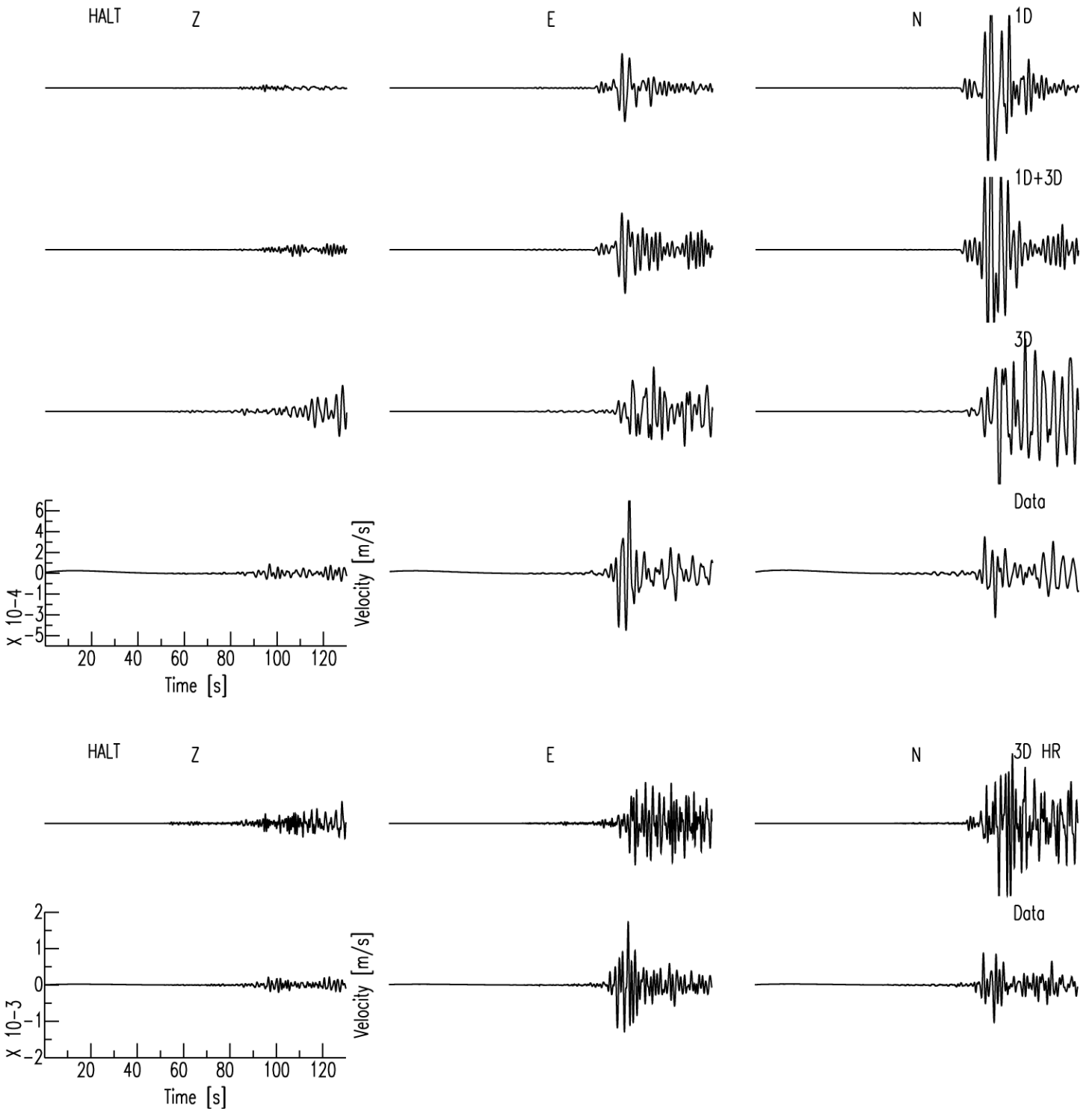


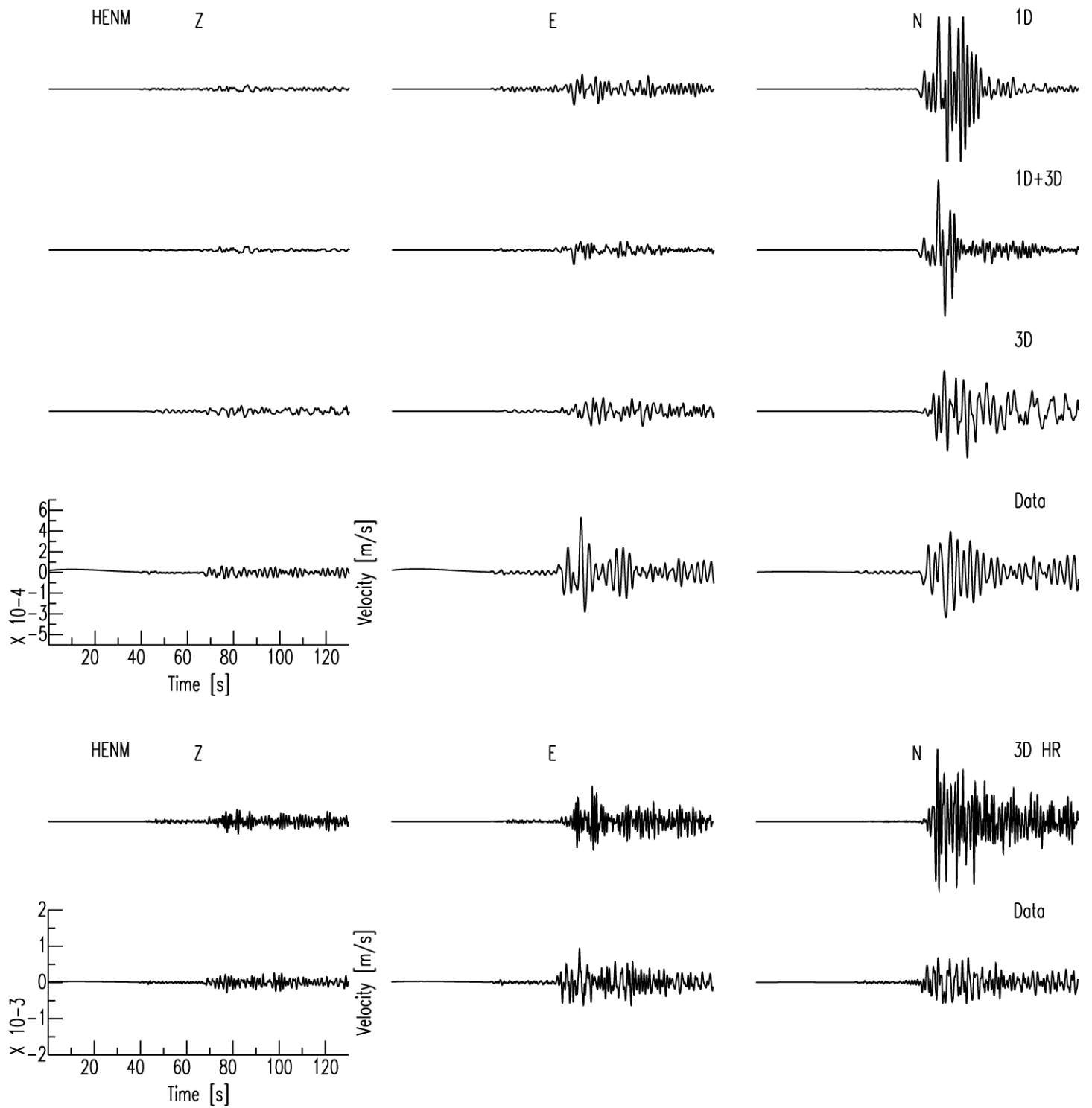
IL



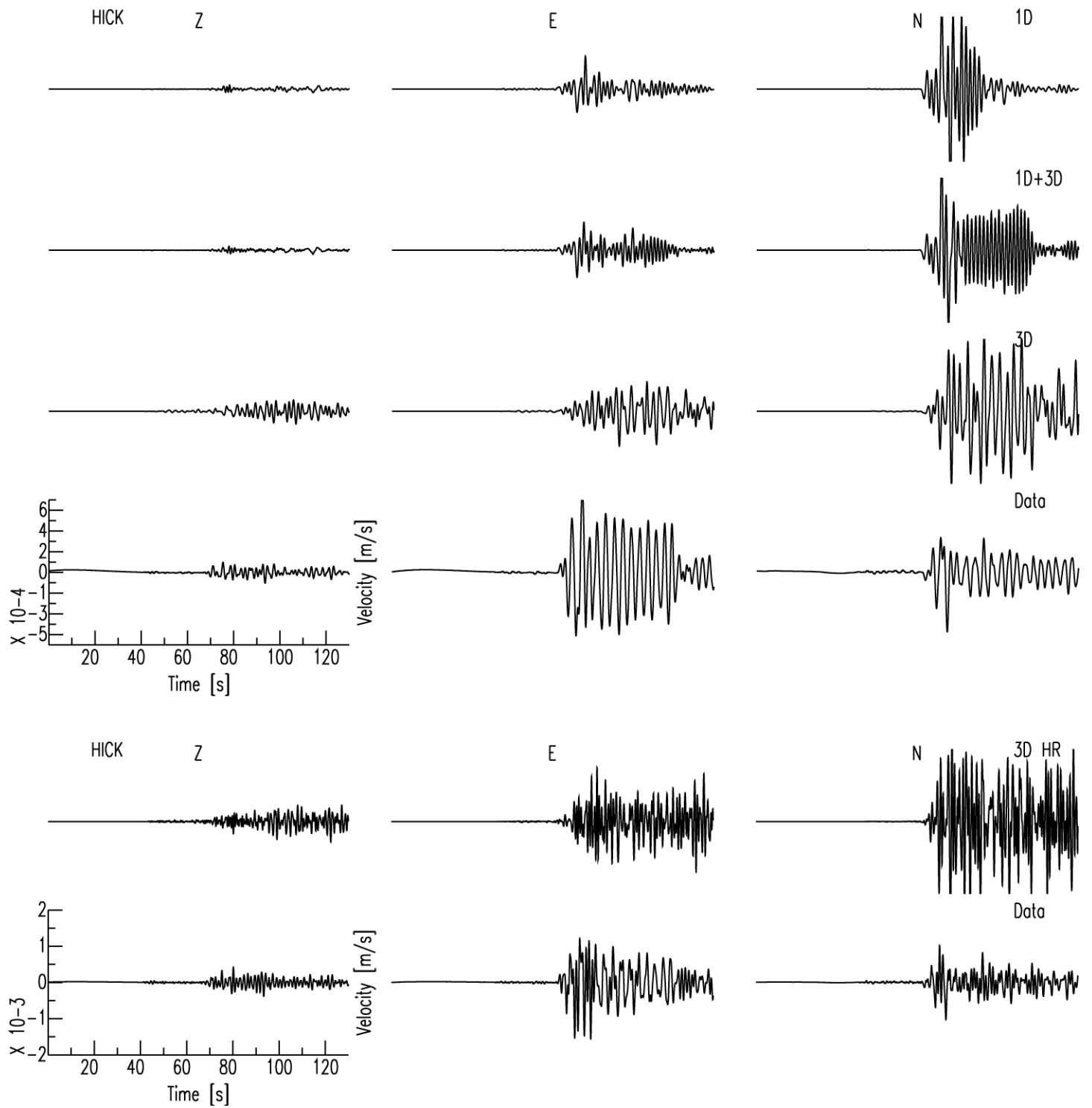


IL

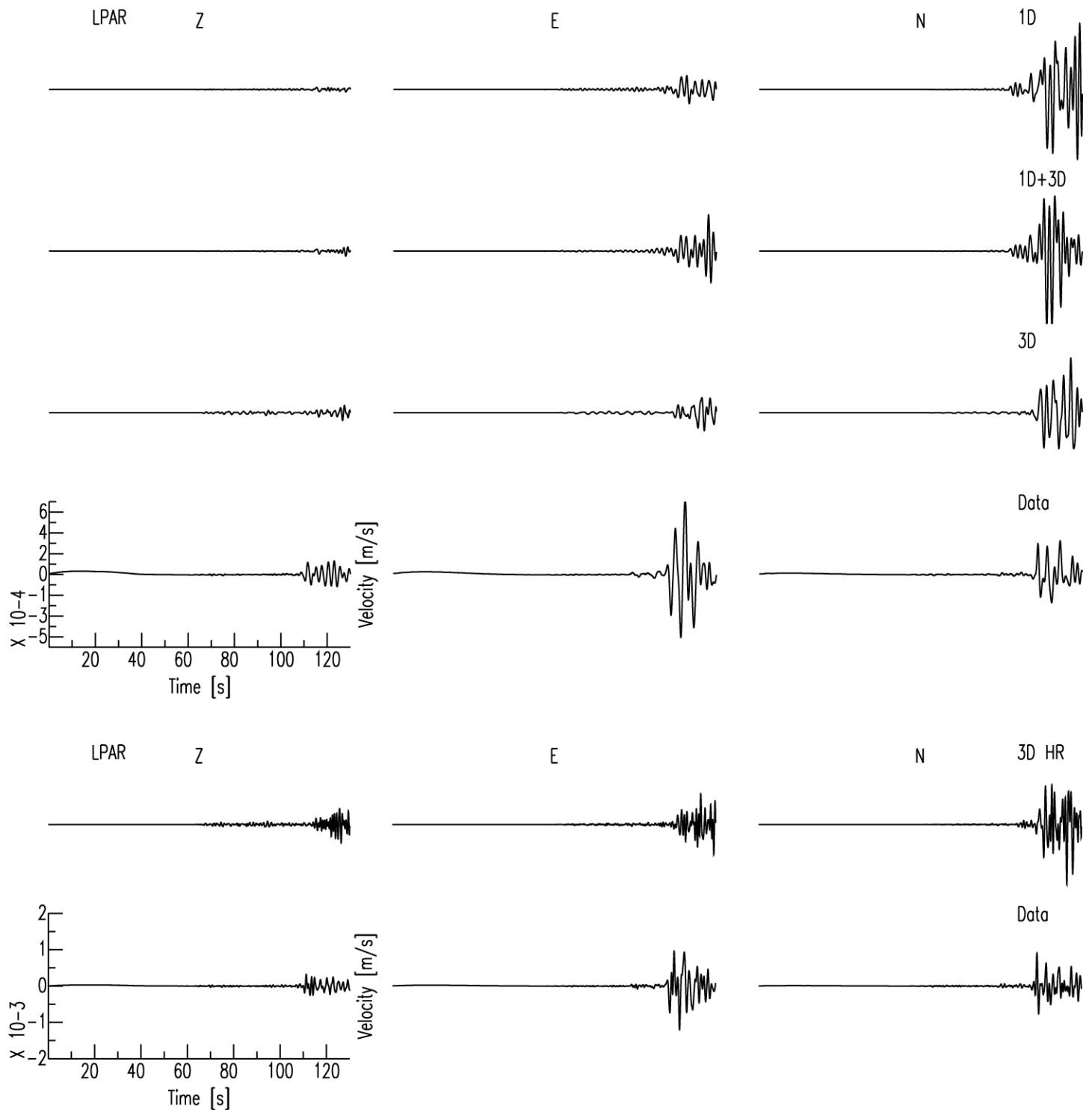


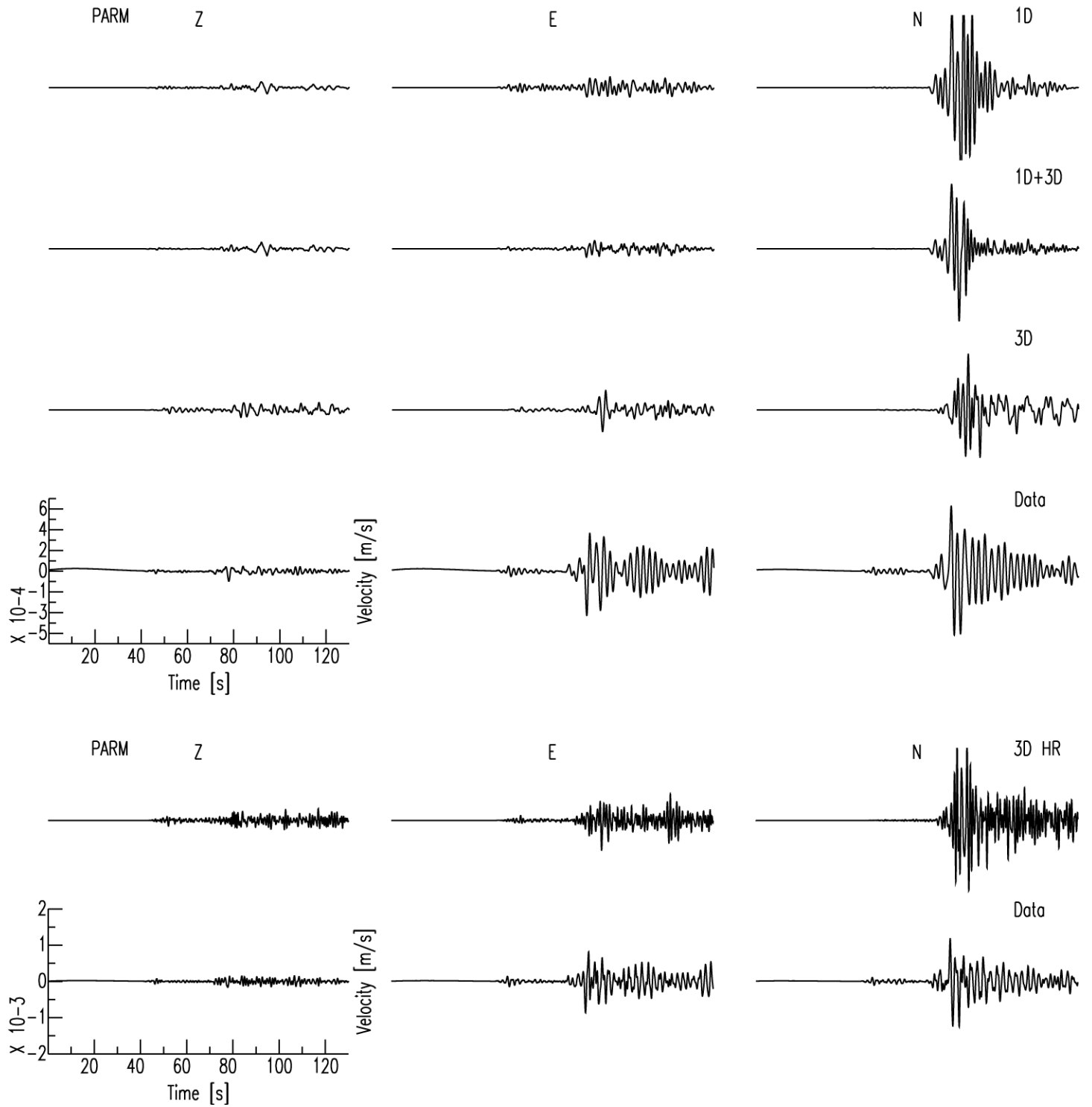


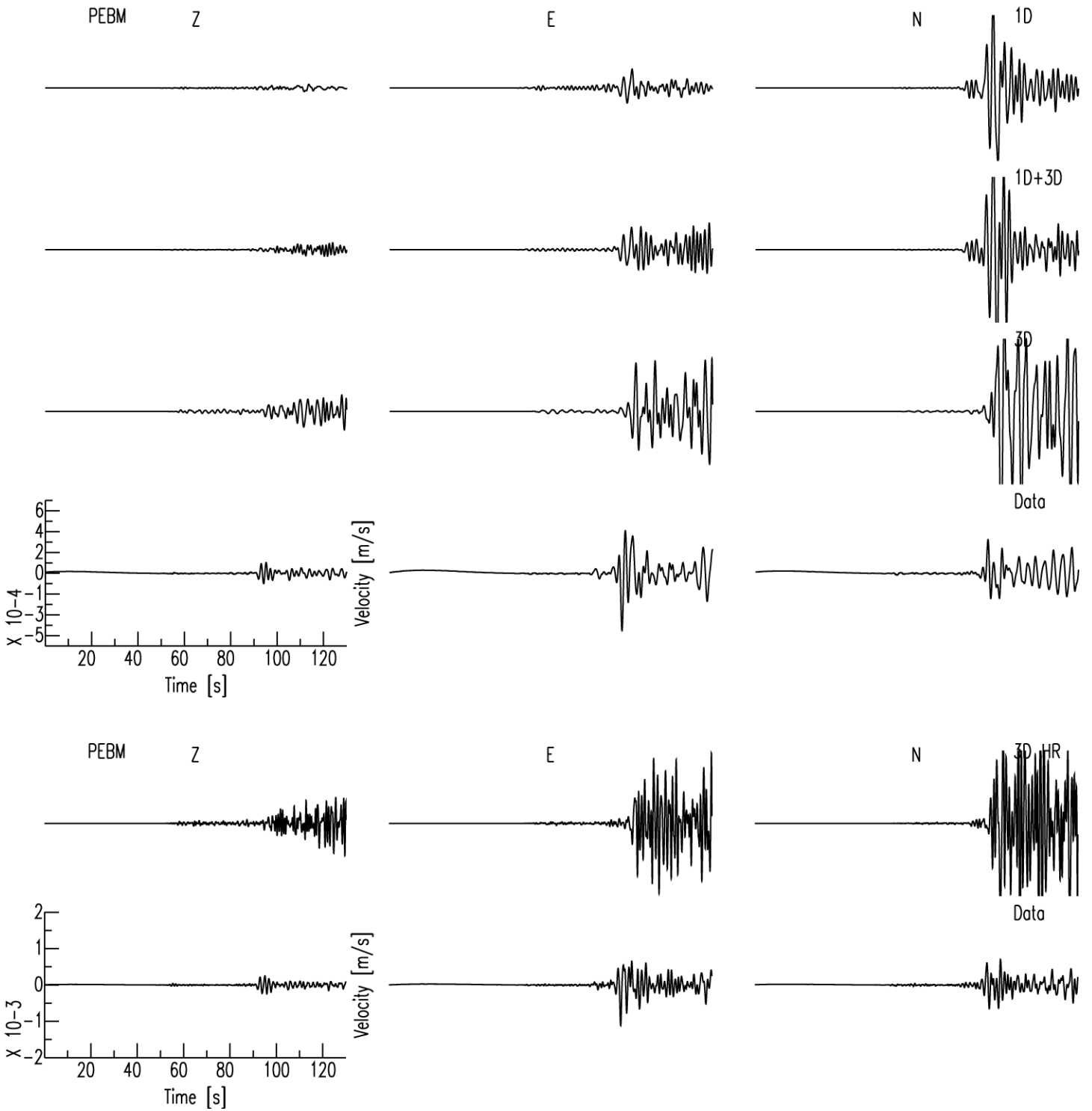
IL

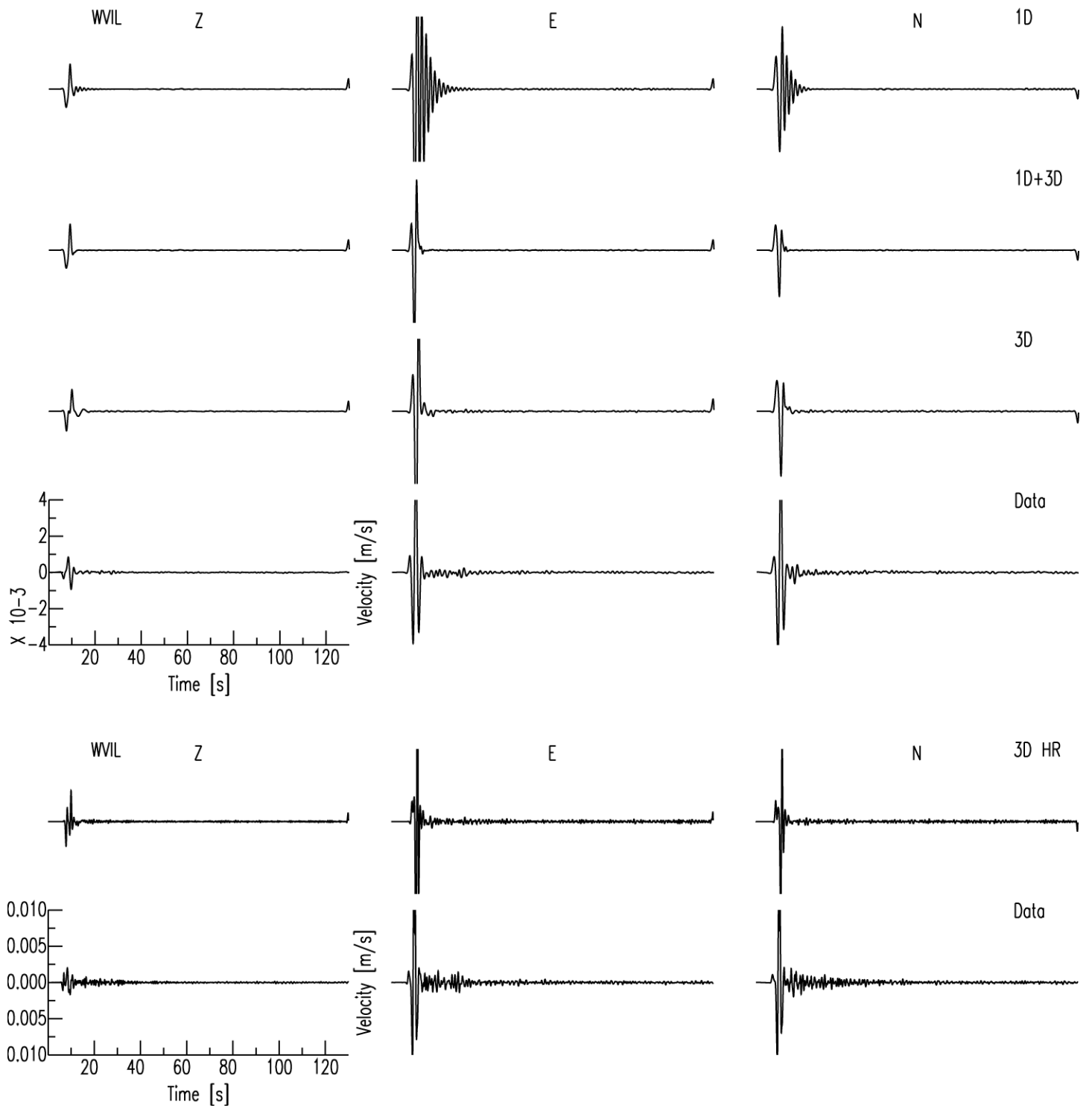


IL









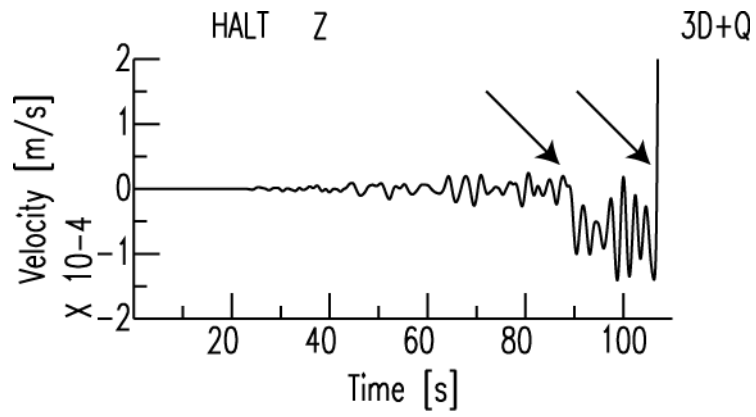


Figure 9. Simulated waveforms for the event BDWL using the 3D velocity model with attenuation. WPP simulations that included attenuation resulted in waveforms that included random steps and artificial arrivals.